



Investigation of Temporal Integration in Cochlear Implant Users Using Electrically-Evoked Auditory Brainstem Responses

Ali Saeedi

Vollständiger Abdruck der von der Fakultät für Elektrotechnik und Informationstechnik der Technischen Universität München zur Erlangung des akademischen Grades eines

Doktors der Ingenieurwissenschaften (Dr.-Ing.)

genehmigten Dissertation.

Vorsitzender:

Prof. Dr.-Ing. Gerhard Rigoll

Prüfende der Dissertation:

1. Prof. Dr.-Ing. Werner Hemmert
2. Prof. Dr. Tobias Rader

Die Dissertation wurde am 17.11.2021 bei der Technischen Universität München eingereicht und durch die Fakultät für Elektrotechnik und Informationstechnik am 15.02.2022 angenommen.

Abstract

Electric hearing with cochlear implants (CIs) can restore hearing sensation of people with severe to profound hearing loss to a high degree. Yet, many temporal and spectral aspects available to normal hearing listeners are missing. Temporal integration in CI users is an area of active research, because temporal integration is a dominating factor in clinical coding strategies, where stimulation rates in the order of 1000 pulses per second (pps) are applied. Objective tests to determine the stimulation thresholds like the measurement of electrically evoked compound action potentials or electrically evoked brainstem responses only work with single pulses so far. In this thesis, single pulses were put together in the time domain to construct multi-pulse stimuli with a burst rate of 10,000 pps. The use of multi-pulse (MP) stimuli to investigate temporal integration in CI users could shed light on the temporal integration effects to electric stimulation at the level of the brainstem and be useful as a clinical tool to determine stimulation thresholds, which is important for example for very young children.

In Chapter 3, the effects of electric MP stimulation with a high burst rate were studied. Psychophysical thresholds (THR) and maximum comfortable levels (MCLs), as well as eABR recordings were investigated. Psychophysical temporal integration functions, i.e. slopes of THR and MCLs as a function of number of pulses, decreased with slopes of -1.30 and -0.93 dB/doubling the number of pulses, respectively. The morphology of eABRs to MP stimuli did not differ from those to conventional single pulses. At a fixed stimulation amplitude, an increasing number of pulses caused increasing wave eV amplitudes up to a certain, subject-dependent number of pulses. Then, amplitudes either saturated or even decreased. This contradiction to the expected amplitude growth function was resolved and attributed to destructive interference, where peaks and troughs of responses to the first pulses were suppressed by those of successive pulses in the train.

In Chapter 4, eABR THR to MPs were estimated. The growth functions of features extracted from eABRs showed shallower growth slopes when the number of pulses increased. The eABR THR estimated at a higher number of pulses were closer to the clinical THR, when compared to low ones. However, the smallest difference between estimated eABR THR and clinical THR was not always achieved from the same number of pulses. Pearson's correlation coefficients (PCCs) between eABR THR and psychophysical THR were significant and relatively large in all but the highest MP conditions. The PCCs between eABR THR and clinical THR, however, were smaller and in less cases significant. Results of this study showed that eABRs to multi-pulse stimulation could represent clinical stimulation paradigms more closely than measurements with single pulses and lead to an improved estimate of clinical THR with smaller deviations.

Zusammenfassung

Elektrisches Hören mit Cochlea-Implantaten (CIs) kann das Hörempfinden von Menschen mit schwerem bis hochgradigem Hörverlust in hohem Maße wiederherstellen. Dennoch fehlen ihnen viele zeitliche und spektrale Aspekte, die Normalhörenden zur Verfügung stehen. Die zeitliche Integration bei CI-Nutzern ist ein aktives Forschungsgebiet, da die zeitliche Integration ein dominierender Faktor bei klinischen Kodierungsstrategien ist, bei denen Stimulationsraten in der Größenordnung von 1000 Impulsen pro Sekunde (pps) angewendet werden. Objektive Tests zur Bestimmung der Stimulationsschwellen, wie die Messung elektrisch evozierter Potentiale, die direkt in der Cochlea oder im Hirnstamm abgeleitet werden, funktionieren bisher nur mit Einzelimpulsen. In dieser Arbeit wurden Einzelpulse im Zeitbereich zusammengesetzt, um Multipuls-Stimuli mit einer Burst-Rate von 10.000 pps zu erzeugen. Die Verwendung von Multi-Puls-Stimuli (MP) zur Untersuchung der zeitlichen Integration bei CI-Trägern könnten die zeitlichen Integrationseffekte bei elektrischer Stimulationen auf der Ebene des Hirnstamms erklären und als klinisches Instrument zur Bestimmung von Stimulationsschwellen nützlich sein, was z. B. für sehr junge Kinder wichtig ist.

In Kapitel 3 wurden die Auswirkungen der elektrischen MP-Stimulation mit einer hohen Burst-Rate untersucht. Ausgewertet wurden psychophysikalische Schwellenwerte (THR_s) und maximal angenehme Werte (MCL_s) sowie eABR-Ableitungen. Die psychophysikalisch gemessenen zeitlichen Integrationsfunktionen der THR_s und MCL_s nahmen mit Steigungen von -1,30 bzw. -0,93 dB/Verdoppelung der Impulszahl ab. Die Morphologie der eABR_s auf MP-Reize unterschied sich dabei nicht von denen auf herkömmliche Einzelimpulse. Bei einer festen Stimulationsamplitude verursachte eine zunehmende Anzahl von Impulsen steigende Amplituden der eV-Wellen bis zu einer bestimmten, subjektabhängigen Anzahl von Impulsen. Danach sättigten die Amplituden entweder oder nahmen sogar ab. Dieser Widerspruch zur erwarteten Amplitudenwachstumsfunktion wurde aufgelöst und auf destruktive Interferenz zurückgeführt, bei der die Spitzen und Täler der Reaktionen auf die ersten Impulse durch die der nachfolgenden Impulse unterdrückt wurden.

In Kapitel 4 wurden die eABR-THR_s für MPs geschätzt. Die Wachstumsfunktionen der aus den eABR_s extrahierten Merkmale wiesen mit zunehmender Anzahl von Impulsen flachere Wachstumskurven auf. Die eABR-THR_s, die mit einer höheren Anzahl von Impulsen geschätzt wurden, lagen dabei näher an den klinischen THR_s als die mit weniger Impulsen. Der geringste Unterschied zwischen den geschätzten eABR-THR_s und den klinischen THR_s wurde jedoch nicht immer mit der gleichen Anzahl von Impulsen erreicht. Die Pearson-Korrelationskoeffizienten (PCC_s) zwischen den eABR-THR_s und den psychophysikalisch gemessenen THR_s waren signifikant und bei allen Bedingungen relativ groß, außer den MPs mit den meisten Impulsen. Die PCC_s zwischen eABR-THR_s und klinischen THR_s waren jedoch kleiner und in weniger Fällen signifikant. Die Ergebnisse dieser Studie zeigen, dass eABR_s zu Multi-Puls-Stimulationen klinische Stimulationsparadigmen besser repräsentieren können als Messungen mit einzelnen Impulsen und eine genauere Schätzung klinischer THR_s ermöglichen.

Acknowledgments

Here I would like to acknowledge some of the people who made it possible and easier for me to start, do, and finish my PhD. My greatest appreciations, of course, go to my supervisor, Prof. Werner Hemmert, whose continuous supports began way before I arrived in Germany. I would like to thank him for his great guidance and support throughout my study at the BAI group.

I would like to thank all members of BAI group, who were always warm, friendly, and ready-to-help: Sonja Karg, Siwei Bai, Andrej Voss, Anja Kenn, Florian Völk, Robin Weiß, Jörg Encke, Christian Wirtz, Miguel Obando, Albert Croner, Carmen Castaneda, and Lukas Driendl. Without them and the nice environment they created, it would have been very hard to finish this work.

I also would like to express my acknowledgements to all of the CI users who participated the measurements detailed in this study, with their admirable commitment and motivation. Also, many thanks to Auguste Schulz and Ludwig Englert, who helped me a lot during the CI measurement.

I deeply thank my parents, two brothers, and one sister, whose support brought me so far. Lastly, my special gratitude goes to my wife, Taban, for all of her support, motivation, and unconditional love during these years.

Munich, 29. October, 2021

Content

Chapter 1 Introduction.....	1
1.1 Hearing with a cochlear implant	1
1.2 Importance of fitting	2
1.2.1 Lower and upper limits	4
1.2.2 Stimulation rate	6
1.3 Coding Strategies	6
1.3.1 Continues interleaved sampling (CIS)	7
1.3.2 HiResolution	8
1.3.3 Fine Structure Processing (FSP) and FS4	8
1.3.4 <i>n-of-m</i> strategies.....	9
1.4 THR determination.....	10
1.5 Electrically-evoked compound action potentials (eCAP)	10
1.6 Electrically-evoked auditory brainstem response (eABR).....	12
1.7 Cortical auditory evoked potentials (CAEPs)	14
Chapter 2 Fundamentals and a Brief Literature Overview	16
2.1.1 Refractoriness.....	16
2.1.2 Temporal summation (facilitation).....	17
2.1.3 Accommodation	19
2.1.4 Spike-rate adaptation.....	19
2.2 Temporal and multi-pulse integration.....	19
2.3 Objective THRs in CI users	21
2.3.1 eCAP THRs.....	22
2.3.2 eABR THRs	23
2.3.3 CAEP THRs	25
2.4 Objectives of this thesis	26
Chapter 3 Investigation of Electrically-Evoked Auditory Brainstem Responses to Multi-Pulse Stimulation of High Frequency in Cochlear Implant Users.....	28
3.1 Introduction	28
3.2 Material and Methods	31
3.2.1 Stimuli.....	31
3.2.2 Pretest.....	32
3.2.3 eABR multi-pulse stimuli	33
3.2.4 eABR recording	34
3.2.5 eABR processing.....	36
3.2.6 Statistical analysis	38

3.3	Results	39
3.3.1	Psychophysical results.....	39
3.3.2	eABR results.....	40
3.4	Discussion	44
3.4.1	Artifact suppression.....	44
3.4.2	TI functions in psychophysical data	46
3.4.3	eABRs to multi-pulse stimulation	48
3.4.4	Efficacy of multi-pulse stimulation	50
3.4.5	Temporal effects in eABRs to fast pulse trains	51
Chapter 4 eABR THR Estimation Using High-Rate Multi-Pulse Stimulation in Cochlear Implant Users.....		53
4.1	Introduction	53
4.2	Material and Methods.....	55
4.2.1	Stimuli	56
4.2.2	Pretest	57
4.2.3	eABR stimulation	57
4.2.4	eABR recording.....	58
4.2.5	eABR THR estimation	58
4.2.6	Statistical Analysis	60
4.3	Results.....	61
4.3.1	Psychophysical thresholds.....	61
4.3.2	eABR results.....	61
4.4	Discussion	70
4.4.1	eABR THR estimation	72
4.4.2	eABR THRs vs. psychophysical THRs and clinical THRs.....	73
Chapter 5 Summary, Conclusion, and Outlook		76
A Supplementary material for Chapter 3		80
List of Figures.....		81
List of Tables.....		85
References		86

List of Publications

Journal Papers

Saeedi, A.; Englert, L.; Hemmert, W., "eABR THR Estimation Using High-Rate MultiPulse Stimulation in Cochlear Implant Users", *Frontiers in Neuroscience*, 15:937, 2021. doi: 10.3389/fnins.2021.705189.

Saeedi, A.; Hemmert, W., "Investigation of Electrically-Evoked Auditory Brainstem Responses to Multi-Pulse Stimulation of High Frequency in Cochlear Implant Users", *Frontiers in Neuroscience*, 14:615, 2020. doi: 10.3389/fnins.2020.00615.

Talks

Saeedi, A.; Hemmert W.; Englert, L., "eABR Thresholds in Response to High-Rate Multi-Pulse Stimulations in CI Users", *AG-ERA 2018*, 23-24 Nov., Freiburg.

Hemmert W.; **Saeedi, A.**; Schulz, A., "Elektrisch evozierte auditorische Hirnstampfpotentiale bei Multi-Puls Stimulation in Cochlea Implantat Nutzern", *DGMP 2018*, 19-22 Sep., Nürnberg.

Posters

Saeedi, A.; Hemmert, W.; Englert, L., "Using Stimuli of High-Rate Multi-pulse Trains to Estimate Clinical Thresholds in Cochlear Implant Users", *CIAP 2021*, 11-16 July., Online conference.

Saeedi, A.; Hemmert W.; Englert, L., "Estimation of Clinical Thresholds by Means of eABR Thresholds in Response to Multi-pulse Trains in Cochlear Implant Users", *AESoP 2019*, 16-18 Sep., Leuven, Belgium.

Englert, L.; **Saeedi, A.**; Hemmert W., "Wave eV eABR Amplitude and Latency in Response to Multi-Pulse Train Stimulation", *AESoP 2019*, 16-18 Sep., Leuven, Belgium.

Saeedi, A.; Hemmert W.; Schulz, A., "Electrically-Evoked Auditory Brainstem Responses to Multi-Pulse Train Stimulation", *DGMP 2018*, 19-22 Sep., Nürnberg, Germany.

Glossary

(e)ABR	(Electrically-Evoked) Auditory Brainstem Responses
ABI	Auditory Brainstem Implants
ACE	Advanced Combination Encoder
AGF	Amplitude Growth Function
AME	Absolute Magnitude Estimation
ANF	Auditory Nerve Fiber
ANOVA	Analysis of Variance
AP	Action Potential
ARP	Absolute Refractory Period
CAEP	Cortical Auditory Evoked Potentials
CI	Cochlear Implant
CIS	Continues Interleaved Sampling
CLS	Categorical Loudness Scaling
CNC	Consonant-Nucleus-Consonant
CU	Clinical/Current Unit
DR	Dynamic Range
eASSR	Electrically-Evoked Auditory Steady State Response
eCAP	Electrically-Evoked Compound Action Potentials
FF	Fitting Function
FSP	Fine Structure Processing
GFP	Global Field Power
IHCs	Inner Hair Cells
IPG	Inter-Phase Gap
LVDP	Lowest Valid Data Point
MAL	Maximum Acceptable Levels
MCL	Most Comfortable Level
MP	Multi-Pulse
MPI	Multi-Pulse Integration
NH	Normal Hearing
OHC	Outer Hair Cell
PCC	Pearson Correlation Coefficients
PD	Phase Duration
PLV	Phase Locking Value
pps	Pulses-Per-Second
RF	Radio Frequency
RIB II	Research Interface Box
RME	Relative Magnitude Estimation
RN	Residual Noise
RRP	Relative Refractory Period
SGC	Spiral Ganglion Cell
speak	Spectral Peak
THR	Threshold
TI	Temporal Integration

Structure of the thesis

Chapter 1 *Introduction* provides a general introduction on hearing and cochlear implants (CI), as well as on importance of clinical fitting. It also includes an overview of important fitting parameters such as lower and upper limits of stimulation amplitudes, stimulation rate and coding strategies used in at-present modern CIs. The chapter ends with a short introduction on objective measurements in CI users, like eCAP, eABR, and CAEP.

In Chapter 2 *Fundamentals and a Brief Literature* will be discussed. Particularly, four temporal response phenomena, refractoriness, facilitation, accommodation, and spike-rate adaptation and their interactions in temporal and multi-pulse integration (TI and MPI) in CIs are described. The chapter ends with a review on the use of objective measures for THR determination in CI users.

Chapter 3 is based on a previously published paper, where the eABRs to multi-pulse stimulations at high rates were investigated. This includes describing amplitude growth and latency functions of responses to MP stimuli, efficiency of MPs, and the temporal effects involved. Following this, the content of Chapter 4 describes how the growth functions of eABR wave eV amplitude, and features such as the RMS and peak of the phase-locking values in response to MPs could be used to estimate objective THRs. Correlations between the eABR THR estimates and their psychophysical counterparts, and clinical THRs were presented.

Chapter 5 summarizes findings of the thesis, provides a general discussion, and concludes the work. A bibliography closes the document.

Chapter 1

Introduction

1.1 Hearing with a cochlear implant

Hearing loss is very common worldwide. In its first-ever report on hearing, the WHO estimated that by 2050, about 2.5 billion people will be living with hearing loss of different degrees and types. At least, 700 million of this population will need rehabilitation services (WHO 2021). This includes providing auditory prosthesis such as hearing aids, cochlear implants (CI), and auditory brainstem implants (ABIs) to patients who need such prosthesis. Particularly, CIs have been shown to be capable of restoring hearing sensations to people with severe to profound sensorineural hearing loss.

CIs with multiple channels (at least 12) can mimic the acousto-chemical transduction of sound to electric pulses, which is the case in normal hearing, up to an excellent extent as long as enough auditory nerve fibers have survived in the cochlea. CIs consist of two parts, an external battery-powered part, which encloses microphone, speech processing unit, and transmitting induction coil, and an internal part, which is responsible for receiving coded radio frequency (RF) pulses from the external part, decoding and delivering them to an array of electrodes. The CI microphone collects environmental sounds. The speech processor codes the sound into electric pulses based on a chain of processing steps, which are known as coding strategy. These electric pulses, as well as the energy needed for operation of the internal part, are then transmitted via the external coil to the internal coil, which is beneath the skin. In the implanted part, the data is decoded and converted to electrical pulses, which are delivered to the electrode array.

Despite between-individual variations, research shows that early implantation of pre-lingually deaf children, results in a more rapid development of speech perception as well as spoken language skills (Grant *et al.* 1999; Sharma *et al.* 2002) compared to later implantation. When lacking normal acoustic hearing, there is a crucial period of less than 3.5 years for the early born babies to undergo implantation. During this period, the plasticity of the central auditory system remains high enough for an optimal benefit from cochlear implantation (Sharma *et al.* 2002). This finding motivated doctors to implant CIs in children as early as possible and the age of implantation decreased continuously over the years from 6 years (Papsin *et al.* 2001), to 5 years (Fryauf-Bertschy *et al.* 1997; Brackett and Zara 1998), 3 years (Miyamoto *et al.* 1999; Kirk *et al.* 2002) and 2 years (Boons *et al.* 2012). More recently, research has suggested that in order to develop language skills similar to normal hearing peers, profoundly deaf children should receive their CIs before the age of 1 year (Valencia *et al.* 2008; Dettman *et al.* 2016), or

Introduction

immediately after the confirmation of the diagnosis (Colletti *et al.* 2011). In addition to children, also post-lingually deaf adults who received a CI can reach very good speech perception (Tyler *et al.* 1997; Helms *et al.* 2004).

However, hearing with cochlear implants still involves many challenges and lacks behind normal hearing. Some CI users are limited by poor performance even in basic speech tests with no background noise. Many CI users have poor performances in telephone conversations, where they lack visual cues. Music perception, understanding of speech in noise, auditory attention (cocktail party), and sound localization is limited in all CI users compared to normal hearing subjects.

1.2 Importance of fitting

Besides technological limitations of to-date CIs, such as a thousand times larger size and a thousand times less number of electrodes compared to those of auditory nerve fibers (Zeng 2017), performance of CIs is influenced by many other factors. These factors can be categorized in implantee-related (e.g. age at implantation, health state of residual nerve fibers), clinical (e.g. fitting and postoperative rehabilitation, see Harris *et al.* (2016)), and pedagogical (e.g. educational programs, see Geers *et al.* (2003)) aspects. In order to take the most of the CI functionality, each of these factors needs to be optimized.

Clinical parameters affecting performance of CIs are set by the audiologist during a process known as *fitting* or *programming*. This process is normally divided into 4 phases: initial programming, on-operation, initial activation, and follow-ups, and aims to adjust the device parameters so that the recipient can benefit from the device maximally (Shapiro and Bradham 2012). Reports from clinicians/audiologists suggest that later performance of CIs is bounded to the quality of their programming. Appropriate fitting of CIs contributes to remarkable performance, while inappropriate fitting leads to poor outcomes (Geers *et al.* 2003; Wolfe and Kasulis 2008). Particularly, pertinent fitting is of high importance for babies, who are not able to provide oral feedback on their sound perception (Wolfe and Schafer 2014).

As a global perspective, these clinical parameters can be categorized into intensity, time, and frequency domains. In the second chapter of their book, Wolfe and Schafer (2014) comprehensively reviewed these parameters and their specifications for the three manufacturers of CIs at the time of writing: Advanced Bionics, Cochlear, and Med-El. The intensity domain includes parameters such as stimulus level, threshold of hearing sensation, upper limit of stimulation, pulse-shape characteristic (e.g. pulse width, inter-phase gap), compression, channel gain, (microphone) sensitivity, and volume control. The two latter are known as patient-controlled parameters, which are said to be underused or misunderstood by them (Shapiro and Bradham 2012).

Clinical parameters which belong to the frequency domain are mainly concerned with the electrode contacts, their corresponding channels and their frequency range. The reason is the

so-called *tonotopic organization* of the cochlea, which implies that the frequency information of the input sounds is *coded* at different *places* along the cochlea, with low- to high- frequencies being coded in the apical-to-basal direction of the cochlea. Multi-channel CIs intuitively take advantage of the place-code theory and map frequency content of the input signal into electrode contacts with decreasing (Med-El and Advanced Bionics) or increasing (Cochlear) electrode number from the base to the apex.

Although current multi-channel CIs have become more advanced compared to the first single-channel CI developed in the 1950s (Djourno and Eyries 1957), one of the still-remaining challenges is poor frequency resolution especially at low frequencies. In a healthy cochlea, there are more than 3000 inner hair cells (IHCs), each of which is tuned to a small and specific frequency range along the cochlea. With such a specialized design, the human auditory system is able to remarkably distinguish tones of 2 Hz difference. With impaired IHCs, CIs must compensate this high resolution with only a very limited number of electrodes (at the time of writing, up to 25 electrodes). It is useless to add more electrodes (or channels) to increase the frequency resolution, as the electric field generated by stimulation of a given electrode spreads broadly over the neighboring channels. This causes severe channel interaction, thus independent information or frequency content cannot be delivered. To overcome this problem, a few solutions have been proposed and implemented. One is using bipolar stimulation, which is an alternative to monopolar stimulation¹. In the bipolar configuration (**Figure 1.1C**), two equal and opposite stimulation currents are delivered to two neighboring electrodes, rather than stimulating a single electrode relative to an extra-cochlear ground electrode (**Figure 1.1B**).

As **Figure 1.1** suggests, opposite current flows generated by the two opposite phases of the bipolar pulse cancel out each other and therefore, the equivalent electric field in the near distance fades away faster, when compared to the monopolar configuration. Although the electric field in bipolar arrangement is more focused than that in monopolar, the cortical activation achieved in the former is only modestly more focal than the latter, in guinea pigs (Bierer and Middlebrooks 2002; Snyder *et al.* 2008), as well as in human speech recognition studies (Wilson 2004).

Another strategy to manipulate the spatial location of the electrical stimulation in the cochlea is the concept of virtual electrodes or current steering. In this concept, pairs of adjacent electrodes are stimulated simultaneously. Based on the proportion of stimulation currents at the electrodes, the location of stimulated neurons will be accordingly shifted between the two electrodes. Therefore, many more intermediate stimulation sites (pitches) than the number of electrode contacts can be, at least theoretically, elicited. As shown in **Figure 1.2**, when stimulation currents are equal, the focus of stimulation will be at the midpoint of the two electrodes, while for a dominant stimulation on one side, the focus will be shifted toward that side. Koch *et al.* (2007) employed current steering to investigate the spectral resolution in users with CII and HiRes 90K (Advanced Bionics) implants at basal, mid-array, and apical sites (2

¹ Bipolar electrode configuration should not be confused with biphasic pulse stimulation. The latter refers to two opposite phases of an electrical pulse delivered to CI electrodes.

Introduction

and 3, 8, and 9, 13 and 14). On average, they found that their CI users could discriminate 5.4, 8.7 and 7.2 spectral (virtual) channels for the three electrode pairs, respectively, and when generalizing to all electrodes, they reported an average of 93 virtual electrodes.

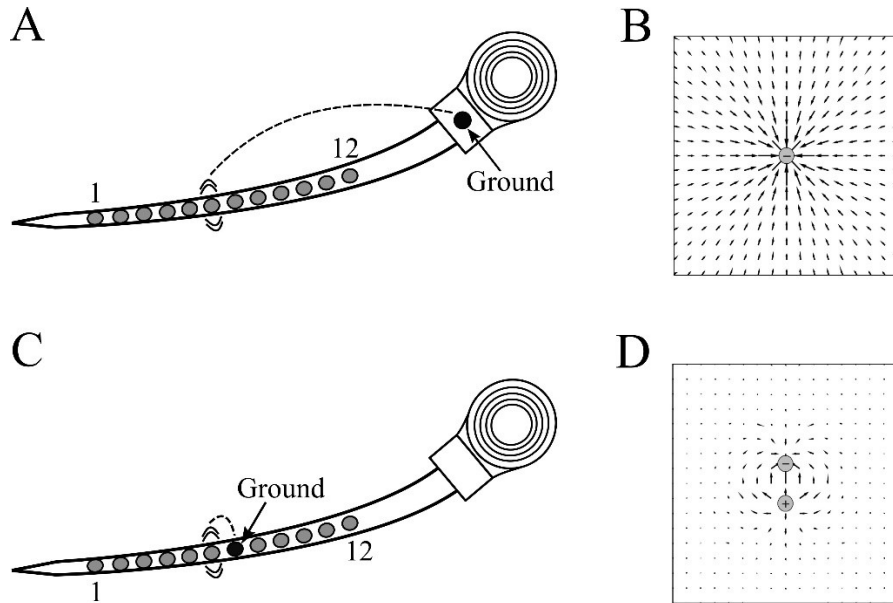


Figure 1.1 Monopolar (A) and Bipolar (C) stimulation configuration and their corresponding electric fields (B and D). The drawings in B and D were adapted with modification from (Schnupp *et al.* 2011).

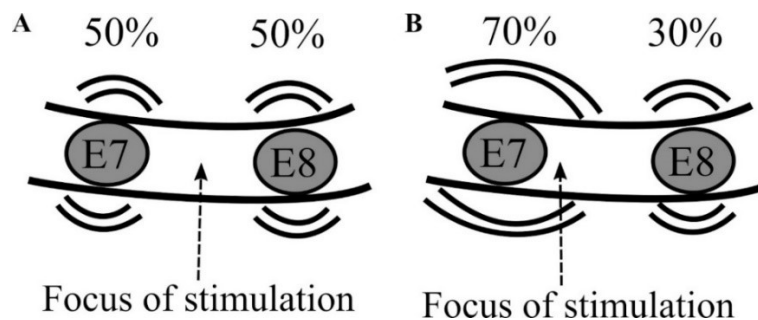


Figure 1.2 Schematic illustration of virtual electrode (current steering). The focus of stimulation will be in the midpoint of the two electrodes when the stimulation currents on the two adjacent electrodes are equal (A). When the stimulation current dominates at one electrode, the stimulation focus will be toward that electrode (B).

1.2.1 Lower and upper limits

Two basic intensity parameters that most of the clinics' effort goes to their determination (Vaerenberg *et al.* 2014), are the lower and the upper stimulation limits. In literature, the former is known as 'threshold', 'THR', 'T-level', and 'THS' and for a given electrode, it is generally

defined as the least stimulation current needed for the CI user to perceive it. Nevertheless, the exact definition of the threshold differs among the manufacturers: the minimum amount of stimulation detected by the recipients with an accuracy of 50% (Advanced Bionics), or 100% (Cochlear), or the highest amount of stimulation just below user's perception (Med-El). As the THR is likely to change only slightly in adult and children users in the first 2 months post-implantation (Hughes *et al.* 2001), it is not critical to set the THR very accurately during the first few days of CI experience. However, appropriate determination of THR is necessary thereafter in order for the recipients to benefit from the optimal performance of the implant. Yet, some studies suggested that CI recipients pertain their speech understanding, when T-levels are set differently from the pre-measured behavioral ones. Spahr and Dorman (2005) observed that for users of the Med-El Tempo+ speech processor, speech understanding did not significantly change when reducing the minimum stimulation THR to 10% of MCL or to 0 μ A. In a Nucleus Cochlear implant study, Busby and Arora (2016) found that \pm 30% deviation from behavioral THR (compression or expansion of the electric DR) did not affect the performance of users in consonant-nucleus-consonant (CNC) word scores.

If THR is set too low, users might lose their ability to perceive low level sounds, which is suggested to improve understanding of soft speech sounds (Skinner *et al.* 2000; Holden *et al.* 2011). Busby and Arora (2016) reported reduced speech understanding in quiet when the electric DR was expanded by 60% and 90% (THR was adjusted lower, while the MCLs were fixed). Moreover, due to unnecessary functioning of the implant for sub-THR levels, setting T-levels too low would lead to stimulation without perception in the range between where the electrode THR and the true THR. On the other hand, setting the THR too high might result in inducing a background noise (Busby and Arora 2016), and also part of already-limited electrical dynamic range would be unnecessarily discarded (Wolfe and Schafer 2014).

The terminology describing the upper stimulation limit varies, like THR, in literature and market. It is referred to as the maximum/most comfort/comfortable level/loudness (MCL), M-level, C-level and is considered to "loud but not uncomfortable" or "loud but comfortable". Similar to THR, setting the upper stimulation levels appropriately is critical for CI users to benefit from their implants. With improper setting of the MCLs, CI users would have difficulties in accessing good sound quality and speech recognition. In case of MCL overestimation, it would induce discomfort or even unpleasant feelings. For CI wearers with proper communication abilities, the MCLs are adjusted via psychophysical loudness scaling methods such as categorical loudness scaling (CLS, see for example Allen *et al.* (1990); Launer (1995)) or absolute/relative magnitude estimation (AME/RME). In CLS, CI users subdivide the dynamic ranges of their CI electrodes using verbal expressions such as "audible", "soft", or "comfortable". In AME/RME, instead of words, subjects assign numerals that corresponds to the loudness of the input stimuli. Although it is unclear which of the two methods (CLS or AME) provides more reliable results (Launer 1995), data from Elberling and Nielsen (1993) indicated that magnitude estimation methods could be more reliable. There exist loudness scaling methods combined from CLS and AME (e.g. Brand and Hohmann (2002)), where the individuals first choose among all possible verbal categories available in the method and in the

Introduction

second step, a fine numeral scale around the chosen category in the step is presented (Hellbruück and Moser 1985).

1.2.2 Stimulation rate

Modern CIs provide stimulation rates between 250 and 5000 pulses-per-second (pps) per electrode. However, stimulation rates used in clinical settings vary between 900 and 2000 pps. Performance of CI recipients when changing the stimulation rate is reported to be highly individual (Vandali *et al.* 2000; Büchner *et al.* 2004; Verschuur 2005; Büchner *et al.* 2010; Shader *et al.* 2020) or of no significance (Friesen *et al.* 2005; Balkany *et al.* 2007; Weber *et al.* 2007), although a general trend exists for all manufacturers towards higher (total) stimulation rates (Zeng *et al.* 2008). Büchner *et al.* (2004) found that on average, employing high-rate coding strategies (e.g. 3000 pps/ch) led to a remarkable improvement in speech understanding, when compared to low rate configurations (1500 pps/ch). However, they observed cases with moderate or even worse effects for high stimulation rates. Shader *et al.* (2020) investigate stimulation rates of 500, 720, 900, and 1200 pps/ch, as well as a higher-than-1200 pps for those with default rate of 1200 pps for three CI manufacturers. They found that for Cochlear-brand users the performance with default rate (900 pps) was slightly better than for the non-default rates. However, the overall performance of Med-El and Advanced Bionics users was modestly higher at non-default rate (720 pps) when compared to the default setting (higher than 1200 pps).

In a large study with the Nucleus Freedom implant, Balkany *et al.* (2007) measured hearing outcomes as a function of two sets of stimulation frequencies: 500, 900, and 1200 pps as low-rate set, and 1800, 2400, 3500 pps as high-rate set. About 67% of participants preferred to choose lower rates in both sets. They observed no advantage or improved performance when using high-rate configurations. Verschuur (2005) investigated the effect of stimulation rate in Med-El CI users using a categorical identification task and a consonant recognition task. They employed rates between 400 and 2020 pps and found no variation in the results as a function of stimulation rate. However, they reported that two subjects showed reduced performance at lower stimulation rates. Verschuur (2005); Balkany *et al.* (2007); Weber *et al.* (2007) came to the conclusion that although in most cases CI performance is optimal for rates below 1200 pps, an individual optimal stimulation rate might exist for CI users. However, Wolfe and Schafer (2014) explicitly suggested that for very old patients, those with long CI experience, as well as patients with auditory nerve dysfunction, low stimulation rates (below 1200 pps) should be used in their clinical maps. They also suggested that in order for the CI users to find their individual optimized rates, they should be provided with a wide variety of stimulation rates (e.g. 250 to 3000 pps), especially within the first months of CI activation. This is, however, challenging, due to the already limited time that clinics offer for CI fittings (Shader *et al.* 2020).

1.3 Coding Strategies

The term coding strategy refers to as the algorithm which codes the important aspects of the

acoustic signals into electrical pulses. The ultimate goal of such an algorithm is to convey the most important features of the incoming sound, such as temporal and spectral information, to the auditory nerve and to the brain. Continuous interleaved sampling (CIS) and the *n-of-m* strategy are two categories of coding strategies being used in modern CIs. Both strategies avoid simultaneous stimulation of electrodes because the summation of the wide spreading electric currents emitted from electrode contacts activated at the same time would rapidly lead to overstimulation, given the small dynamic range available in electric hearing.

1.3.1 Continuous interleaved sampling (CIS)

For this reason, the CIS strategy stimulates only one electrode after the other. As shown in **Figure 1.3**, the envelope of each channel output of the filter bank is calculated as the input of the map-law transformation. The output of map-law is then multiplied by a pulse train. From apex to base (in a tonotopic fashion of low to high frequency), pulse trains are shifted in time by the duration of at least one complete length of a biphasic pulse (blue dotted line in **Figure 1.3**). This prevents superposition of electric current spread from different electrodes, and thus, provides access to higher stimulation amplitudes. The modulated pulse trains will be then delivered to the electrode contacts with preserved tonotopic organization. Normally 8 to 16 electrodes are used by CIS and the typical stimulation rates vary between 800 and 1600 pps per channel/electrode (Wolfe and Schafer 2014).

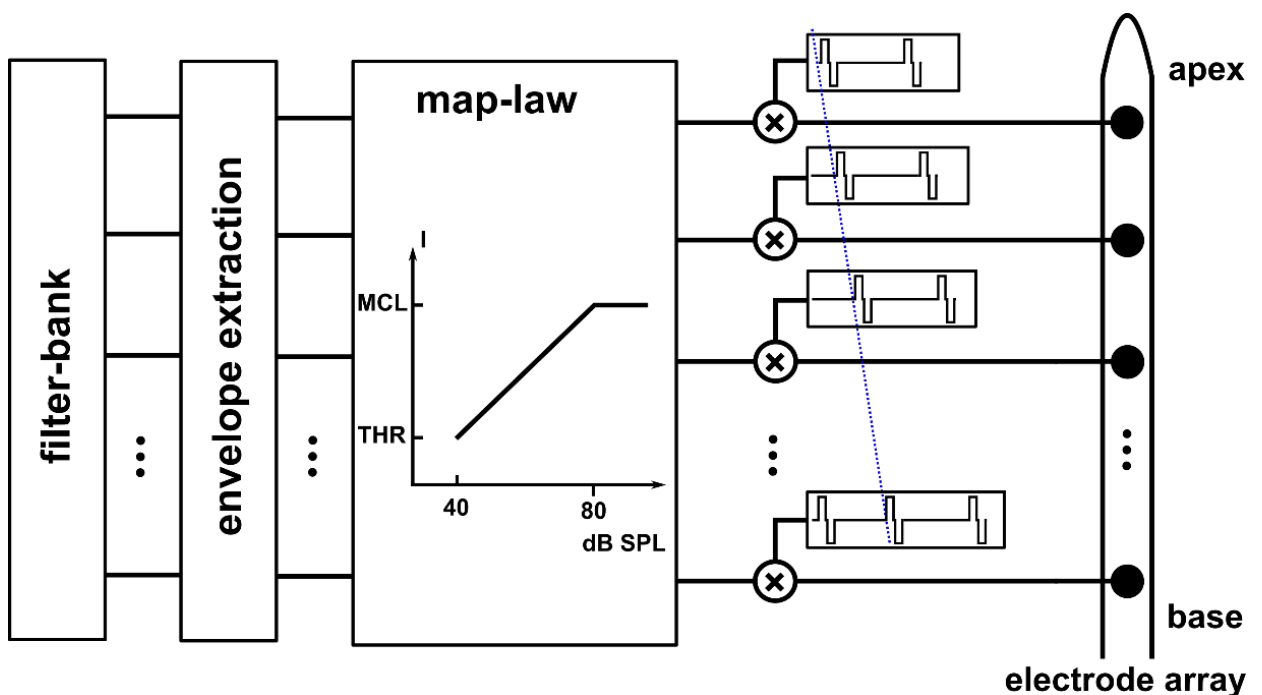


Figure 1.3 Schematic illustration of continuous interleaved sampling (CIS).

Introduction

Variations of CIS are used by different CI manufacturers. For instance, Med-El uses CIS+ and high definition CIS (HDCIS). CIS+ basically resembles CIS, but the stimulation rate is expanded and a Hilbert transform is employed instead of rectification and low-pass filtering to provide more accurate extraction of the envelopes. HDCIS aims to perform current steering (virtual electrodes) by sequential stimulation of adjacent electrodes such that the stimulation is focused at a point between the two electrodes. Advanced Bionics employs simultaneous stimulation of two remotely distant electrodes. This way the overlap between current spreads are low enough to ensure avoidance of overstimulation (for more details, see pp 84-91 of Wolfe and Schafer (2014)).

1.3.2 HiResolution

HiResolution sound coding strategy is another variation of the CIS strategy, which was introduced by Advanced Bionics in 2003. The major differences between HiRes and the classical CIS are the usage of 16 active channels compared to 8 in CIS and greatly increased stimulation rates per channel (up to about 5000 pps). Recently, a new version of HiRes, known as HiRes120 has been released by Advanced Bionics. HiRes120 aims to deliver finer special resolution to the electrodes by utilizing the current steering approach. As described before, different current ratios at two neighboring electrodes can steer the effective current between the two electrodes. Having 16 electrode contacts provides 15 adjacent electrode pairs, and with 8 defined current ratios, up to 120 virtual stimulation channels can be achieved (Wouters *et al.* 2015). Although Koch *et al.* (2004) reported significant improvement in consonant recognition tests in quiet and noise with the HiRes strategy compared with conventional sound processing, no significant influence of processing strategies on speech and music perception has been reported (Wouters *et al.* 2015).

1.3.3 Fine Structure Processing (FSP) and FS4

In a similar attempt to establish current steering paradigm, Med-El introduced a CIS-type processing strategy referred to as fine structure processing (FSP). FSP's primary differences with the traditional CIS strategy include 1) provision of intermediate pitches and 2) modulating timing of stimulation to code the temporal fine structure. Access to intermediate pitches is achieved by employing bell-shaped band-pass filters which also allow for smooth transitions from one electrode to the neighboring basal or apical electrode (Hochmair *et al.* 2006). Modulation of time in FSP is achieved by means of a series of burst pulses, which take place after each negative-to-positive zero-crossing. The bursts aims to code the temporal fine structure in the lower frequency bands (up to 500 Hz), which is missing in the envelope of those bands (Wouters *et al.* 2015). While in the FSP, timing modulation is typically applied to one or two apical channels to provide fine temporal processing up to 500 Hz (Hochmair *et al.* 2006), in FS4, which is a newer version of FSP, up to four apical electrodes are programmed to deliver fine structure information (Wolfe and Schafer 2014).

1.3.4 *n-of-m* strategies

Unlike sequential or partially simultaneous stimulation used for all electrodes in CIS-type strategies, the *n-of-m* strategies deliver from the outputs of m band-pass filters with the highest amplitudes a maximum of n electrodes. Channels other than n are not activated during the activation cycle of the n channels. The first obvious benefits from activation of n out of m channels are increased stimulation rate and reduced channel crosstalk. Spectral peak (SPEAK) and advanced combination encoder (ACE) are two well-established versions of the *n-of-m* strategy. The ACE, which was introduced and is being used by Cochlear, differs from SPEAK in the stimulation rate, with ACE using higher rates (up to 1800 pps for $n = 8$).

SPEAK and CIS strategies share pre-processing stages prior to channel selection and the delivery of current to electrodes. In SPEAK, n usually varies between 8 and 12, but is typically set to 8, which means that the output of 8 channels with the highest amplitudes are modulated with biphasic pulse trains and, still in an interleaved manner, delivered to 8 electrodes. The stimulation rate is usually set to 900 pps and the time frames in which the maximum amplitudes are selected ranges between 2.5 to 4 ms (Zeng *et al.* 2008).

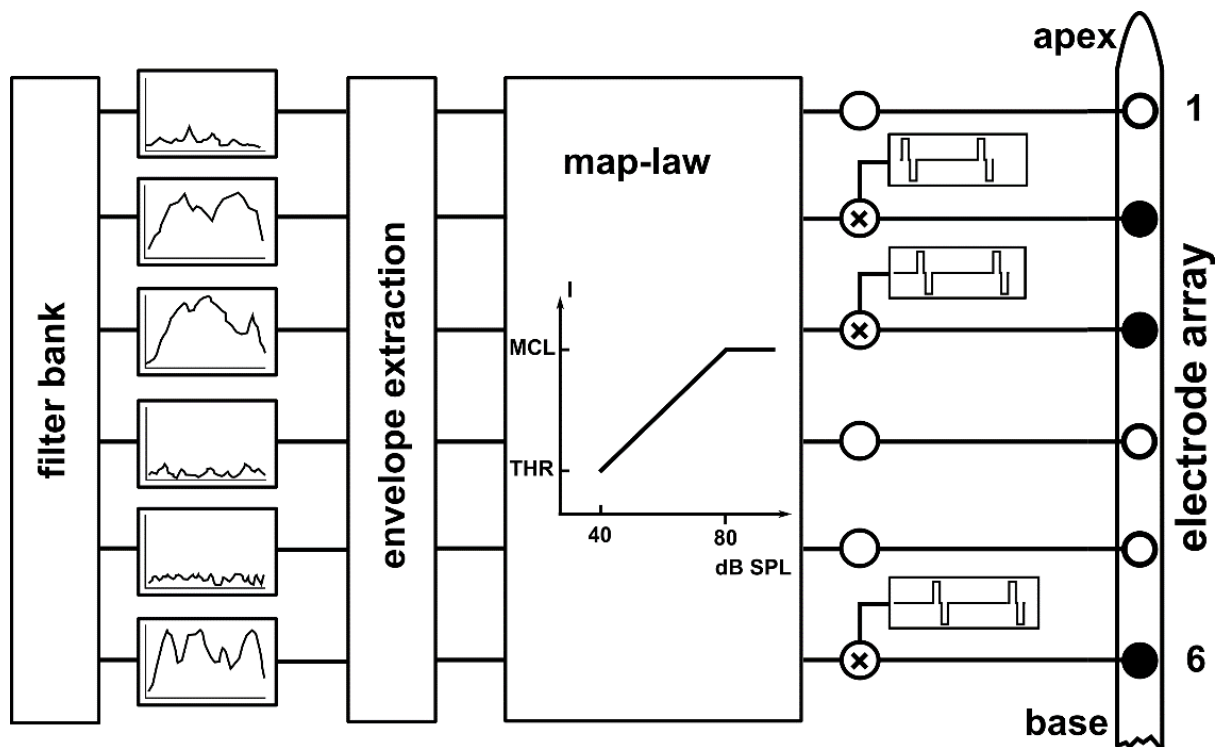


Figure 1.4 Schematic presentation of *n-of-m* strategies (e.g. ACE). Filter outputs with the highest amplitude are with electric pulses and delivered to the electrodes (here electrodes 2, 3, and 6). The remaining channels are not used during this cycle, as they had lower amplitudes.

Introduction

1.4 THR determination

Determination of THRs for recipients with proper communication skills is straightforward and there are several methods to do so. Basic and traditional methods are the method of limits, e.g. the modified Hughson-Westlake procedure (Carhart and Jerger 1959) and the method of adjustment. In the method of adjustment, the listener adjusts the intensities so that the signal is just audible. Since employing this method requires experience and is more prone for unexpected harmful events, it is less common in clinical routines. There are other clinically applicable methods for setting the THRs in CI users such as ‘count THR estimation’ (Skinner *et al.* 1995), categorical loudness scaling (explained in section 1.2.1), ‘interval choice’ (Van Wieringen and Wouters 2001), and the ‘percT’ method (Rader *et al.* 2018). In ‘count THR estimation’, which is also known as ‘count the pulses/beeps’, the THR is the level at which the listener counts the right number of pulses, which are presented with different amplitudes, in three different sets. In the ‘choose the interval’ method, users determine the interval (out of 4) in which a pulse train is played. Van Wieringen and Wouters (2001) reported generally higher detection THRs for the ‘count the pulses’ compared to ‘choose the interval’ method and suggested the latter to be used for research purposes. The ‘percT’ (Rader *et al.* 2018) is based on a gradual adaptive procedure in which two stimuli with different levels ($\Delta L = 10, 6, \text{ or } 3 \text{ CU}$ in a rough to precise manner) are presented to the listener, who should determine whether none, exactly one, or the two of the stimuli was/were perceived. The ‘precise’ THR was determined at the point where exactly one stimulus was perceived by the listener, and the THR value being the average of the two stimuli.

Although it is feasible to establish the T-levels in most children with traditional methods, such as behavioral observation audiometry or visual reinforcement audiometry, it is still challenging and sometimes impossible to measure the THR levels with psychophysical procedures.

Alternative methods for such conditions are objective measurements, where the listener does not need to actively cooperate in the THR determination procedure. These objective measures are usually neural rhythms recorded at a location from peripheral to the central auditory pathway. Here we briefly review the most common objective measurements in CI studies: electrically-evoked compound action potentials (eCAP), electrically-evoked auditory brainstem responses (eABR), electrically-evoked auditory steady state responses (eASSR), and cortical auditory evoked potentials (CAEP).

1.5 Electrically-evoked compound action potentials (eCAP)

eCAPs are the measures of the activation of the auditory nerve in the cochlea. Measurement of eCAPs is provided by the neural response telemetry (NRT¹) systems embedded in the CI hardware. The same electrodes which are normally used to deliver electric current to the

¹ The term neural response telemetry (NRT) is specifically used by Cochlear. The equivalent telemetry systems for Advanced Bionics and Med-El are referred to as neural response imaging (NRI) and auditory nerve response telemetry (ART), respectively.

auditory nerves now read back the intracochlear potentials shortly after the stimulation. eCAPs are relatively robust responses and are less muscle artifact prone (Miller *et al.* 2000), when compared to e.g. eABRs. Due to close vicinity of electrode and nerves, as well as relatively short latencies, eCAPs can be easily contaminated with the stimulation artifacts. Different methods have been proposed to suppress the stimulation artifact in eCAP measurements. One employs stimuli with alternating polarities, as shown in the left column of **Figure 1.5**. Equal numbers of responses to multiple biphasic pulses of each leading-polarity (i.e. cathodic-first or anodic-first) are averaged. With the assumption of linearity, averaging in the time-domain suppresses the electrical artifact drastically. In the alternating polarity method, it is assumed that physiological responses to both polarities are identical, thus averaging them would not influence the eCAP signal. This assumption is, however, under question, as research suggests that cat and guinea pig (Miller *et al.* 1998), as well as human (Frijns *et al.* 2002; Baudhuin *et al.* 2016) auditory nerve responses are polarity sensitive, with cat and guinea pig nerves being more sensitive to the cathodic phase and human nerves being more sensitive to anodic phase of the pulses (Macherey *et al.* 2006; Undurraga *et al.* 2013).

A second method to reduce the stimulation artifact is referred to as subthreshold template (Miller *et al.* (1998); middle panel in **Figure 1.5**). First, a stimulation artifact template is measured using a subthreshold stimulation, which assumes that no neural activity exists in the response. The response to the subthreshold stimulus is then scaled to that of a suprathreshold stimulation to match the amplitude of the latter. The scaled response is then subtracted from the suprathreshold response in order to eliminate the stimulation artifact. An alternative to the subthreshold template is the forward masking paradigm, proposed by Brown *et al.* (1990). As shown in the right panel of **Figure 1.5**, the method utilizes a series of probe-only (sequence A), masker-only (sequence B), masker-probe stimuli (sequence C), and a zero-amplitude template (sequence D) to suppress the stimulation artifact. Responses to probe-only and masker-only stimuli contain neural activity and stimulation artifact. For masker-probe stimuli (sequence B), the response to the masker pulse contains neural activity and the stimulation artifact, while the probe pulse is assumed to contain only the stimulation artifact and no neural responses as with a sufficiently short masker-probe interval, the neural population would be in its refractory period due to the response to the masker pulse (Brown *et al.* 1990).

eCAP show a biphasic-like morphology in 80% of measurable conditions in human: a trough (negative peak; N1) which occurs around 0.2-0.4 ms after stimulus onset, followed by a positive peak (P2) within 0.6-0.8 ms (Brown *et al.* 1990; Abbas *et al.* 1999). eCAPs are assumed to be a robust measure, as their amplitude is relatively large (up to 2 mV). Because they are recorded inside the cochlea and not on the skin, the contamination by myogenic activity is smaller compared to eABRs, ASSRs and CAEPs. On the other hand, since eCAPs are a peripheral neural measure, in contrast to a central measure such as CAEP, they are not affected by maturation of the central auditory system (see Sharma *et al.* (2002)). However, the peak amplitude and latency of eCAPs can be influenced by many factors, e.g. stimulation amplitude (see Brown *et al.* (1990); Kim *et al.* (2010)), inter-phase gap (IPG) and phase duration (PD; for instance Prado-Guitierrez *et al.* (2006); Ramekers *et al.* (2014)), electrode distance from the

Introduction

nerves, location of stimulation (basal vs. apical; see for example (Frijns *et al.* 2002; Polak *et al.* 2004; Tejani *et al.* 2017)), polarity of stimulation pulses (e.g. Macherey *et al.* (2006); Undurraga *et al.* (2013); Baudhuin *et al.* (2016)). eCAP amplitudes and latency changes in response to these factors could shed light on CI performance and the health state of the auditory nerve. More details on this will be presented in Chapter 2.

1.6 Electrically-evoked auditory brainstem response (eABR)

eABRs are evoked potentials elicited from the auditory brainstem and are counterparts for the auditory brainstem responses (ABRs) in normal hearing listeners. eABRs can be recorded using surface electrodes and are normally evaluated with a series of waves named from eI to eV as a function of their latencies ('e' denotes electrically evoked), each represents neural activities of auditory periphery and brainstem nuclei in a bottom-up direction. The first eABR recordings date back to the late 1980's, when Starr and Brackmann (1979) recorded eABRs from three CI users. They found reproducible waves eIII and eV for both positive- and negative-leading pulses. eABR measurements with poor reliability were reported by Chouard *et al.* (1979), who use round window electrodes, and Simmons *et al.* (1984), who observed considerable eABR variations between trials and reported different morphologies from the conventional ABRs.

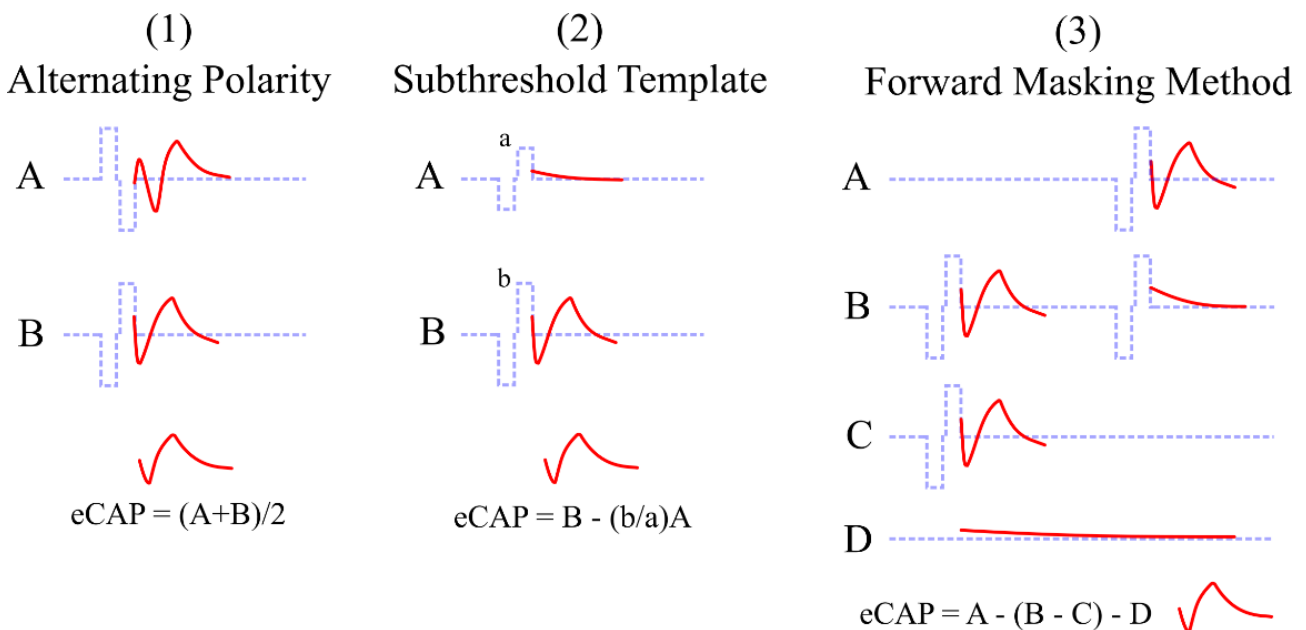


Figure 1.5 Schematic illustration of three common methods to reduce artifact stimulation in calculation of eCAPs.

Particularly, the amplitudes and absolute- and relative latencies of eABR waves are of interests for researchers and clinicians. eABR studies usually investigate wave eIII and eV as they have higher amplitudes and show more robustness against the electrical stimulation artifacts induced by the CI. Although ABRs and eABRs share characteristics such as morphology and amplitude range (Starr and Brackmann 1979; Miyamoto 1986), they differ in some aspects. Due to the electrical stimulation used for eABR measurements, compared to the acoustic stimuli used in ABRs, eABRs are more sensitive to the stimulation artifacts and myogenic activity (van den Honert and Stypulkowski 1986). Due to the absence of the mechanical traveling wave propagation, OHC and IHC transduction, and synaptic activation in CI users, eABR wave latencies tend to be shorter by about 1.0 to 2.5 ms compared to those in ABRs (Starr and Brackmann 1979; Shallop *et al.* 1990; Hodges *et al.* 1994; Truy *et al.* 1998). **Figure 1.6** shows examples of ABRs of a normal hearing individual and eABRs of a CI recipient for low, medium and high stimulation amplitudes. Response amplitudes increased as a function of electric and acoustic stimulation amplitude in ABR and eABR, respectively. This is referred to as amplitude growth function (AGF).

Latencies of eABR waves are reported to be independent form the stimulation level (van den Honert and Stypulkowski 1986), which differs from those in ABRs, where higher stimulation levels result in waves with shorter latencies. As shown in **Figure 1.6A**, ABR wave III and V occurred at around 4.5 and 6.5 ms after the acoustic stimulus onset, respectively, while their electrical counterpart appeared already at latencies of 2.0 and 3.5 ms, respectively. Yet, it is observed that eABR latencies are influenced by the stimulation site of the cochlea. Shallop *et al.* (1990), Miller *et al.* (1993), and Lundin *et al.* (2015) observed shorter latencies at more apical regions of the human cochlea, but in guinea pigs, the two former studies observed shorter latencies of wave I and III at the basal sites.

Animal studies showed that eABR characteristics such as input-output function or IPG effect, could indicate the anatomical survival/degradation of neural elements within the cochlea (Walsh and Leake-Jones 1982; Black *et al.* 1983; Smith and Simmons 1983; Prado-Guitierrez *et al.* 2006). Extended to human, associations between eABR characteristics and speech recognition (Gallégo *et al.* 1997; Kileny *et al.* 1997; Gallégo *et al.* 1998; Danieli *et al.* 2021), auditory neuropathy (Hosoya *et al.* 2018), distribution of neuronal tissue (Yamazaki *et al.* 2014), and developmental plasticity (Gordon *et al.* 2003), were reported.

In earlier times, eABRs were widely used for pre-, intra- and postoperative applications in cochlear implantation. It is important to ascertain the effectiveness of cochlear implantation before performing the surgery. This possibly also avoids implantations that may end with irresponsiveness to electrical stimulation (Kileny *et al.* 1997). On the other hand, assessing the functionality of cochlear or brainstem implants during implantation, as well as appropriate initial configuration of THR and upper limits could be facilitated by utilizing eABRs (Anwar *et al.* 2017). However, introducing neural response telemetry systems by CI manufacturers in their devices has faded such applications of eABRs away (Brown 2003). As such telemetry systems can provide eCAPs with much less time and cooperative efforts, applications of eABRs

Introduction

have been shifted to other directions. Yet, in conditions such as auditory neuropathy (Walton *et al.* 2008; Jeon *et al.* 2013; Hosoya *et al.* 2018), inner ear malformation (Kim *et al.* 2008; Yamazaki *et al.* 2014; Lundin *et al.* 2015), absence of eCAPs, and conditions with auditory brainstem implants (Anwar *et al.* 2017), which might be related to auditory neuropathy, one would prefer to employ eABRs instead of/in conjunction with eCAPs. Studies that investigated the relation between eABR characteristics and postoperative CI performance have revealed contrary results. While, for instance, Gallégo *et al.* (1997) and (1998), Wang *et al.* (2015), and Walton *et al.* (2008) reported correlations between speech intelligibility and eABR parameters, other studies such as Abbas and Brown (1991), Makhdoum *et al.* (1998), Firszt *et al.* (2002), and Lundin *et al.* (2015) found no significant correlations between eABR parameters and speech outcomes. Brown (2003) suggested that, as there exists no correlation between the acoustic ABRs and speech performance in normal hearing, one should not expect strong correlations between those in CI users.

1.7 Cortical auditory evoked potentials (CAEPs)

CAEPs are potentials elicited from neural activity of the auditory cortex. Similar to eCAPs and eABRs, CAEPs are described by a set of positive (P) and negative (N) extrema. CAEPs of adults normally consist of successive P1, N1, and P2 waves, which occur 50, 100, and 175 ms after acoustic/electric stimulus onset, respectively (Davis 1965). CAEPs exist regardless of the state of the listener being attentive/ inattentive to the stimuli, or even sleep (Van Dun *et al.* 2015). However, the amplitude and morphology of CAEPs may change drastically during different stages of sleep (Davis 1965; Colrain and Campbell 2007). The applicability of CAEPs for the determination of THR in CI users will be discussed in chapter 2.3.3.

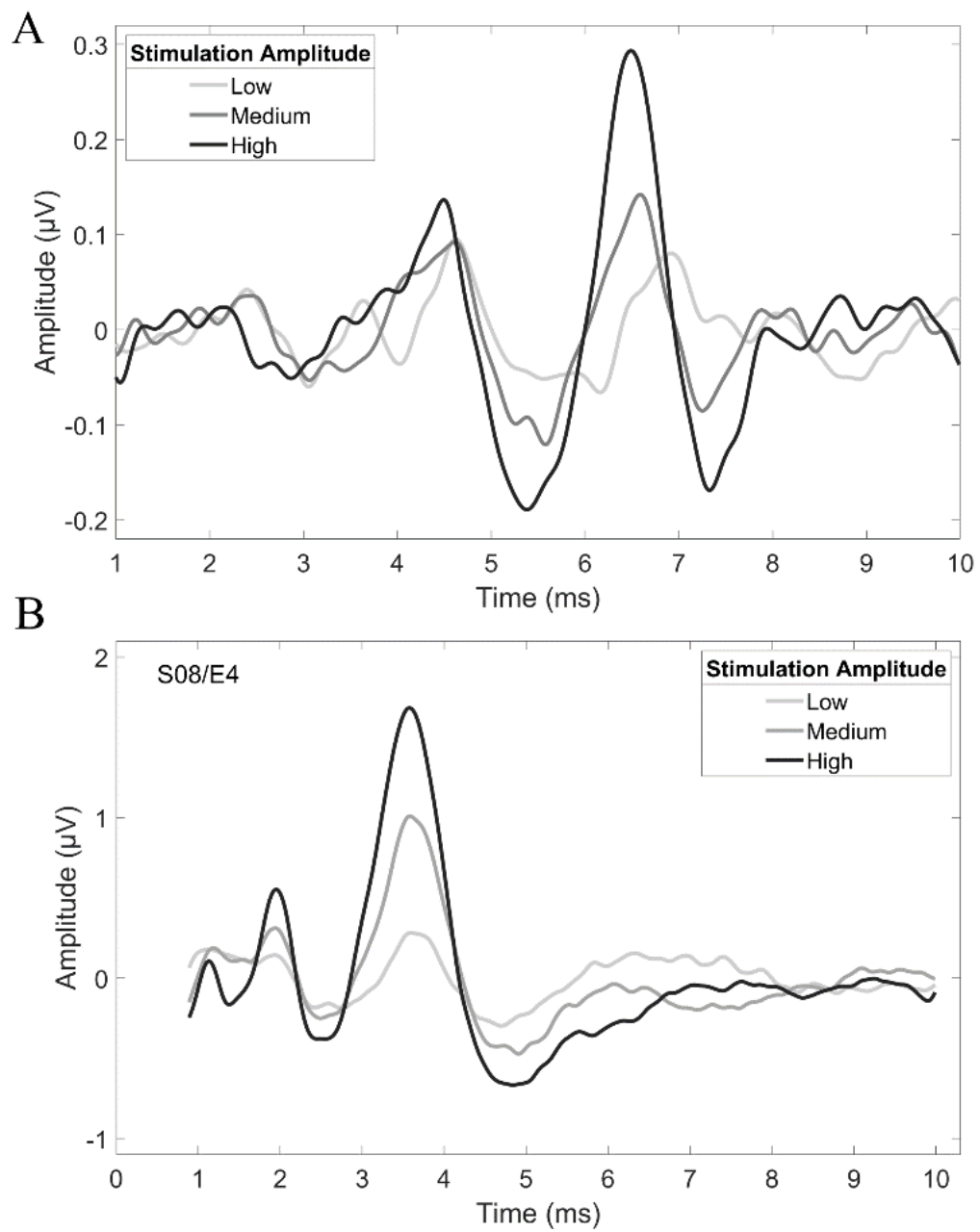


Figure 1.6 Sample ABR (A) and eABR (B) signals in response to low, medium, and high stimulation amplitudes.

Chapter 2

Fundamentals and a Brief Literature

Overview

In this chapter, fundamentals of temporal response properties of auditory nerve fibers will be presented. Then, a brief summary of temporal- and multi-pulse integration in normal- and electric hearing will be discussed. In the end, the literature investigated objective THR determination in CI users will be reviewed. More details on the latter can be found in the introduction sections of the two research papers available in chapters 3 and 4.

As stated in Chapter 1, the outcomes of speech understanding as a function of stimulation rate have been reported to be highly subject-dependent. While some CI wearers prefer high single-channel stimulation rates above 1700 pps (Verschuur 2005; Nie *et al.* 2006), other CI users benefit more from stimulation rates below 1200 pps (Vandali *et al.* 2000; Balkany *et al.* 2007; Wolfe and Schafer 2014). The reasons for such a large variation is not clear to CI researchers. The interaction between auditory nerve fibers and electrical stimulation at high stimulation rates seems to be more complicated compared to that at low to moderate rates (Boulet *et al.* 2016). In order to gain a better insight, it is worthwhile to review first the most important temporal response phenomena which occur when the spiral ganglion neurons (SGNs) are stimulated with electric pulses.

As Boulet *et al.* (2016) reviewed, there exist four stimulus-response phenomena in most of the excitable cells: refractoriness, temporal summation, accommodation, and spike-rate adaptation. While at low stimulation rates, some of these phenomena might be absent, the firing patterns at high rates are influenced not only by the separate effects of these factors, but they also interact.

2.1.1 Refractoriness

Refractoriness is known since over a decade, and is defined as the diminished/reduced sensitivity of a neuron immediately after firing in response to an excitation. Within a short enough post-stimulation duration, the neuron completely loses its ability to respond to a second pulse, which is referred to as the absolute refractory period (ARP). During that period, regardless of the magnitude of the second pulse, no more action potential can be elicited from the neuron. After a longer post-stimulation duration, the nerve gradually recovers from the absolute refractoriness and enters into the so-called relative refractory period (RRP), where with an elevated firing threshold (suprathreshold stimulation amplitude), the nerve can elicit another AP in response to a stimulus. **Figure 2.1A**

schematically illustrates refractoriness, where the gray curves represent stimuli and black ones show the responses. The dominant effects of the ARP are suggested to be the inactivation of Na⁺ channels and the high conductance of K⁺ channels, while for RRP, only being the inactivation of Na⁺ channels (Boulet *et al.* 2016). Data from cat shows the ARP of 0.33 ms, while being 2-4 ms for the RRP (Miller *et al.* 2001). However, Cartee *et al.* (2000) found RRP of 0.70 ms from cat data, and while not explicitly mentioning the ARP, refractory function fit to their data showed ARP of 2-3 ms. Boulet *et al.* (2016) suggests that extraction of refractory-related parameters is difficult due to reasons such as the sensitivity of parameters to the number of data points in the averaging pool, initial guesses made for parameters, and constraints introduced to the fitting process.

Reduced excitability of a neuron as a result of refractoriness introduces limitations to the rates with which the neuron can fire. Considering durations of 0.33 and 4 ms for ARP and RRP, respectively, maximum firing rates of around 3000 and 250 Hz for absolute and relative refractions can be expected. The 3000 Hz limitation is especially important for CI stimulation as it could also restrict the maximum stimulation rate per channel. However, it should be noted, that when dealing with CI stimulation, the whole nerve, rather than a single neuron, is involved. Therefore, if a single neuron is in its refractory state, this does not imply a reduction in the excitability of other neurons (Botros and Psarros 2010). Given this, Botros and Psarros (2010) suggested that eCAP recovery functions do not reflect refractory properties at the level of a single neuron, but instead, expresses the refractoriness of the whole nerve.

2.1.2 Temporal summation (facilitation)

The presence of a second subthreshold pulse following a first one can further charge a neuron and change its sensitivity. For inter-pulse-intervals (IPIs) up to 300 μ s, the excitability of neurons increases due to the membrane charge which remained from the first subthreshold pulse (**Figure 2.1B**). Using data from nerve fibers of different animals, Cartee *et al.* (2000) expressed the summation threshold as an exponential function of ISI with a summation time constant of 147 μ s, where shorter ISIs ‘facilitated’ eliciting an AP. While Dynes (1996); Cartee *et al.* (2000); (2006) investigated facilitation effects of a single probe pulse in animals, Heffer *et al.* (2010) studied the effects of facilitation provided by multi-pulse stimulation of rates between 200 and 5000 pps, also in animals. They observed decreased THRs as a function of number of pulses (or equivalently stimulation rate, given the fixed 2-ms stimulation duration), which was attributed to the facilitation effect of pulsatile stimulation.

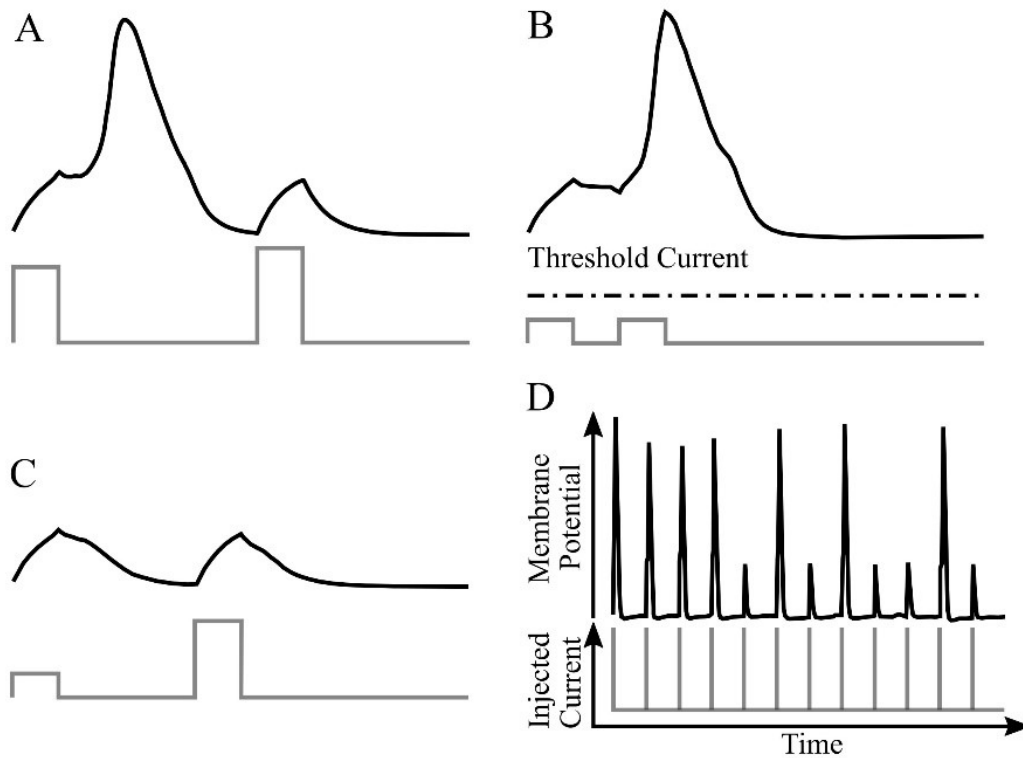


Figure 2.1 Temporal response properties of stimulus-response phenomena in auditory nerve fiber. (A): Refractoriness, (B): facilitation (temporal summation), (C) accommodation (subthreshold adaptation), and (D): spike-rate adaptation. The gray curves represent stimuli and the black ones show nerve responses. Figure adapted and modified from Boulet *et al.* (2016).

In a psychophysical human CI study, Karg *et al.* (2013) found facilitation effects for IPIs up to 600 μ s for biphasic pulses. They also investigated the effects of pulse polarity on the degree of facilitation by varying the polarities of the first and second probe pulse. Strongest facilitation effects occurred when the second phase of the masker pulse and the first phase of the probe pulse were identical, that means, the polarity of the second pulse was inverted. Using eCAP measurements, Tabibi *et al.* (2019) measured recovery facilitation effects in CI users. Although not directly mentioned in their study, they found summation time constants in the range of about 100 to 140 μ s, which are comparable to the ones reported in Cartee *et al.* (2000). A positive correlation between the eCAP AGF slope and facilitation magnitude was found, which implies that stronger facilitations might indicate better neural survival in CI users. Similarly, Tabibi *et al.* (2020) have found high correlation between the facilitation amplitude and time constants and the speech understanding outcomes. Results from Tabibi *et al.* (2020) also showed that facilitation shows stronger effects on the speech recognition performance of CI users, compared to other temporal response phenomena.

2.1.3 Accommodation

When the ISI between the masker and probe pulses exceeds a certain duration (between 1 and 5 ms to 10 ms, Dynes (1996) and Boulet *et al.* (2016)), the ability of the neuron to fire in response to the probe pulse decreases. This is schematically illustrated in **Figure 2.1C**, where the probe pulse, even having a larger amplitude than the first pulse, could not make the neuron fire an AP. The underlying mechanism responsible for accommodation is attributed to the hyperpolarization-activated cyclic nucleotide-gated (HCN) channels of the nerve fiber (Liu *et al.* 2014; Negm and Bruce 2014). Long after a subthreshold pulse, the neural excitability to respond to a second pulse decreases as the membrane potential has dropped below resting membrane potential.

2.1.4 Spike-rate adaptation

Spike rate adaptation is referred to as the tendency of a neuron to reduce its excitability after an initial response to stimuli with extended-durations. The time course within which spike-rate adaptation occurs covers a range of a few tens of milliseconds (Heffer *et al.* 2010; Miller *et al.* 2011; Hughes *et al.* 2012) up to 1-2 minutes (Litvak *et al.* 2003). **Figure 2.1D** shows how a neuron adapts in a high stimulation rate paradigm. In the beginning, the neuron spikes following the rate of the stimulus, but then its firing probability decreases. The degree of spike-rate adaptation is typically quantified by the difference/ratio between the maximum and minimum of the spike rate and is thought to depend on the stimulation rate, with bigger adaptation effects at higher rates (Zhang *et al.* 2007; Miller *et al.* 2008; Hughes *et al.* 2012). Such an increase at high rates has been suggested to be associated with desynchronization effects in a population of fibers (Rubinstein *et al.* 1999; Hughes *et al.* 2012). In a CI eCAP study, Hughes *et al.* (2012) extracted eCAP responses to each of the 21 stimulation pulses at rates between 900 and 3500 pps. For slower rates, they observed a ‘zig-zag’ pattern in the eCAP amplitudes, which was attributed to the refractoriness of the nerve fibers. This alternating pattern diminished at higher rates, suggesting stronger desynchronization effects of ANFs. The rate at which the zig-zag pattern disappeared was referred to as the ‘stochastic’ rate (Rubinstein *et al.* 1999; Hughes *et al.* 2012), where the refractory state of the neural population started to change from a two-pool paradigm (responsible for the dents of the zig-zag pattern) to a multi-pool paradigm with equal size (Rubinstein *et al.* 1999). Such a behavior of ANFs is similar to the spontaneous activity observed in the nerves of normal hearing listeners, and thus might be able to provide a better temporal representation (Rubinstein *et al.* 1999) and therefore improved transmission of information at very high stimulation rates (Hughes *et al.* 2012).

2.2 Temporal and multi-pulse integration

In the context of hearing, temporal integration (TI) is attributed to the observation that THRs increase when stimulation durations are reduced below about 200 ms. It is also

Fundamentals and a Brief Literature Overview

extended to suprathreshold levels, where longer stimuli, compared to shorter ones, need smaller amplitudes to induce an equal loudness. The amount of TI is normally quantified by the slope of detection THR reduction per decade or doubling the duration. For normal hearing listeners, TI is found to be about 8-10 dB when the stimulation duration is increased by a factor of ten (Florentine *et al.* 1988), which is approximately equivalent to a reduction of 2.5 dB/doubling the duration for durations up to 300 ms (Gerken *et al.* 1990; Zhou *et al.* 2015). For longer stimulation durations, the slope of TI becomes shallower, which implies the existence of a *critical duration*.

In a human CI study, Obando Leitón (2019) measured TI functions at a typical clinical rate of 1200 pps and a very high rate of 25000 pps, and for durations up to 1000 ms. For the higher rate, the TI slope was steeper than that for the lower rate. Compared to the critical duration of 200 ms in normal hearing (NH), no consistent critical duration was found for CI users in their study. For durations up to 100 ms, the TI functions were clearly decreasing, thereafter the inter-subject and inter-electrode differences started to become large. For the decreasing part of TI function, a median slope of -2.90 dB/doubling the number of pulses was observed, which is comparable with that for NH listeners, e.g. ~ -2.5 dB/doubling the stimulus duration, summarized by (Gerken *et al.* 1990). In an attempt to mimic the stimulation paradigm used in MED-EL devices, Obando Leitón (2019) also investigated TI effects at the rates of 1500 and 18000 pps. The former is the rate at which single electrodes of MED-EL arrays deliver the currents, and given 12 electrodes in the array, the latter is the maximum global rate induced by all electrodes. Similarly, a shallower TI slope of -1.03 dB/doubling the duration was observed, compared to steeper slope of -1.65 dB/doubling, at 18000 pps.

Due to the pulsatile stimulation used in electric hearing, the term TI is used in conjunction with a specific term known as multi-pulse integration (MPI) in electric hearing. TI effects are usually studied by investigating the effect of stimulation duration while keeping the rate fixed, while in MPI, duration is fixed and the effects are investigated as a function of stimulation rate. Carlyon *et al.* (2015) suggested that at higher stimulation rates, the *number*, *rate*, and *probability* of firing of ANFs increase in MPI paradigms, therefore THRs improve. At rates up to a few hundred pps, individual nerve fibers might lock to the stimulus and respond to each pulse. Thus, increasing the input rate probably also increases the *rate* of ANFs' responses. Assuming enough neurons in the ensemble, further pulses might make other nerve fibers spike; other than those already in refractory state following an early pulse. Therefore, increasing the stimulation rate could increase the *number* of fibers firing APs. Finally, in case of no neural firing following a stimulation pulse, it can still facilitate firing an AP by subsequent pulses (facilitation). In other words, higher stimulation rates, also increase the *probability* of neural spiking, eliciting an AP from partially-depolarized ANFs is facilitated by closely-spaced pulses at these rates (Middlebrooks 2004).

The effects of MPI are reported to be stronger at rates above 1000 pps, with steeper

integration slopes observed both in humans (Carlyon *et al.* 2015; Zhou *et al.* 2015) and guinea pigs (Middlebrooks 2004; Pfungst *et al.* 2011; Zhou *et al.* 2015). Middlebrooks (2004) measured THR_s at rates between 254 and 12200 pps and found that for rates below 1000 pps, the integration effects were minor and the MPI slopes were almost flat (median slope of -0.8/doubling the rate) when compared to rates above 1000 pps (median slope of ~ -2 /doubling the rate). He speculated that a smaller effect at rates < 1000 pps is due to the fact that the second pulse at these rates falls outside the integration window for a single neuron (duration ~ 1 ms), during which most of the integration effects occur.

Carlyon *et al.* (2015) investigated TI and MPI effects in users of cochlear- and auditory brainstem implants (ABI). They measured THR_s at rates of 500 and 3500 pps, and for durations from 2 to 32 ms in steps of doubling. Effects of TI were observed at both rates and for both types of implants, but at the slower rate, TI slope was steeper for ABI users, compared to CI users. However, for ABI users the slope remained almost unchanged at the higher rate, while it dropped steeper for CI recipients. The authors also measured behavioral THR_s at the rates 71, 500, 3500 pps, for durations of 40 and 400 ms. For CI users, they observed THR reductions of 3.9 dB and 7.7 dB when the rate increased from 71 to 500 pps, and from 500 to 3500 pps, respectively. For ABI users, the slope from 71 to 500 pps was shallower than that for CI users and from 500 to 3500 pps, almost no effect of MPI was observed. Although they did not measure THR_s at a larger number of rates to let one judge the MPI slopes below and above 1000 pps, the amount of reduction from 71 to 500 pps, (-1.38 dB/doubling the rate), was lower than that when the rate increased from 500 to 3500 pps (-2.75 dB/doubling the rate), all for CI users.

Given the differences between neurons of the cochlea and the brainstem, psychophysical results from Carlyon *et al.* (2015) could not identify the detailed mechanisms behind the different performances between CI and ABI users. Nonetheless, the authors speculated that such differences probably originate from mechanisms with time constants within a few milliseconds, e.g. 1 ms as suggested by (Middlebrooks 2004). Such interactions within a few milliseconds seem to be absent in ABI users, as the extra five pulses within the 2-ms window at the rate 3500 pps could not effectively contribute in THR reduction.

A more detailed review on the literature of temporal- and multi-pulse integration is provided in Chapter 3 (sections 3.1).

2.3 Objective THR_s in CI users

There exists a rich literature on measuring objective THR_s in CI users, where indirect physiological responses of subjects, without their active participation, are captured. The main purpose of such studies are usually finding relations between the THR_s estimated with objective measures and those from psychophysical responses. Objective measures cover the full auditory pathway, from the most peripheral measure being eCAP, through the measures in the midway, e.g. eABRs and evoked auditory middle latency responses

Fundamentals and a Brief Literature Overview

(eAMLRs), to the recordings from the central auditory pathway, such as CAEPs. Here a relatively short review on these objective measures used for THR determination in CI users is presented.

2.3.1 eCAP THRs

The growth function of eCAPs has been found to be correlated with human CI users' performance in speech perception by Brown *et al.* (1990); Kim *et al.* (2010), while no association between these two measures was found in studies such as (Turner *et al.* 2002). The slope of eCAP I/O functions was also found to correlate with longer hearing loss durations (Schvartz-Leyzac and Pfingst 2016) in humans as well as for neural survival or spiral ganglion cells' (SGCs) density in guinea pigs (Kang *et al.* 2010; Ramekers *et al.* 2014; Pfingst *et al.* 2015). Both in animal (Ramekers *et al.* 2014) and human studies (Schvartz-Leyzac and Pfingst 2016; Brochier *et al.* 2021), it has been observed that the effect of IPG on eCAP amplitude growth function could correlate with neural health. Increased IPG and/or phase duration would increase eCAP amplitude, while small SGC populations revealed decreased eCAP amplitudes.

Many studies have investigated the feasibility of predicting behavioral THRs using eCAP measures and almost all of them found only low to moderate correlations between these two measures (Abbas *et al.* 1999; Hughes *et al.* 2000; Dees *et al.* 2005; McKay *et al.* 2005; McKay *et al.* 2013; McKay and Smale 2017), which even deteriorates for high behavioral stimulation rates. Although eCAPs THRs are utilized together with one or two behavioral measures for initial CI THR settings in infants and young babies, eCAP still lacks enough predictive power to be used for fully objective CI programing alone. It is suggested that the poor correlation between these two measures stems, at least to some extent, is due to the different stimuli used in each (McKay *et al.* 2005). Stimuli in the former are normally single biphasic pulses, while in the latter, pulse trains with rates of at least 300 pps are used. Responses to a single pulse seems to reflect no information on the history of neurophysiological activity of the auditory nerve such as temporal summation, or spike-rate adaptation. However, stimulating with pulse trains seem to be able to do so. Therefore, in an attempt to mimic the effects of pulse trains employed for behavioral measures, pulse trains of different rates have also been used for eCAP measurements.

McKay *et al.* (2013) measured eCAPs in response to a pulse train of different rates in the range of 500 - 2400 pps. They extracted responses to each individual pulse of the first 20 pulses in the train, which were then averaged to provide a single eCAP amplitude at each rate. Although their proposed model, when fed with the average eCAP data, well predicted the behavioral THR change, individual slope of THRs could not be well predicted with individual eCAP data. They concluded that their proposed eCAP measures combined with eCAP THRs is not capable of predicting high-rate behavioral THRs with sufficient precision. In another study, McKay and Smale (2017) used two IPGs and two PDs as eCAP parameters to improve the accuracy of the prediction of behavioral THRs

with eCAP measures. They measured eCAP THR_s changes associated with these two parameters as a function of stimulation rate. They showed that inclusion of IPG and PD for the prediction of eCAP THR_s could improve the accuracy of prediction of behavioral THR_s significantly. However, they mentioned that even with incorporating eCAP parameters, eCAP measures lack sufficient predictive power to be used for totally objective programming of CIs.

2.3.2 eABR THR_s

eABRs are also reported to be useful for CI programming, i.e. in setting the THR_s and comfort levels. When using stimulation rates in the range of clinical configurations (above 500 pps), eABR THR_s showed only weak correlations with behavioral THR_s (Brown *et al.* 1999). However, for rates below 100 pps, eABRs have shown to provide high correlations with other behavioral measures (Abbas and Brown 1991; Gallégo *et al.* 1997; Truy *et al.* 1998; Brown *et al.* 1999). **Table 2.1** summarizes studies that investigated correlations between eABR THR_s and those of behavioral measures. Firszt *et al.* (1999) measured eABRs from a small group of Clarion CI users (three adults and three pediatrics). They observed that, within each group, 2 of 3 subjects had eABR THR_s within their behavioral dynamic range, while for 1 subject per group the eABR THR exceeded either the comfortable level or the upper limit. Similarly, Shallop *et al.* (1991) observed that eABR THR_s seem to be more capable of predicting comfort levels, rather than behavioral T-levels. Due to such a large overestimation, Firszt *et al.* (1999) suggested that configuring the THR levels using eABR THR_s for young children, who cannot provide reliable feedback, should be performed conservatively. Brown *et al.* (1999) performed a series of eABR measurements to investigate the relationship between eABR THR_s and behavioral THR_s. They found that, eABR THR_s overestimated the behavioral T-levels for all subjects ($r = 0.69$), the comfortable levels in half of subjects ($r = 0.54$), and the uncomfortable levels in a few subjects.

Brown *et al.* (1999) also measured behavioral THR_s in response to single pulses and pulses trains of 250-ms duration delivered at rates of 400 pps and 1000 pps, as well as eABR THR_s in response to single pulse stimulation with a rate of 13.1 pps. There was a strong correlation between eABR THR_s and behavioral THR when stimuli were single pulses ($r = 0.84$). Correlations declined when pulse trains were used, where correlations of 0.74 and 0.69 were found for 400 and 1000 pps, respectively. Brown *et al.* (1999) attributed the decline of the correlation coefficients to the high variability in subjects' temporal integration, and concluded that in order to improve the THR estimation by eABRs, a proper estimation of temporal integration is required for each individual. Similar to the rationale that McKay *et al.* (2005) provided for the poor correlation between eCAP THR_s and behavioral measures, Brown (2003) stated that the weak correlation between eABR THR_s and those used for programming CIs stem in the nature of relatively low (<60 pps) and high (>250 pps) stimulation rates used in the former and latter, respectively.

Fundamentals and a Brief Literature Overview

Table 2.1 Details of studies that investigated the eABR THR and behavioral THR.

Study	Behavioral stimulation duration (ms)	Rate at behavioral THRs (pps)	Rate at eABR THRs (pps)	Note (r: Correlation btw. the two THRs)
Shallop <i>et al.</i> (1991)	n.m.	10-14	10-14	eABR THRs were near comfort levels
Hodges <i>et al.</i> (1994)	n.m.	10	10	T-level: r = 0.89
Truy <i>et al.</i> (1998)	n.m.	300	60	T-level: r = 0.98 Perceptual threshold = $1.06 \times \text{eABR threshold} + 0.76$
Firszt <i>et al.</i> (1999)	n.m.	833	20.03	eABR THRs for two subjects exceeded comfortable levels
Brown <i>et al.</i> (1999)	250 (at 400 and 1000 pps)	Single pulse 400 1000	13.1 13.1 13.1	T-level: r = 0.84 T-level: r = 0.74 T-level: r = 0.69
Brown <i>et al.</i> (2000)	500	250	49	T-level: r = 0.83 C-level: r = 0.90
Danieli <i>et al.</i> (2021)	n.m.	500	21	T-level: r = 0.54 C-level: r = 0.74
Macherey <i>et al.</i> (2021)	419.3 - 451.3	1000	11600 - 29240	T-level over all subjects: 0.89 T-level at BUPS: 0.49 – 0.72

n.m. not mentioned.

In a similar study with those presented in the next two Chapters of this work, Macherey *et al.* (2021) measured eABRs to short-duration pulse trains with high stimulation rates (11.60 to 29.24 kpps). They used closely ‘bunched-up’ pulse stimuli (BUPS) for eABR measurements, where the number of pulses in BUPS varied from 1 to 32 with steps of two-fold. For clinical measurements (CLIN), the same configuration as in eABR measurements, but with stimulation rates of 1000 pps, was used. The estimated eABR THRs decreased as a function of number of pulses, and over all subjects and BUPS conditions, the correlation between eABR THRs and clinical THRs was quite high ($r = 0.89$). However, for individual BUPS conditions, the correlation between the two THRs varied between 0.49 and 0.72.

Macherey *et al.* (2021) found that psychophysical THRs measured at BUPS conditions were lower than those at clinical THRs, with increasing differences as the number of pulses increased. This finding was mostly contributed to counteracting temporal integration effects and refractoriness, where shorter inter-pulse gaps of BUPS tended to boost refractoriness effects and thus reduced interaction between pulses. However, the short inter-pulse gap for BUPS led to more compressed activities in the integration window (for more details, see Middlebrooks (2004)), when compared to that for stimuli used to measure clinical THRs. Macherey *et al.* (2021) concluded that their measurements considered only the effects of refractoriness and temporal integration, but more complex

interactions between other temporal response properties such as facilitation, accommodation and spike-rate adaptation could also play important roles.

2.3.3 CAEP THR_s

The use of CAEPs to estimate behavioral THR_s dates back to the 1950s, (Perl *et al.* 1953; Davis 1965), and has continued until recently (Abbas and Brown 2015; Visram *et al.* 2015; Mao *et al.* 2019; Mao *et al.* 2021). Employing CAEPs for the determination of behavioral THR is particularly of interest as this measure represents central auditory activities, which also reflects the origins of behavioral responses. Additionally, due to late responses of CAEP, one can use longer stimuli to possibly account for temporal integration effects occurring at the cortical levels to a larger extent. In comparison to eCAPs and eABRs, CAEPs have the benefit of being more robust due to relatively larger wave amplitudes. On the other hand, the CAEPs suffer from the fact that the patient needs to remain awake and as calm as possible, which might not be easy to achieve in younger children (Van Dun *et al.* 2015).

In an early study, Davis (1965) measured CAEPs from fifty children with severe hearing loss using filtered clicks for frequencies of 300, 600, 1200, 2400, and 4800 Hz and related the CAEP THR_s to their corresponding behavioral THR_s. On average, he found a difference of 2.5 dB between the two THR_s, while for two children, average errors of more than 18 dB was found for all frequencies tested. Picton (2011) has summarized studies between 1967 and 2007 that investigated behavioral THR estimation using CAEPs (late auditory evoked potentials, LAEPs in the original study) and described their results as being more accurate than expected. Some of the studies he investigated, had used cortical evoked response audiometry (CERA), thus they employed tones with durations of up to 200-ms (Prasher *et al.* 1993; Yeung and Wong 2007). However, for eCAEP purposes one can only use stimuli with durations of up to 60 ms to avoid overlap of response and stimulation artifact.

In a series of studies, McKay and her colleagues measured CAEP THR_s in normal hearing (Mao *et al.* 2018; Mao *et al.* 2021) and CI listeners (Visram *et al.* 2015; Mao *et al.* 2019; Mao *et al.* 2021) and correlated them with the behavioral THR_s. The stimuli they used in all of these studies were 50-ms pulse trains delivered at a rate of 900 pps. They extrapolated the growth functions of different temporal- and spectral features to estimate behavioral THR_s. Visram *et al.* (2015) employed growth functions of the global field power (GFP) of responses, which is a measure of variation over all EEG channels and estimated CAEP THR_s and found a high correlation of 0.93 between the two THR_s. They correlated the THR_s in response to 50-ms stimuli used in both CAEP and behavioral measurements and claimed that their method would also well predict behavioral THR_s in response to stimuli with higher durations (e.g. 500 ms), which are used to determine THR_s in clinical configurations. Their rationale for such a speculation was that first, longer stimulus duration results in lower THR_s, and second, THR_s determined with clinical methods are usually higher than those obtained by the three-interval three-alternative

Fundamentals and a Brief Literature Overview

forced choice method. Therefore, the higher offset of THR_s obtained by 50-ms (compared to 500-ms) stimuli could be compensated by the typical lower THR_s determined by the 3-IFC method. However, their speculation still needs to be further investigated.

In a study with normal hearing subjects, Mao *et al.* (2018) used growth functions of four features to estimate objective hearing THR_s in response to 1-kHz pure tones. The features were N1-P2 amplitude, root-mean-square value (temporal features), peak spectral power (spectral feature) and the peak of the phase-locking value (peak PLV, tempo-spectral feature), among which the peak PLV performed best with mean THR deviation of 2.7 ± 5.9 dB from the behavioral estimates. Therefore, they conducted a follow-up study with CI users and estimated the behavioral THR_s using only the peak PLV feature, where they found a strong correlation of $r = 0.979$ between the two measures (Mao *et al.* 2019). Mao *et al.* (2021) extended their investigation to use spectral features to decode intensity and threshold percepts in normal- and electric hearing modalities. They extracted Fourier magnitude- and phase-related features referred to as event-related spectral perturbations (ERSPs) and inter-trial coherence (ITC), respectively, and correlated them with the stimulus intensity. The linear discriminant analysis classifiers showed that, at low stimulation intensities and in both hearing modalities, using ITC features for training yielded more mutual information (better performance) compared to conditions where the ERSP features were used. They concluded that ITC features are more sensitive than the ERSP features, and therefore, are more suitable for behavioral THR estimation.

2.4 Objectives of this thesis

The main hypothesis of this thesis is that the low correlations between objective THR_s, particularly eABR THR_s, and behavioral ones originate, at least partly, due to the different stimulation/repetition rates and durations used in these measures. Compared to clinical rates, which are between 800 and 2000 pps, rates used in eABR measurements are typically limited to below 100 pps. This limitation arises from the fact that at higher rates, the stimulation artifact would interfere with the eABR characteristics e.g. wave amplitudes. Increased stimulation duration would also lead to the same condition. However, the short stimulation duration (up to 2 ms) allowed in eABR measurements still provide enough room for closely-spaced multiple pulses to be fit within such a window.

In this thesis, multi-pulses of very low inter-pulse intervals have been introduced with the aim of accounting for temporal interactions uncovered in regular eABR. The multi-pulse configuration employed in this thesis provides very high stimulation rates of 10 kpps. As the current spread in the cochlea is quite broad, the effective stimulation rate experienced by a given ANF is probably not only from the nearest electrode(s), but possibly from all electrodes, at least the ones in closest proximity. This would considerably increase the effective stimulation rate, i.e. from f_i to $N \times f_i$, where f_i is the stimulation rate for a given electrode, and N is the number of active electrodes in the array. Therefore, the effects of such a high stimulation rates could be investigated by employing the multi-pulse

stimulation (here 10 kpps).

This thesis aims therefore to investigate: 1) how do the eABRs morphology and characteristics change in response to multi-pulse stimuli at very high rates, 2) how do the amplitude growth functions change for multi-pulse stimulation, 3) how do the eABR THR estimated in MP condition change compared to those at single pulse stimulation, 4) do these THRs correlate better with clinical THRs, and 5) do eABR THRs in response to MPs allow to estimate clinical THRs with higher precision than with single pulses. Objectives 1 and 2 are addressed in Chapter 3 and objectives 3, 4, and 5 are discussed in Chapter 4.

Chapter 3

Investigation of Electrically-Evoked Auditory Brainstem Responses to Multi-Pulse Stimulation of High Frequency in Cochlear Implant Users

The content provided in this chapter was published in a previously peer-reviewed research paper¹:

Saeedi A. and Hemmert W. (2020) Investigation of Electrically Evoked Auditory Brainstem Responses to Multi-Pulse Stimulation of High Frequency in Cochlear Implant Users. *Frontiers in Neuroscience*. 14:615. doi: 10.3389/fnins.2020.00615

which is reproduced here without any content-related changes. To fit the typesetting of this document, only caption numberings of figures, tables, and formulas have been changed.

3.1 Introduction

Cochlear implants (CI) can restore hearing and speech understanding to people with severe to profound hearing loss to a surprisingly high degree by electrically stimulation of the residual auditory nerves (ANs). As the dynamic range of electric stimulation is much narrower than in the intact ear, it is necessary to set sensation thresholds and maximum stimulation levels properly. Both levels depend on the stimulation rate and on the number of pulses (or the length of the pulse train) delivered. These two parameters contribute in temporal phenomena are known as multi-pulse integration (MPI) and temporal integration (TI) functions. For a fixed (usually long) stimulation duration, the MPI function is referred to the function relating the psychophysical detection threshold (THR) with stimulation rate (McKay and McDermott 1998). The TI function describes as how the detection THR varies as a function of stimulation duration when the stimulation rate is fixed. The time range in TI functions varies from tens of milliseconds to hundreds of milliseconds with large individual variations. TI in acoustic hearing leads

¹ The paper is distributed under the terms of the Creative Commons Attribution License (CC BY), which holds its copyright with the authors.

to a THR decrease with a slope of approximately 2.5 dB per doubling of stimulus duration up to about 300 ms (Gerken *et al.* 1990).

Studies which investigated TI functions for electric hearing generally claimed that, similar to MPI functions, TI slopes drop when the stimulation duration (or equivalently, the number of pulses) increased, both in animal studies (Donaldson *et al.* 1997; Zhou *et al.* 2015) and in human studies (Zhou *et al.* 2015). Donaldson *et al.* (1997) found THR TI slopes of 0.42 dB/doubling of number of pulses, ranging from 1 to 64 pulses at 100 pps stimulation rate. Zhou *et al.* (2015) found that for a stimulation rate of 640 pps, mean TI slopes dropped about 0.88 dB/doubling of stimulation duration from 31.25 to 250 ms (20 to 160 pulses). Donaldson *et al.* (1997) found that not only THRs but also loudness levels including maximum acceptable levels (MAL) dropped when the stimulation duration increased. For MALs, they found large inter-subject variabilities of TI slopes, i.e. shallower, equally steep, and steeper TI slopes in comparison to the THR TI slopes. Obando Leitón (2019) measured TI functions for two rates in a very comprehensive study. Slopes showed a large variation between subjects but also for different electrodes within a subject. For a stimulus of 300 ms duration, slopes ranged from -5.24 dB to -2.32 dB/doubling, when stimulation rate increased from 1500 pps to 18000 pps. Over all subjects, Obando Leitón (2019) observed that increasing the stimulation rate from 1500 to 18000 pps caused THR levels to decrease by approximately 11 dB, which corresponds to a decrease of -3.1 dB/rate doubling. Obando Leitón (2019) also found that the MALs dropped by 4 dB when the stimulation rate was increased from 1500 to 18000 pps, which suggests a slope of -1.11 dB/rate doubling. Temporal integration effects between two pulses are usually quite small (Karg *et al.* 2013). Nevertheless, for long pulse trains MPI effects on THR and MAL can be large.

For low stimulation rates (below 1000 pps), THRs in CI users fall only by less than 1 dB/doubling of stimulus duration (Donaldson *et al.* 1997) when the stimulation rate is below 1000 pulses-per-second (pps). When the stimulation rate exceeds 1000 pps, the slope of the MPI function becomes steeper, in guinea pigs (Middlebrooks 2004; Kang *et al.* 2010; Zhou *et al.* 2015) and in humans (Shannon 1985; McKay and McDermott 1998; Zhou *et al.* 2012; Carlyon *et al.* 2015). As an example, Kang *et al.* (2010) found a significant decrease of MPI slopes when rates below 1000 pps increased to above 1000 pps at two stimulation sites (Δ slopes = -2.88 and -2.83 dB/doubling of pulse rate at two stimulation sites). Similarly, Carlyon *et al.* (2015) observed a THR decrease of 7.71 dB when increasing the stimulation rate from 500 to 3500 pps for pulse durations of 400 ms, which is equivalent to a slope of -2.74 dB/rate doubling. An exception was Skinner *et al.* (2000), who found MPI slope to drop by less than 0.1 dB/doubling of the pulse rate for rates above 1000 pps and even less for rates below 1000 pps. Slopes of MPI functions for C-levels are reported to be steeper for rates above 1000 pps compared to rates below 1000 pps (Zhou *et al.* 2012). In a human study, they found that MPI slopes for the C-levels were 0.65 dB, 0.54 dB, and 1.19 dB/doubling or stimulation rate steeper for rates above 1000 pps compared to rates below 1000 pps, respectively for three stimulation sites. Zhou

Investigation of Electrically-Evoked Auditory Brainstem Responses to Multi-Pulse Stimulation of High Frequency in Cochlear Implant Users

et al. (2012) observed that TI slopes for THR were steeper than those for MAL/C-levels. For basal and middle sites, MPI slopes for THR were 1.24 dB and 1.07/doubling of the rate, respectively, which were 0.59 dB and 0.53 dB steeper than their corresponding MPI slopes for C-levels. Since Zhou *et al.* (2012) found no correlation between slopes of C-level and THR MPI functions, they claimed that the underlying mechanisms of these two functions are probably different.

Middlebrooks (2004) and Zhou *et al.* (2012) attributed the steeper MPI slopes at rates above 1000 pps to a residual partial depolarization mechanism, where initial subthreshold pulses partially depolarize a single AN or a group of ANs and further pulses, accruing within a 1-ms time window, increase the chance of firing an action potential thus lowering the THR level. In terms of temporal considerations, this effect is also known as ‘facilitation’, where the elevated membrane potential of the auditory nerve, as the effect of the first pulse in the train, facilitates it for the successive pulses to elicit an action potential (Hodgkin 1938; Hodgkin and Huxley 1952; Boulet *et al.* 2016).

The slopes of MPI functions are suggested to be possibly an indicator of cochlear health in the area close to the stimulation site, either in CI users (Kang *et al.* 2010; Pfungst *et al.* 2011; Zhou *et al.* 2012; Zhou and Pfungst 2016; Zhou *et al.* 2018) or in normal hearing listeners (Shannon 1983). Psychophysical results from (Kang *et al.* 2010; Pfungst *et al.* 2011) indicated that in guinea pigs, for stimulation rates below 1000 pps, there is a correlation between the THR MPI slopes and cochlear health state in terms of hair cell counts, auditory nerves and ensemble spontaneous activity (ESA).

Electrical stimulation with high pulse rates are thought to resemble the spontaneous activity of ANFs in a healthy ear (Rubinstein *et al.* 1999; Litvak *et al.* 2003; Hughes *et al.* 2012). (Rubinstein *et al.* 1999) found that for pulse rates above 2000 pps, human electrically evoked auditory compound action potentials (eCAP) responses to a pulse train dramatically dropped after a strong response to the initial pulse of the train and sustained afterwards. They interpreted this sustained activity as an independent quasi-stochastic activity of ANFs resulting from desynchronization of populations of ANFs. For stimulation rates below 1016 pps, they still observed an alternating amplitude pattern of the eCAP for successive pulses of the train after a relatively strong initial response to the first pulse. The rate at which the alternating pattern seemed to vanish and the sustained pattern appeared, was referred to as ‘stochastic rate’ (Hughes *et al.* 2012), and occurred at rates above 2033 pps in Rubinstein *et al.* (1999). Hughes *et al.* (2012) observed that the stochastic rate was variable (about 2400 to 3500 pps) between different electrodes in human subjects. Similar to human results, Litvak *et al.* (2003) found a sustained discharge rate in cat ANFs in response to a 5000 pps pulse train. They claimed that, since no correlation between simultaneous measurements of pairs of ANF activities was found, the 5000 pps pulse rate desynchronized the auditory nerve activities, which is, again, an evidence that high stimulation rates could improve neural representation to electric stimuli.

Another motivation to use high pulse rates in electric hearing is to represent the global stimulation rate induced by stimulation rate of individual electrodes in CIs. Results of finite element model from Bai *et al.* (2019) and measurement data from Obando Leitón (2019) and many others suggest that stimulation of a single electrode contact leads to a broad spread of current along the cochlea, which means that in electric hearing, neurons are stimulated not only by the nearest electrode, but also by the neighboring electrodes. Therefore, the effective stimulation which reaches a spiral ganglion neuron – at least in the continuous interleaved stimulation (CIS) strategy – is a burst with the global stimulation rate originating from neighboring electrodes, which is very similar to our experiment.

The studies mentioned above investigated the effects of multi-pulse stimulation on either most central (psychophysical studies) or most peripheral (eCAPs or ESA) stages of the auditory system. It is still worth to investigate such an effect at a location between these two extreme regions, which, to our best knowledge, has not yet been done. Such a study will shed light on the temporal integration at the level of the auditory brainstem as well as on how temporal properties such as refractoriness and facilitation would function. Based on these foundations, we designed this study to investigate electrically evoked auditory brainstem responses (eABRs) to high rate electrical multi-pulse stimuli in CI users. We measured eABRs to the stimuli with different number of pulses, but with the same physical stimulation amplitude to see how multi-pulses are integrated in the level of the brainstem. We also evaluated the contribution of nerve responses to each pulse or to a few consecutive pulses in multi-pulse stimulation to estimate the post-stimulus time histogram (PSTH) of the nerve.

3.2 Material and Methods

Sixteen ears from twelve participants (two males, mean age: 56.5 years) implanted with Med-El CIs were measured (Table 3.1). Amplitude growth functions in MP conditions were measured from 8 ears (out of 16; last column of Table 3.1). Participants signed a written informed consent form and were paid for their participation. The experiment was approved by the Ethics Committee of the Klinikum rechts der Isar, Munich.

3.2.1 Stimuli

In this study, we mainly focused on the analysis of eABR wave eV, which usually occurs at around 4 ms after the stimulus onset. This constrains the stimulation duration to be less than 4 ms, otherwise stimulus and response would interfere. A further limitation comes from the large stimulation artifact, which follows the stimulus and limits the stimulation window to be even shorter. Therefore, in order to obtain clear eABR peaks eV, we employed a stimulation window of up to 1.6 ms, within which pulse trains of up to 16 pulses with a pulse rate of 10,000 pulses-per-second (pps) were closely packed together to form multi-pulse stimuli.

Investigation of Electrically-Evoked Auditory Brainstem Responses to Multi-Pulse Stimulation of High Frequency in Cochlear Implant Users

An overview of the stimuli is illustrated in Figure 3.1. Electric pulse trains of 1-pulse, 2-pulses, 4-pulses, 8-pulses and 16-pulses were used. Pulses were anodic-leading charge-balanced biphasic pulses with 45 μ s phase width and 2.1 μ s inter-phase gap. Multi-pulse (MP) stimuli were assembled by putting single pulses together with an inter-pulse gap of 7.9 μ s to achieve a pulse period of 100 μ s and, consequently, a burst rate of 10,000 pps, which is well above standard clinical rates. All MP stimuli were delivered at a repetition rate of 37 Hz through an electrode in the middle of the array (subject specific electrode).

3.2.2 Pretest

In order to select the stimulation electrode for the experiment, trial psychophysical and eABR measurements were performed on electrodes number 4, 5, 6, 7, and 8 (out of 12 electrodes in an apical-to-basal order). Psychophysical THR and MCLs were determined by CI users. The stimulus was a single-pulse (1 pulse condition) with the same parameters mentioned above. For each electrode in eABR measurements, the stimulation amplitude was set to 95% of the corresponding psychophysical dynamic range (DR, defined as MCL - THR). The electrode corresponding to the eABR with the largest wave eV amplitude was selected and used for the entire measurements. In case of electrodes with similar eV amplitudes, the one with larger DR was selected.

Table 3.1 Demographic information of CI subjects participated in the study.

Subject	Side	Age range (years)	Etiology	Dur. deaf (years)	CI use (years)	CI type	Electrode	Data in Figure 3.11
S1	L	50-55	Inherited OM	49	4	Co	6	Yes
S2	L, R	56-60	Congenital	56	12, 10	P, So	6, 4	Yes
S3	L, R	60-65	Unknown	22	4.5, 5	So, So	4, 6	No
S4	L, R	56-60	Unknown	56	11, 10	P, P	6, 7	Yes
S5	L, R	66-70	Unknown	27	12, 6	P, P	7, 7	No
S6	L, R	60-65	Meningitis, Unknown	32	2, 8	Sy, Co	6, 5	No
S7	L	56-60	Unknown	44	3	So	6	No
S8	L	40-45	Congenital	42	5	Co	4	Yes
S10	L	76-80	Unknown	30	20	Sy	4	No
S13	L	40-45	OM	40	3	Sy	7	Yes
S14	R	36-40	Inherited OM	31	6	Co	4	Yes

OM otitis Media; Co: Concerto; P: Pulsar; So: Sonata; Sy: Synchrony

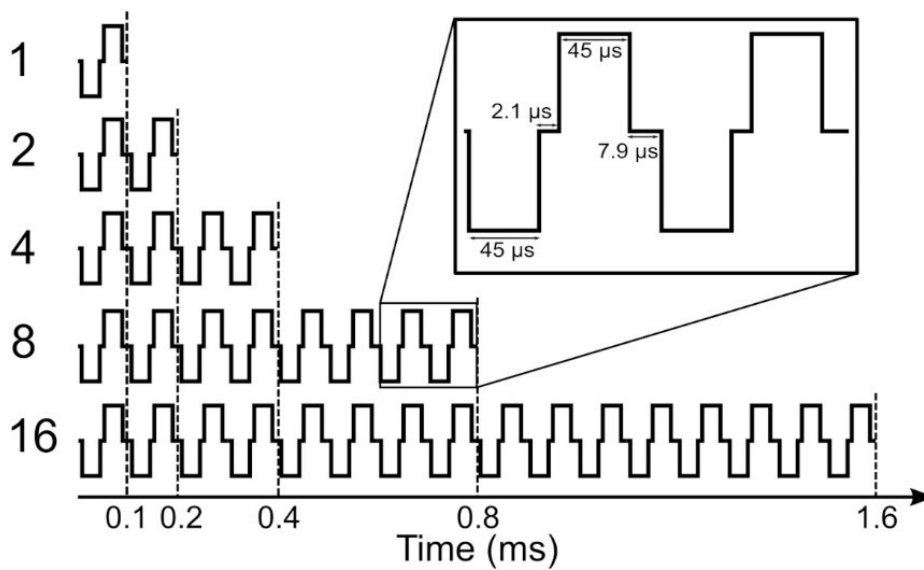


Figure 3.1 Shape of multi-pulse stimuli used in the study.

Once an electrode was determined, psychophysical thresholds (THR) and most comfortable levels (MCL) in MP conditions were adjusted by the subjects while they were seated on a comfortable coach. On a normal keyboard, the subjects used two keys (PgUp and PgDn) for coarse changes and two other keys (up arrow and down arrow) for fine changes. The procedure of adjustment was monitored by the examiners using a custom-designed graphical user interface. In order to avoid any visual biases, subjects did not see the monitor screen. The THRs and MCLs for each MP condition were measured in one trial round and two main rounds. Stimuli were presented randomly but THR and MCL were measured in separate sessions. For THRs, CI users were asked to raise the stimulation amplitude until they could clearly perceive it and then reduced it so that they could not perceive it any more. For MCL measurements, they were asked to increase the stimulation amplitude to the highest level, which they could still comfortably stand for three minutes. This duration is about three times the duration of a single eABR recording trial. Only the results of the main rounds were used for psychophysical analysis and, later, for eABR measurements. The stimuli used in psychophysical measurements were the same as those employed in eABR measurements.

3.2.3 eABR multi-pulse stimuli

We call the measured DRs in 1-, 2-, 4-, 8-, and 16-pulse conditions as DR1, DR2, DR4, DR8, and DR16, respectively. Maximum stimulation amplitudes (MSA) were always limited at 95% of the corresponding DRs to avoid very loud stimulation. They were called MSA1, MSA2, MSA4, MSA8, and MSA16 e.g. MSA4 means stimulation amplitude of 95% of DR4. An exception was subject S14R, where due to a strong artifact at 95% of DRs, 60% was used for all numbers of pulses.

Investigation of Electrically-Evoked Auditory Brainstem Responses to Multi-Pulse Stimulation of High Frequency in Cochlear Implant Users

Figure 3.2 shows a schematic view of all stimulation conditions used in this study. Different numbers of vertical bars depict the number of pulses and different bar sizes indicate stimulation amplitudes. Some conditions were not measured (n.m. in Figure 3.2) because they were above comfortable loudness. In each row of Figure 3.2, the number of pulses is constant, while the stimulation amplitude varies. Thus, row-wise investigation of the table provides amplitude growth functions (AFG) of MP conditions. On the other hand, in each column of the table, the stimulation amplitude is constant, while the number of pulses varies. Thus, investigation of the effect of number of pulses is feasible by column-wise investigation of the table. We also provide eABR amplitude growth functions (AGFs) in MP conditions from 8 ears (out of 16 ears). Stimuli with amplitudes of 5% to 95% the corresponding DRs with steps of 10% were used.

3.2.4 eABR recording

Stimulation scripts were written in MATLAB and executed on a personal computer equipped with a National Instrument (NI) I/O card. Subjects were asked to remove their speech processors before the measurements and stimuli were then generated and delivered to CIs via an external induction coil of a research interface box (RIB II), provided by the University of Innsbruck, Innsbruck, Austria.

The stimulation/recording setup is shown in Figure 3.3. The eABRs were recorded from surface electrodes glued on the skin. The positive electrode was placed behind the ear. The negative and the ground electrodes were placed on the upper and lower forehead, respectively. Raw eABRs were recorded with a Biopac® MP36 system (California, USA) with a sampling rate of 100 kHz, 24-bit A/D converter and amplifier gain of 1000. An internally-implemented hardware band-pass filter with cut-off frequencies of 0.05 Hz and 20 kHz was used in eABR measurements. No trigger signal was recorded, as the electric stimulation artifact was large enough for stimulus onset detection. For each MP condition, 2184 epochs were recorded, each of which had a duration of 27 ms.

The skin beneath electrodes was cleaned with alcohol swabs, smoothly but thoroughly scrubbed to achieve low electrode impedances. Conductive gel was used to increase the impedance match between the electrodes and the skin surfaces. Electrode impedances were controlled by the recording setup and were kept below 10 k Ω . During eABR recording, subjects were either sitting or lying on a couch. They were asked to stay as calm as possible to avoid myogenic artifacts. Breaks were taken on regular intervals or on subjects' demands.

# pulses	Stimulation amplitude				
	MSA16	MSA8	MSA4	MSA2	MSA1
1					
2					n.m.
4				n.m.	n.m.
8			n.m.	n.m.	n.m.
16		n.m.	n.m.	n.m.	n.m.

Amplitude Growth Functions

Effect of Nr. of pulses

Figure 3.2 eABR multi-pulse measurement conditions (n.m. means not measured).

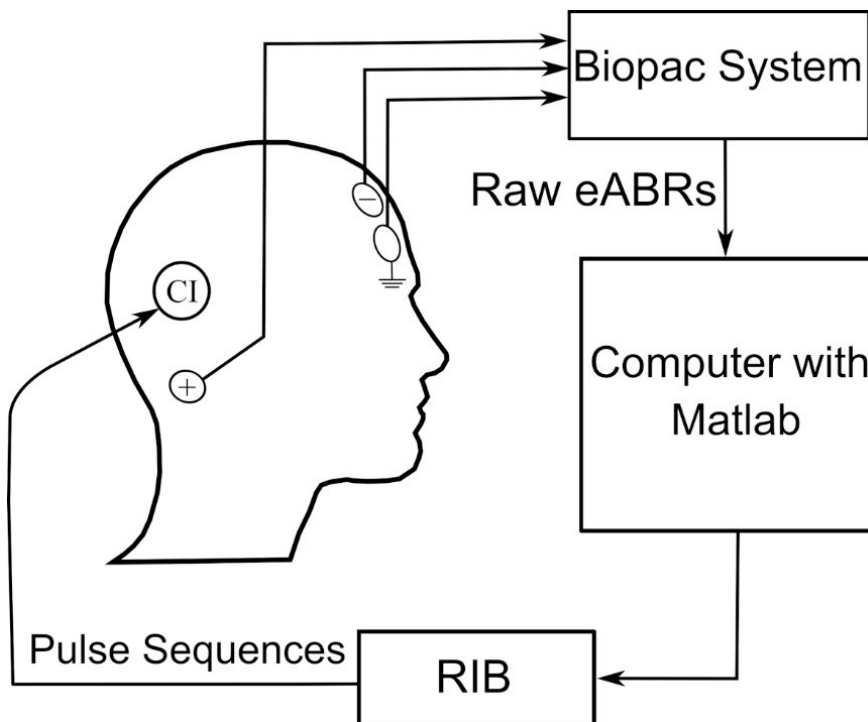


Figure 3.3 Setup for electrical stimulation via CI and eABR recording.

Investigation of Electrically-Evoked Auditory Brainstem Responses to Multi-Pulse Stimulation of High Frequency in Cochlear Implant Users

3.2.5 eABR processing

Raw eABRs were processed offline using MATLAB R2017b in a series of steps. First, stimulus onset detection was performed using the electrical stimulation artifacts (which were larger than about 300 μV). They were orders of magnitudes higher than neuronal responses (maximum of about 2.6 μV). Using onset indices, data were divided into epochs of 27 ms long. Since most of the eABR information is within the first 10 ms, epoch length were reduced to 10 ms. Epochs contaminated with myogenic activities (e.g. eye blink, facial muscle movement) were removed and only ‘clean’ epochs were used in further analysis. In order to determine the clean epochs, the distribution of the RMS values of epochs were used. For all users, the RMS value of epochs had lognormal distribution. A normal distribution was fitted to the logarithm of RMS (logRMS) value of epochs. Epochs with logRMS values in the range of $\mu \pm k\sigma$ were considered as clean epochs. The μ and σ were the mean and standard deviation of the fitted distribution, respectively. The k parameter was subject-specific and varied from 0.7 to 2. Across all subjects, at least 2053 epochs (out of 2184 epochs) remained for averaging.

The next step dealt with electrical artifact suppression. The pattern of the electrical artifacts was subject-dependent. For some subjects, one-exponential fittings worked, while for other subjects, two-exponential fittings were required (blue curves in **Figure 3.4**, compare with Spitzer *et al.* (2006)). Therefore, exponential functions with the general forms of Eqs. 3.1 and 3.2 were used to eliminate electrical artifacts. For each subject, only one function was used for curve fitting, but for each measurement condition, the fitting was performed independently. The decision of using one-exponential or two-exponentials was made by visual inspection of the discharge curve shape. The starting point of the fitting window varied since the duration of electrical artifacts varied due to different number of pulses. Therefore, this parameter was excluded from the fitting curve, as in Hu *et al.* (2015). The end point of the fitting window was always set to 10.0 ms after the stimulus onset. The fitted artifact was subtracted from the individual eABR epochs.

$$f(t) = a_0 + a_1 e^{-b_1 t} + a_2 e^{-b_2 t} \quad 3.1$$

$$f(t) = a_0 + a_1 e^{-b_1 t} \quad 3.2$$

Noise was reduced by zero-phase digital filtering (bandpass 4th order Butterworth filter, passband: 100 Hz to 3 kHz). As a final stage, weighted non-stationary fixed multi-points (WNSFMP) averaging was applied (Silva 2009). In this method the variation of multiple fixed time points in subsets of epochs is analyzed to estimate the variance of the residual noise (RN). The WNSFMP method assumes stationary noise within a subset of epochs, but still lets the noise vary within different subsets. This enables the method to eliminate the effect of non-stationary noise, and, on the other hand, to make a weighted averaging with weights being the inverse of corresponding subsets variances. The WNSFMP

method also provides post-average RN estimation, its variance ($\hat{\sigma}_{RN}^2$) is a measure of RN power. In this study, amplitude variances were estimated as $\hat{\sigma}_{amp}^2 = 2\hat{\sigma}_{RN}^2$, as in Undurraga *et al.* (2013).

Only eABR wave eV amplitudes and latencies were analyzed, as wave eIII was corrupted by the stimulation artifact, especially in the 8- and 16-pulse conditions. Wave eV amplitude was calculated as the difference of peak eV and the next trough and the latency of wave eV was defined as the time point where peak eV occurred. Only amplitudes greater than $\sqrt{2}\hat{\sigma}_{RN}$ were accepted as valid amplitudes and were used for further analysis. Exemplary final eABRs in 1-, 4-, and 8-pulse conditions are shown in Figure 3.5 for three subjects.

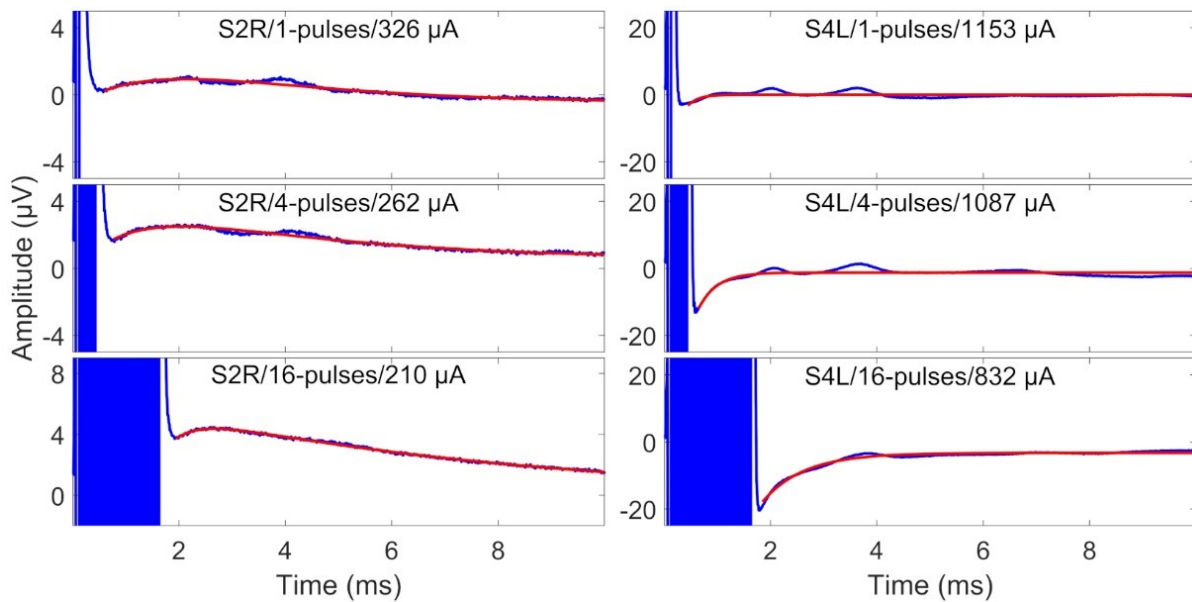


Figure 3.4 Surface electrode recordings (blue curves) and exponential fittings of stimulation artifacts (only after stimulation, red curves). Left column shows two-exponential fittings and right panels show one-exponential fittings. In each panel, the number of pulses and the stimulation amplitude is indicated. Note that the stimulation artifact exceeds the range displayed in the figure.

Investigation of Electrically-Evoked Auditory Brainstem Responses to Multi-Pulse Stimulation of High Frequency in Cochlear Implant Users

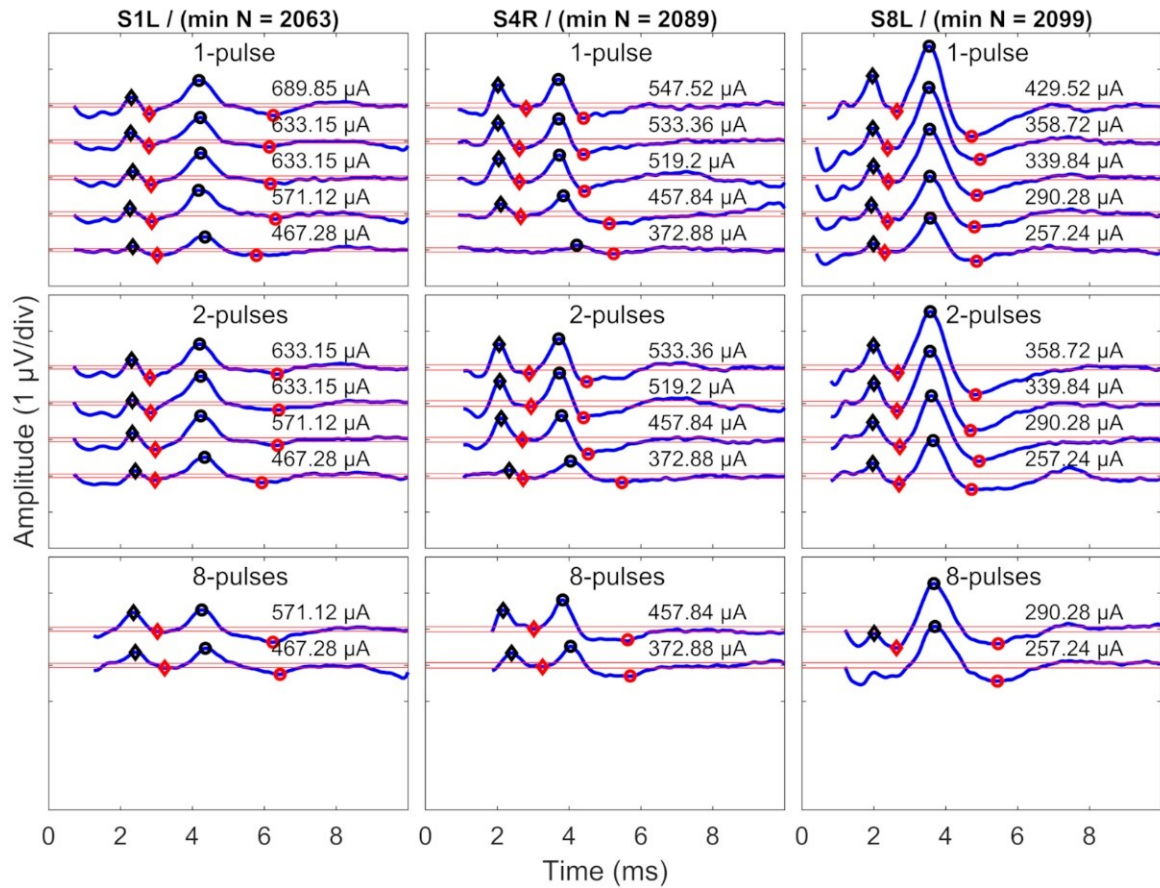


Figure 3.5 Exemplary final eABRs for three subjects (columns) in multi-pulse conditions (rows). The stimulation amplitudes and the number of pulses are indicated in each panel. Significant peaks and troughs eIII are marked with filled black and red diamonds, respectively. Peaks and troughs of eV are shown with filled black and red circles, respectively. Horizontal red lines indicate $\pm\sqrt{2}\hat{\sigma}_{RN}^2$. The minimum number of epochs used for averaging (min N) is indicated for each subject.

3.2.6 Statistical analysis

Repeated measures analysis of variance (ANOVA) was used to statistically test the effect of the number of pulses. Statistical analysis was performed in MATLAB 2017b. In psychophysical data, the within-subject variable was changes in THR and MCL, while in eABR data, the within-subject variable was changes in wave eV amplitudes. For pairwise comparisons, Bonferroni corrected post hoc analysis was applied. The statistical significance level was set to $\alpha=0.05$.

3.3 Results

3.3.1 Psychophysical results

Results of psychophysical experiments are plotted in Figure 3.6. THR and MCLs are plotted for individual subjects in Figure 3.6A with open blue and green circles, respectively. Total burst charges (TBCs) used to reach THR and MCLs, are also depicted in open circles in Figure 3.6B. The TBC was defined as overall charges in positive phases of multi-pulses. The corresponding median values of each set of the data are shown with filled symbols.

The median THR and MCLs for single pulses were 211.8 μA and 514.5 μA , respectively, which corresponds to TBCs (of the integrated positive pulse phases) of 9.4 nC and 23.1 nC, respectively. This corresponds to a dynamic range from 4.65 dB to 12.61 dB (median: 7.17 dB). With increasing number of pulses both THR levels and MCLs decreased monotonically, almost for every measurement and patient, with steeper drops for THR. The median THR levels over all subjects dropped by about 6.30 dB when the number of pulses increased from 1 to 16 pulses, whereas the decrease for MCLs was only 2.90 dB. For the analysis, linear regression was calculated for each set of data and averaged. The THR decreased with an average slope of 1.30/doubling of the number of pulses (ranged from 0.65 to 2.34 dB/doubling), while the MCLs decreased with an average slope of 0.93 dB/doubling of the number of pulses (ranged from 0.66 to 1.32 dB/doubling).

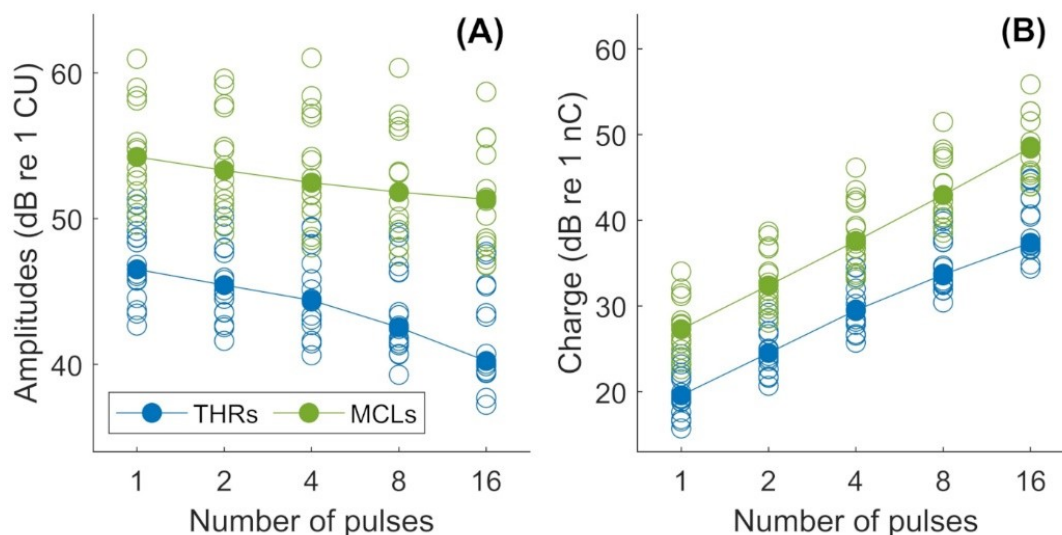


Figure 3.6 (A) Psychophysical THR and MCL currents (in dB re 1 μA) and **(B)** Total burst charge (TBC) (dB re 1 nC) for 14 subjects (19 ears). Values differed significantly between all conditions ($p < 0.05$).

Investigation of Electrically-Evoked Auditory Brainstem Responses to Multi-Pulse Stimulation of High Frequency in Cochlear Implant Users

Two-way repeated measures of ANOVA showed that THR and MCL data (amplitudes and TBCs) in Figure 3.6 dropped significantly as a function of number of pulses. In panel A, both THR and MCL decreased significantly (main effect of the number of pulse; $F(4, 112) = 176.14, p < 0.001$) when the number of pulses increased from 1 to 16. The interaction effects between THRs vs. MCLs were significant ($F(4, 112) = 5.26, p < 0.001$), which indicates a shallower slope for MCLs compared to THRs. In panel B, THR and MCL TBCs increased significantly (main effect of the number of pulse; $F(4, 112) = 3470.2, p < 0.001$) as a function of number of pulses. The interaction effects between THRs vs. MCLs were significant ($F(4, 112) = 5.26, p < 0.001$), which indicates a shallower slope for THR TBCs compared to MCL TBCs.

3.3.2 eABR results

Since eABR wave eIII was corrupted by the multi-pulse stimulation artifact especially in measuring conditions with larger number of pulses, we focused on wave eV amplitudes and latencies. Figure 3.7 and Figure 3.8 show individual eABR wave eV amplitudes and latencies for all CI subjects, respectively. Each panel consists of 15 data points (measurement conditions listed in Figure 3.2). In each panel, data points with the same color represent responses to stimuli with equal current amplitudes, but with different number of pulses. Amplitude growth functions in Figure 3.7 (reading data for identical numbers of pulses) indicate that eV amplitudes grow generally monotonously with stimulus level. Lines in a single color show how wave eV parameters depend on the number of pulses. Note that because of maximum stimulation levels mentioned earlier, measurement conditions differ in number of data points. Since wave eV amplitude was calculated by subtraction of two values (peak eV and the following trough), error bars in Figure 3.7 are equal to $2 \times \hat{\sigma}_{RN}^2$. No efforts were made to estimate error bars for latencies (Figure 3.8). Results of eABR eV amplitudes in multi-pulse conditions over all subjects are plotted in Figure 3.9. In each panel, data were normalized to (divided by) the corresponding responses at the largest number of pulses (2-, 4-, 8-, and 16-pulses in panels A-D, respectively). Data points in gray show individual CI responses to multi-pulses and the colored circles, which match the colors in Figure 3.7, are their corresponding median values. Data for MSA1 are not plotted, as all values were 1 due to normalization.

The stimulation amplitudes in MP conditions were 95% of the corresponding DRs for the longest burst. For shorter bursts, however, this stimulation amplitude was far below this value. Over all subjects, stimulation amplitudes of MSA16 (95% of DRs in 16-pulses conditions), corresponded to averages of 35%, 46%, 60%, and 74% of the DRs in 1-, 2-, 4-, and 8-pulses conditions, respectively. Similarly, stimulation amplitudes of MSA8 (95% of DRs in 8-pulses conditions) corresponded to averages of 52%, 63%, and 78% of the DRs in 1-, 2-, and 4-pulses conditions, respectively. For example, for the 1-pulse conditions, the stimulation amplitudes were at 35%, 52%, 65%, 80% and 95% of the DR (averaged over all subjects; more details are available in supplementary Figures 1 and 2). Visual inspection of the curves from individual CI subjects in Figure 3.7 shows that

inter-subject variability is high. Yet, some trends could be detected. For most subjects, and particularly in 8-pulse and 16-pulse conditions, eABR wave eV amplitudes tend to increase when the number of pulses increased from 1-pulse up to a certain number of pulses, i.e. up to 2-, 4-, or 8-pulses, then they seem to saturate or even decrease. Such an increase was not found for the stimulation amplitude MSA16 (cyan data points in Figure 3.7) for S7L and S10L, where a monotonically decreasing trend was observed. The points where wave eV amplitudes reached their maximum depended on the subject, but also on level within a subject. Due to a facial nerve artifact, eABRs in some conditions were not reliably measured, thus excluded from the dataset (e.g. subject S3R). Similar to the amplitudes, latencies across subjects showed high variability, as depicted in Figure 3.8. However, for a fixed stimulation amplitude (lines with single colors), the general trend was that latency was increasing with the number of pulses. Moreover, for a fixed number of pulses, higher stimulation amplitudes resulted in shorter latencies, as expected.

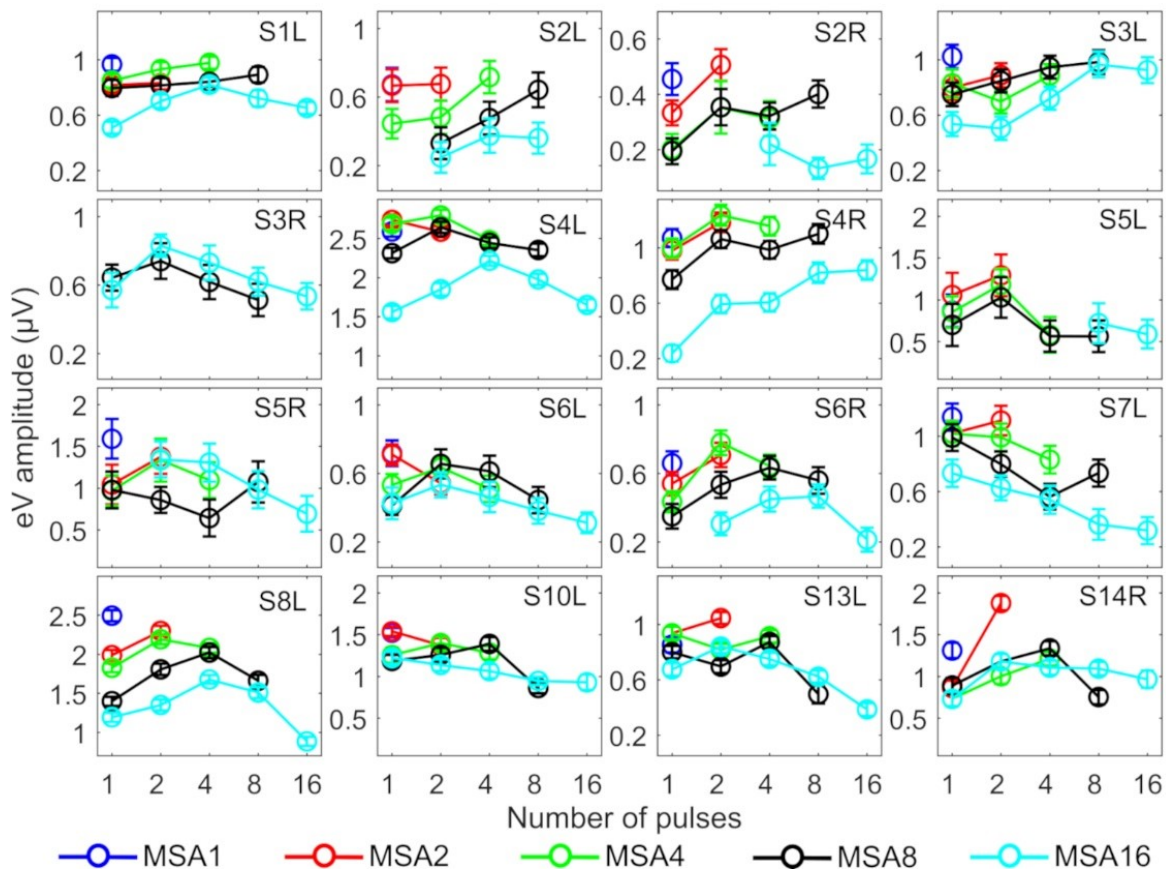


Figure 3.7 eABR wave eV amplitudes corresponding to the 15 measurement conditions mentioned in Figure 3.2. Curves with specific colors represent responses to stimuli with fixed stimulation amplitude and varying number of pulses. Error bars indicate $\pm\sqrt{2}\hat{\sigma}_{RN}^2$.

Investigation of Electrically-Evoked Auditory Brainstem Responses to Multi-Pulse Stimulation of High Frequency in Cochlear Implant Users

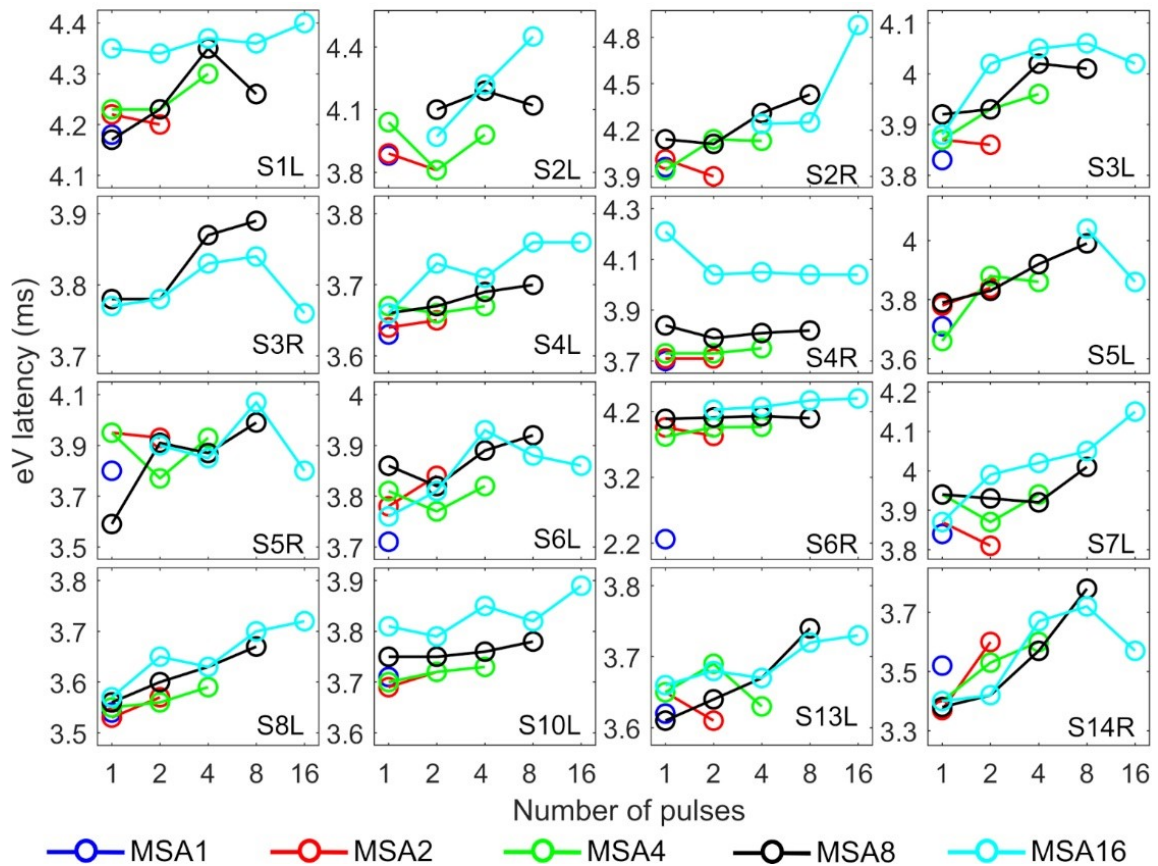


Figure 3.8 eABR wave eV latencies corresponding to the 15 measurement conditions mentioned in Figure 3.2. Curves with specific colors represent responses to stimuli with fixed stimulation amplitude and varying number of pulses.

Amplitude averaged over all subjects, depicted in Figure 3.9, suggest that wave eV grows when the number of pulses increased from 1 to 2-pulses and then tended to decrease for further pulses. Statistical analysis on overall results showed a significant difference only between 1 and 2-pulse conditions when the stimulation amplitude was MSA2 ($F(1, 14) = 4.73, p < 0.05$) (red data points in Figure 3.9) and MSA4 ($F(2, 28) = 3.66, p < 0.02$) (green data points in Figure 3.9).

Overall results of wave eV latencies corresponding to data in Figure 3.9, is depicted in Figure 3.10. Data in each panel were normalized to (subtracted from) the corresponding latencies at conditions with the largest number of pulses, i.e. MSA2, MSA4, MSA8, and MSA16 in panels A to D, respectively. Note that data for MSA1 are not plotted. Statistical analysis shows significant differences between 1-pulse and 4-pulses ($F(2, 28) = 3.15, p < 0.05$) when the stimulation amplitude was MSA4 and also between four pairs when the stimulation amplitude is MSA8 ($F(3, 42) = 12.29; p < 0.01$ for 1-pulse and 4-pulses, $p < 0.01$ for 1-pulse and 8-pulses; $p < 0.02$ for 2-pulses and 4-pulses; $p < 0.01$ for 2-pulses and 8-pulses). In 16-pulses condition, only the difference between 2-pulse and 16-pulse conditions was significant ($F(4, 40) = 4.80; p < 0.05$).

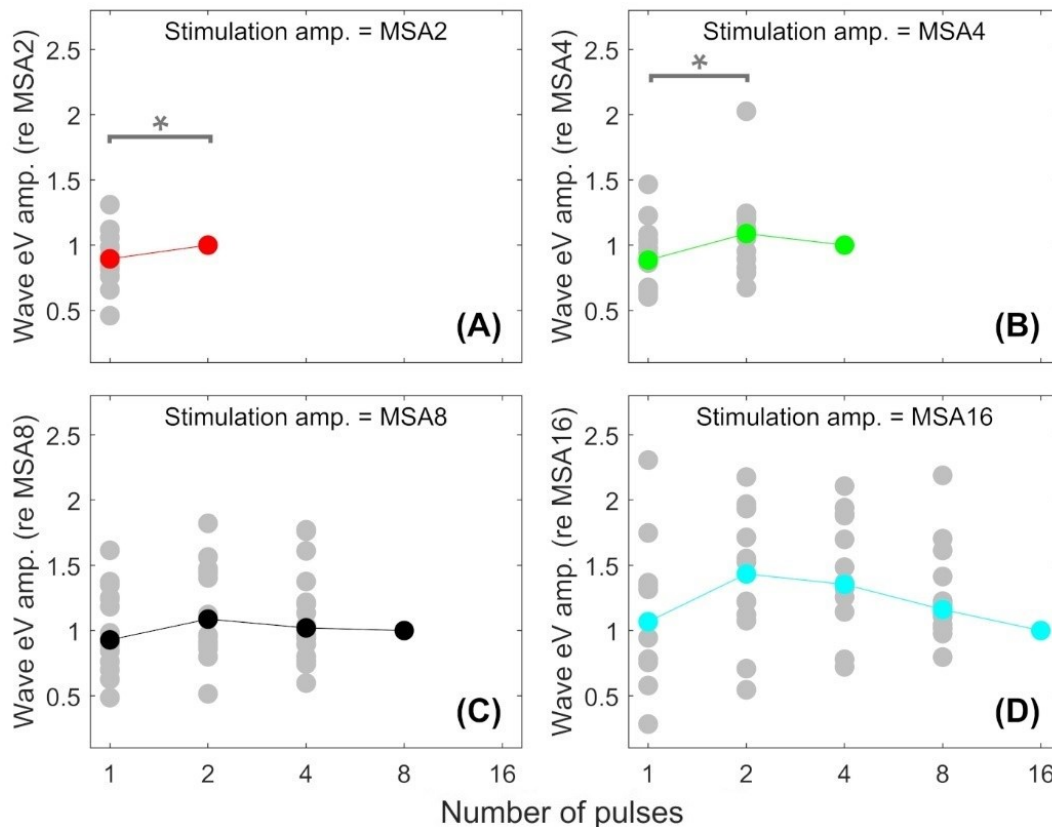


Figure 3.9 eABR eV amplitudes of multi-pulse conditions over all subjects. In each panel, the stimulation amplitude is constant (MSA2, MSA4, MSA8, MSA16 in panels (A-D), respectively). Data from individual subjects are plotted in gray circles and their corresponding median values in colors, which match the colors in Figure 3.7. In each panel, data were normalized to (divided by) the corresponding responses at the largest number of pulses (2-, 4-, 8-, and 16-pulses in panels A-D, respectively). Data of MSA1 condition (blue points in Figure 3.7) are not plotted, as all were 1 due to normalization. The asterisk shows pairs with significant difference.

Figure 3.11 shows wave eV amplitudes and latencies as a function of stimulation amplitudes (%DR) in different MP conditions for 8 ears (out of 16 ears). Columns show results for different number of pulses, while top and bottom rows show results of wave eV amplitudes and latencies, respectively. The amplitude data in top panels was normalized to the largest wave eV amplitudes that could be measured in 1-pulse condition (mostly 95%DR). Data from individual ears are in gray and the corresponding median values are depicted in black. The median AGFs showed a monotonic increasing trend except for few cases. Due to the small latency variabilities between subjects, latency data in bottom panels were not normalized. Visual inspection in top panels show a saturating tendency for the AGFs in MP conditions. The variation of range of eV amplitudes as a function of number of pulses was insignificant only between 2-pulses and 16-pulses ($F(4, 24) = 7.55, p < 0.02$). The variation of ranges of eV latencies as a function of number of pulses was significant only between 1-pulse and 8-pulses ($F(4, 24) = 5.24, p < 0.02$) and between 2-pulses and 8-pulses ($F(4, 24) = 5.24, p < 0.03$).

Investigation of Electrically-Evoked Auditory Brainstem Responses to Multi-Pulse Stimulation of High Frequency in Cochlear Implant Users

The structure of data on AGFs in MP conditions is different from that presented in Figure 3.9 and Figure 3.10. In the latter, we used fixed stimulation amplitudes for different number of pulses, while in the former, the stimulation amplitudes of the same percentage of the DRs were not identical. For instance, the physical stimulation amplitudes at 65% DR in 1-, 2-, 4-, 8-, and 16-pulses were not the same. Therefore, we could not apply the same analysis to both datasets.

3.4 Discussion

3.4.1 Artifact suppression

In neurophysiological measurements such as eABRs or eCAPs, electrical stimulation artifacts are inevitable. Factors such as stimulation mode, amplitude, phase width, polarity of the stimulus as well as stimulation site affect the magnitude and morphology of the stimulation artifact. Low stimulation amplitudes generate small artifacts, it may still be possible to extract eABRs without further processing (Gordon *et al.*). Often even large artifacts decay rapidly, such that they do not interfere with the eABR waves and blanking of the artifact-contaminated region is sufficient (Tykocinski *et al.* 1995; Truy *et al.* 1998). When long and strong artifacts corrupt the eABRs, stimulation with alternating polarity is a further option to reduce artifacts (Abbas and Brown 1991; Spitzer *et al.* 2006; Bahmer *et al.* 2008). However, due to nonlinearities of the eABR generation (probably mostly due to the stimulation electrodes), residual artifacts may remain even with alternating polarity stimulation. A different approach was proposed by Bahmer *et al.* (2010), who measured eABRs in response to triphasic pulses. They varied the distribution of charge over the three phases and selected a configuration, where the artifact was minimal. However, adopting this procedure for pulse train stimulation is not straightforward. In this case as well as when only single polarity stimuli are used, exponential fitting can be used to subtract artifacts (Undurraga *et al.* 2013; Hu *et al.* 2015). For stimuli consisting of multi-pulses, accumulated charges remaining from individual pulses yield to higher artifacts compared to single pulse stimulation. This could be the reason why in this study it became apparent that the stimulation artifacts obviously had two components, which can be fitted by two exponential functions. This was already found in a few studies even for conventional biphasic (Spitzer *et al.* 2006) or tri-phasic stimuli (Bahmer and Baumann 2012). Two-exponential fitting functions used in this study appeared to robustly and reliably remove the artifact even for long stimuli, e.g. 16-pulses, where the artifact superimposed with the eABR wave eV.

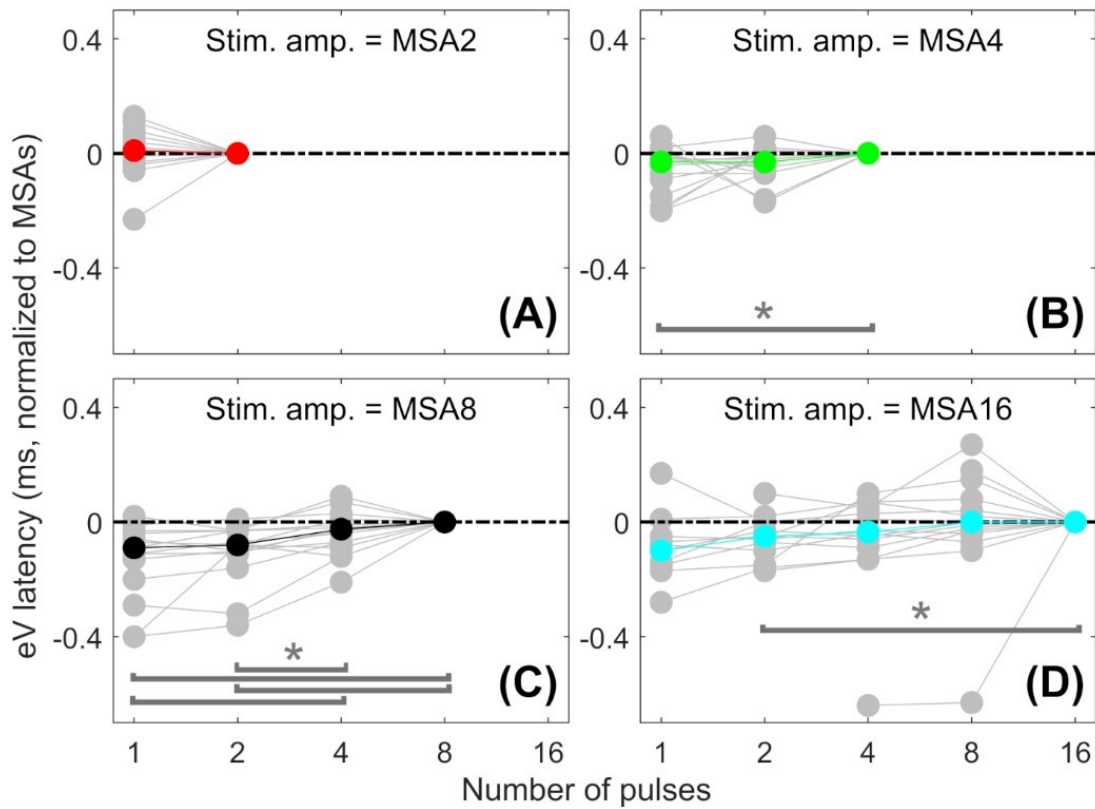


Figure 3.10 eABR eV latencies of multi-pulse conditions over all subjects. In each panel, the stimulation amplitude is constant (MSA2, MSA4, MSA8, MSA16 in panels (A-D), respectively). Data from individual subjects are plotted in gray circles and their corresponding median values in colors, which match the colors in Figure 3.7. Data of MSA1 condition (blue points in Figure 3.7) are not plotted, as all were 0 due to normalization. The asterisk shows pairs with significant difference.

Investigation of Electrically-Evoked Auditory Brainstem Responses to Multi-Pulse Stimulation of High Frequency in Cochlear Implant Users

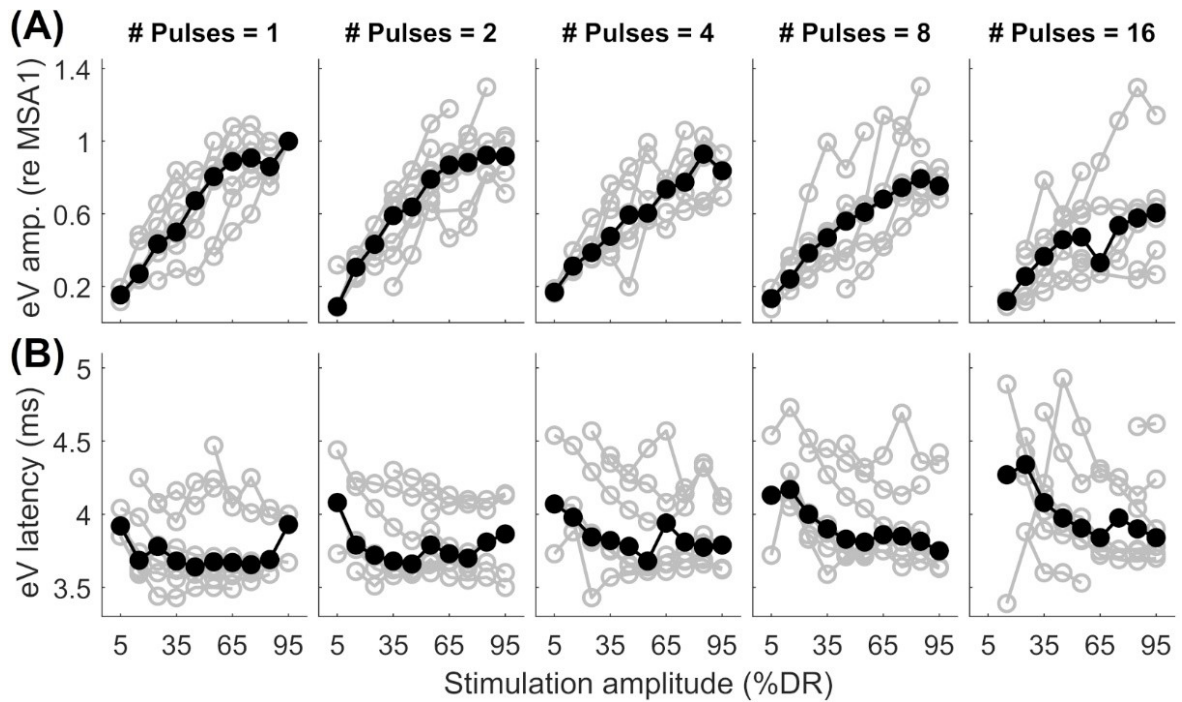


Figure 3.11 Wave eV amplitude growth functions (A) and latency functions (B) as a function of stimulation amplitude in all MP conditions for 8 ears (last column of Table 3.1). The amplitude data was normalized to the largest valid wave eV amplitudes in 1-pulse condition for each ear. Results from individual subjects are plotted in open gray circles, while the corresponding median values are plotted in filled black circles.

3.4.2 TI functions in psychophysical data

The first part of this study examined the TI functions of THR and MCLs as a function of stimulation duration, which increased from a single pulse to 1600 μ s (16-pulses). As the psychophysical THR and MCLs in this study were determined for the purpose of eABR measurement, the stimulation pattern differed fundamentally from those usually used for psychophysical measurements in other studies e.g. (McKay and McDermott 1999; Zhou *et al.* 2015). In this study, besides the high stimulation rate of 10,000 pps, a repetition (burst) rate of 37 bursts-per-second was presented, which was essential to record eABRs which require fast averaging. This way it was possible to apply identical stimuli for both psychophysical measurements and eABR recordings. Nevertheless, even with these deviations in stimulation pattern, results were in line with previous studies. We observed a decrease of -1.31 dB/doubling of stimulation duration in TI slopes of THR levels. If this is combined with the TI slopes of -0.42 dB (Donaldson *et al.* 1997), -0.88 dB (Zhou *et al.* 2015), -1.0 dB, and -2.6 dB/doubling the number of pulses (Obando Leitón 2019), one can see that the TI slopes decrease monotonically when the stimulation rate increased. We also compared the TI slopes of THR levels with those of wave eV amplitudes, for conditions of fixed stimulation amplitude (MSA8 and MSA16), while the number of pulses changed, as well as for conditions of fixed number of pulses, while the

stimulation amplitude changed (AGFs in 1-pulse and 2-pulses conditions). Details of these comparisons is available in supplementary Figures 2-6. TI slopes for MCLs showed a shallower decline of 0.78 dB/doubling the number of pulses, when compared to that of THR. This was consistent with findings of Zhou *et al.* (2012) and Obando Leitón (2019), where shallower TI slopes were found for comfortable levels and MCLs, respectively. Nevertheless, given this shallow decline and that TBC is proportional to the power consumption of the implant, our results also show that very high pulse rates (when using biphasic pulses) are not very efficiently stimulating neurons (A schematic illustration of the integration of charges in 16-pulses condition is depicted in supplementary Figure A.1).

The fact that not only a pulse rate (10,000 pps), but also a burst rate (37 bps) were employed in the study, might raise the hypothesis that a combination of both rates, and not only the pulse rate, contributes to temporal integration functions. This needs us to investigate phenomena related to temporal processing of ANFs including refractoriness, facilitation, accommodation and high-frequency spike rate adaptation (see Boulet *et al.* (2016) for review). Each of the mentioned phenomena is effective in certain conditions and time ranges. Refractoriness and high-frequency spike rate adaptation are related to conditions where the stimulation amplitude is (well-) above thresholds (e.g. MCLs), whereas the facilitation and accommodation deal with subthreshold amplitudes. Refractoriness states that a single nerve fiber has an elevated threshold after firing an action potential (relative refractory period), in a short period after a first action potential it is even impossible to elicit another action potential (absolute refractory period). The duration of the absolute refractory period is around 0.5 ms (Hodgkin and Huxley 1952; Matsuoka *et al.* 2001; Boulet *et al.* 2016), relative refractory period for the auditory nerve is about 4 ms (Boulet *et al.* 2016). This means that the high pulse rate used in this study (10 kHz) interacts with the refractory time for multi-pulse stimulation. That is, the population of nerves that responded to the first pulse of a multi-pulse burst cannot be activated by further pulses of the burst and instead, only a population other than that responded to the first pulse may respond to the second pulse of the burst.

Spike rate adaptation characterizes the reduced ability of ANs to elicit action potentials in response to pulse trains with relatively high-rates (> 250 pps). The time course of spike rate adaptation effect is reported to be between 10 and 100 ms (Zhang *et al.* 2007; Miller *et al.* 2011; Boulet *et al.* 2016), when the stimulation lasts 300 ms, i.e. excitability of neurons starts to decrease immediately after the first spike and then with a time constant between 10 ms and 90 ms. In this study, although we used a high stimulation rate of 10,000 pps, the stimulation duration was not in the same range of that in abovementioned studies. Therefore, spike rate adaptation has a massive effect on temporal response properties in the present study, it can be concluded that responses are dominated by the first pulse, which is supported by the relatively small changes in MCL amplitudes when the number of pulses was increased. The time course of facilitation and accommodation is reported to be 0.5 ms and between 0.5 and 1 to 10 ms, respectively (Boulet *et al.* 2016). Therefore, ANFs could integrate residual charge for multi-pulse stimulation, which leads

Investigation of Electrically-Evoked Auditory Brainstem Responses to Multi-Pulse Stimulation of High Frequency in Cochlear Implant Users

to lower THR. On the other hand, the inter-burst interval of 27 ms is longer than the 0.5 to 10 ms accommodation window, so that ANF had enough time to recover.

3.4.3 eABRs to multi-pulse stimulation

The notion that responses to a high-frequency burst are dominated by the first pulse is also supported by the relatively small changes in eABR responses when the number of pulses increased (Figure 3.9 and Figure 3.10). The averaged changes in amplitudes were smaller than 2.22 dB and 0.1 ms in latency compared to the single-pulse response with the same amplitude. Figure 3.9 shows even a decreasing trend for eV amplitude in MSA4, MSA8, and MSA16 after an initial increase from MSA1 to MSA2, which suggests that response amplitude falls. Although the stimulation current in each panel of Figure 3.9 is constant, the number of stimulation pulses and with it, the stimulation TBC increased. Therefore, higher wave eV amplitudes in response to stronger stimuli would be expected, but this was not observed here. One possible explanation for this observation is destructive interferences, where peaks and troughs of responses to the first pulse are reduced by anti-phasic (because of the delay) responses to later pulses in the train. For instance, the eABR in the 16-pulse condition could be assumed as an arithmetic summation of responses to individual pulses (as in Eq. 3.3) or groups of pulses (as in Eq. 3.4). The responses to groups of pulses can be extracted by simple subtractions: for example, the response to the second pulse is $eABR_2 = eABR_{2p} - eABR_{1p}$ and the response to the third and fourth pulses could be derived as $eABR_{3..4} = eABR_{4p} - eABR_{2p}$, where $eABR_{ip}$ is the measured eABR to a train of i -pulses. Figure 3.12 depicts such a decomposition of the responses to groups of pulses in the 16-pulse condition for subject S8L. It can be easily observed how the responses to successive pulses, especially $eABR_{5..8}$ and $eABR_{9..16}$ (cyan and magenta curves), contribute to suppressing the wave eV amplitude of $eABR_1$ by pushing down the peak of eV of $eABR_{1p}$ as well as by pulling up its trough, both resulting in a smaller wave eV amplitude of $eABR_{16p}$. Similar analysis on S8L' data in MSA2, MSA4, MSA8 conditions (not shown) supports the claim that the first pulse of the train has the dominant effect and responses to other pulses suppress the response to the first pulse. Therefore, the drop in eABR wave eV amplitudes of MSA4, MSA8, and MSA16 conditions might not be because of a weaker response but seems likely to be caused by destructive interference with eABR responses to later stimulation pulses. The effect of the destructive interference could be also observed in Figure 3.11, where the range of eV amplitudes decreased as a function of number of pulses (significant difference only between 2-pulses and 16-pulses) and latencies and their ranges were elevated (significant differences only between 1-pulses and 8-pulses and between 2-pulses and 8-pulses).

$$eABR_{16p} = eABR_1 + eABR_2 + \dots + eABR_{15} + eABR_{16} \quad 3.3$$

$$eABR_{16p} = eABR_1 + eABR_2 + eABR_{3..4} + eABR_{5..8} + eABR_{9..16} \quad 3.4$$

Here an additional support for the destructive interference rationale mentioned above is provided. As mentioned in Methods section, at each multi-pulse condition, eABRs to MSAs, which were defined as 95% of psychophysical MCLs, were measured. Assuming that all MSAs induce the same hearing impression (loudest tolerable level) to each CI subject, similar eABR signals and consequently, similar wave eV amplitudes are expected. However, as shown in Figure 3.13A, when the number of pulses increased, the eABR wave eV amplitudes in response to MSAs tended to decrease, but not to preserve. The opposite trends in stimulation TBCs (Figure 3.13B) and wave eV amplitudes (Figure 3.13A) also support the rationale of destructive interference, as more TBC would mean more activated ANFs and, consequently, larger eV amplitudes. Additionally, such a destructive effect was found to reverse the tendency of latency, where normally shorter latencies are expected for higher stimulation amplitudes. Figure 3.10, however, suggests longer wave eV latencies (maximum of about 0.1 ms) over all subjects, when the number of pulses increased.

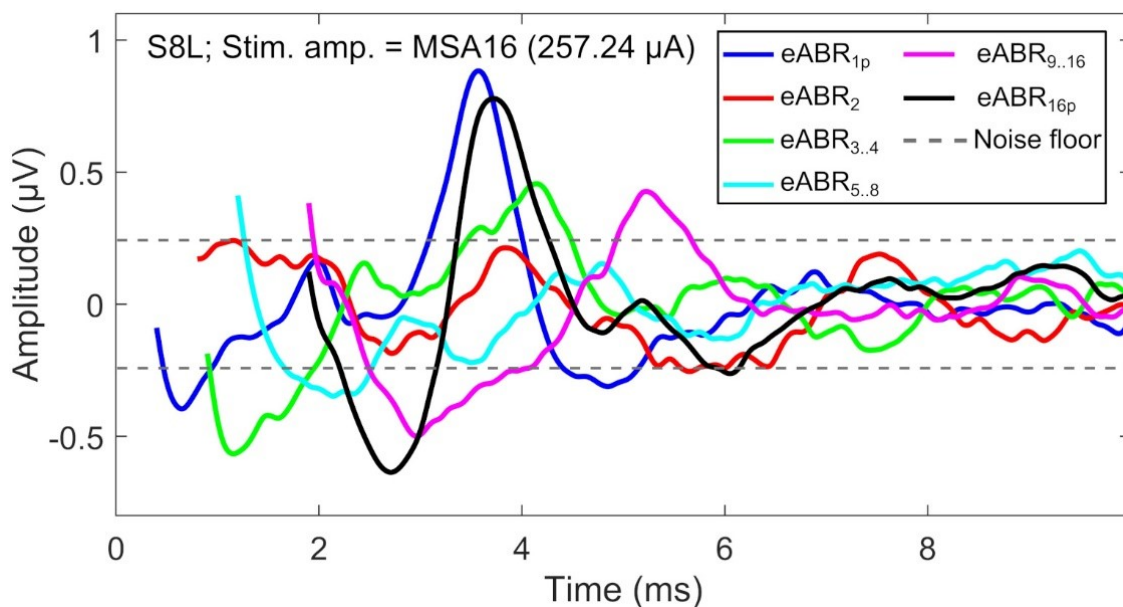


Figure 3.12 eABRs to individual pulses and groups of pulses in 16-pulses condition for subject S8L. Note the peaks and troughs of responses to successive pulses and groups of pulses, which suppress the response to the first pulse ($eABR_{1p}$). This destructive interference effect may explain the decrease of the eV amplitude in multi-pulse conditions.

Investigation of Electrically-Evoked Auditory Brainstem Responses to Multi-Pulse Stimulation of High Frequency in Cochlear Implant Users

3.4.4 Efficacy of multi-pulse stimulation

For electric biphasic stimulation, pulse shape could affect the detection THR_s at the level of a single ANF, eCAPs or eABRs. It is known that pulses with longer phase durations evoke stronger neural responses when compared to pulses with shorter durations and equal stimulation amplitude. This means, in comparison to shorter phases, pulses with longer phases need less current to reach THR. However, according to the fact that nerve membrane functions more as a leaky integrator rather than a perfect one, pulses with longer phases seem to be less efficient than those with shorter phase durations of same overall charges (Abbas and Brown 1991; Shepherd *et al.* 2001). For single pulses, Moon *et al.* (1993) observed mean slopes of -3.60 and -5.71 dB/doubling of phase duration when pulse duration was less or more than 0.5 ms/phase, respectively. The effect of phase duration on eCAP and eABR was also found to be correlated with auditory nerve survival in guinea pigs (Prado-Guitierrez *et al.* 2006). Shepherd and Javel (1999) investigated the efficacy of pulses of different shapes. They found that, not only ordinary biphasic pulses, but also chopped pulses could make a single ANF elicit an action potential. Shepherd and Javel (1999) also found that charge packages of 2×30, 3×20, and 6×10 μs of same polarity, followed by a series of reversed polarity, could charge the nerve membrane even up to eliciting an action potential. This packet-structure, which was called a ‘chopped pulse’, was found to show 1.5 dB higher THR_s (less efficient) than a 60 μs/phase biphasic pulse with 60 μs inter-phase gap and, interestingly, at least about 1.5 dB lower THR_s (more efficient) when compared to a 60 μs/phase biphasic pulse without inter-phase gap.

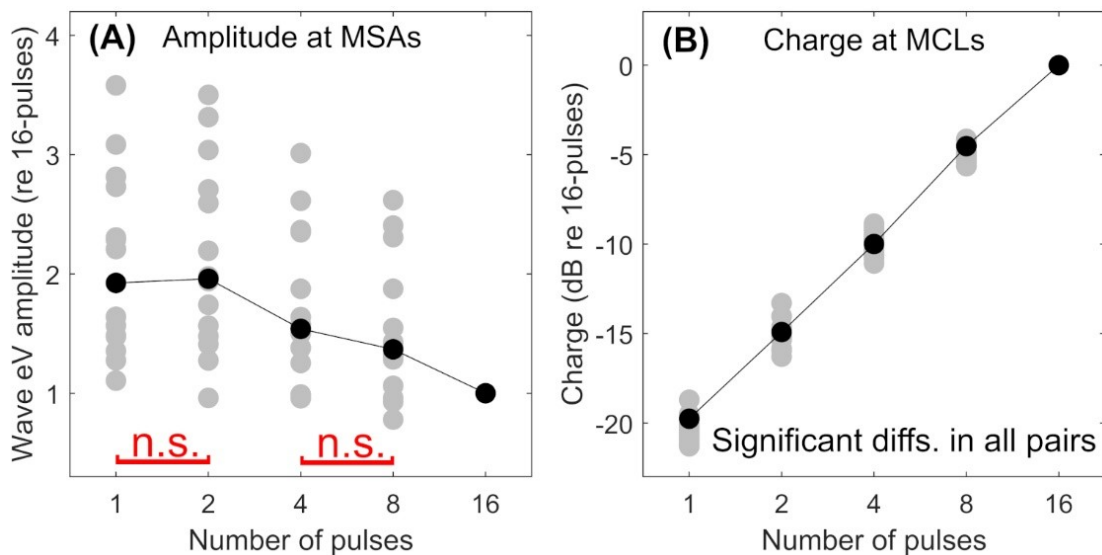


Figure 3.13 Comparison of psychophysical and eABR results. eABR wave eV amplitude at MSAs (95% of psychophysical MCLs) (A), and corresponding stimulation TBCs led to psychophysical MCLs (B). All data are normalized to their corresponding values at 16-pulses condition. The ‘n.s.’ in red in panel (A) show *not significant* differences between 1-pulse and 2-pulses and between 4-pulses and 8-pulses. The difference between the rest of the pairs were significant. In panel (B), all pairs were significantly different.

Although the electric current and charge are closely related, in electric hearing, the current, rather than the charge, plays the main role in stimulating auditory nerves. Moreover, in MED-EL implants there is a coupling capacitor, which forces the net charge to be zero. A net residual potential of the electrodes should have no effect in the resistive fluid. In such a structure, if stimulation mode was 100% efficient, it could be expected that the total charge required to elicit THR/MCL remained constant. In such a condition, the stimulation amplitude in a m -pulse condition should decrease by a factor of $\frac{1}{m}$, compared to the 1-pulse condition. This was not found in the data of the present study. Figure 3.6 highlights the inefficiency of multi-pulse stimulation. The TBC of the positive phases in a multi-pulse condition is plotted as a function of number of pulses for THR and MCL. In both THR and MCL data (Figure 3.6B), the TBC needed to elicit THR/MCL increased drastically as a function of number of pulses (see also supplementary Figure 7). The steeper slope for THRs show a stronger inefficiency compare to that for MCLs. The inefficiency found in this study can be attributed to rapid phase switching of pulses, therefore multi-pulse stimuli are far less efficient than single pulses.

3.4.5 Temporal effects in eABRs to fast pulse trains

Since all multi-pulse stimuli used in eABR section of this study were (well-) above THR, temporal phenomena such as facilitation and accommodation would not be involved in temporal processing of ANFs. Refractoriness however, is the likely occurring phenomenon and the eABR measurements might shed light on this effect. Abbas and Brown (1991) employed a masker-probe paradigm in which an initial pulse, termed masker, followed by a second pulse, named probe, with varying inter-pulse interval from the masker was used to measure eABRs. They found that average durations of 5.10 and 4.63 ms, respectively, were needed for the probe (second) pulse to fully recover, using two different CI types. Their findings seem to be consistent with the relative refractory period of about 4 ms, as reported in Boulet *et al.* (2016). This also suggests that, in the 16-pulse condition of the present study, where the stimulation lasted for 1.6 ms, a portion of the ANFs might fire twice during the train. This portion would probably be those ANFs which responded to the first pulses, and later, most likely to the pulses close to the end of the train, due to their recovery after their absolute refractory period.

Particularly in multi-pulse stimulation employed in this study, the initial pulse activated a population of ANFs, which consequently led to a detectable eABR in the brainstem. This population is not capable to respond to the second pulse and has only limited responses during the rest of the pulses in the burst, because of the refractoriness. Therefore, another population of ANFs, other than the one responded to the first pulse and presumably farther than that, might be capable of eliciting action potentials as a response to the second pulse. In case that the second pulse alone is not strong enough, a group of pulses might be able to make ANFs fire, as described in Eq. 3.4. Generalized to further pulses, characteristics of wave eV amplitudes in response to multi-pulse stimulation provide insight into how multi-pulse stimuli are integrated at the level of the

Investigation of Electrically-Evoked Auditory Brainstem Responses to Multi-Pulse Stimulation of High Frequency in Cochlear Implant Users

brainstem and they might be a potential measure of health state and/or survival of ANFs.

Obando Leitón (2019) and Bai *et al.* (2019) confirmed that stimulation of a single electrode of the CI leads to a broad spread of current along the cochlea, which means, the auditory nerves are stimulated not only by the nearest electrode, but also by a number of neighboring electrodes. This would mean that in the CIS strategy the effective stimulation rate in electric hearing is not the rate of individual electrodes, but a burst with the global stimulation rate originating from neighboring electrodes with overlapping current spread. Considering a typical stimulation rate of 800-2000 pps for individual electrodes, the high stimulation rate of 10,000 pps used in this study represents the global stimulation rate induced by stimulation of N neighboring electrodes. Thus, eABRs in response to multi-pulse stimuli of high rate could be used for estimation of THRs like those used in clinics. This assumption of course requires further investigation.

Chapter 4

eABR THR Estimation Using High-Rate Multi-Pulse Stimulation in Cochlear Implant Users

The content provided in this chapter was published in a previously peer-reviewed research paper¹:

Saeedi A., Englert L., and Hemmert W. (2021) eABR THR Estimation Using High-Rate Multi-Pulse Stimulation in Cochlear Implant Users. *Frontiers in Neuroscience*. 15:705189. doi: 10.3389/fnins.2021.705189

which is reproduced here without any content-related changes. To fit the typesetting of this document, only caption numberings of figures, tables, and formulas have been changed.

4.1 Introduction

Appropriate adjustment of hearing threshold (THR) levels is important in cochlear implant (CI) fitting in order to make the best use of the limited dynamic range (DR) available in electric hearing. Precise THR estimation, especially for the first fit after implantation, can provide the user with improved perception of soft sounds, which in turn helps for a better speech perception (Holden *et al.* 2011; Rader *et al.* 2018). Setting the THRs too low or too high results in suboptimal usage of the available DR. In the former case, quiet sounds cannot be perceived and in the latter, the available DR is reduced and CI users might even perceive an irritating background noise (Busby and Arora 2016). Clinically, THR levels are determined by direct adjustment/feedback from the implantee. The procedure of THR determination becomes hard if the implantee is unable to cooperate, e.g. infants or users with lack of proper communication. In such situations, objective estimation of THRs, where electrically-evoked objective measures of the auditory pathway are used, could be an alternative. Among these measures are electrically-evoked compound action potentials (eCAP, peripheral measure), electrically-evoked auditory brainstem responses (eABR), electrically-evoked auditory steady state

¹ The paper is distributed under the terms of the Creative Commons Attribution License (CC BY), which holds its copyright with the authors.

response (eASSR), and cortically evoked potentials (CAEP) (central measures). The extent to which the THRs estimated in each of these measures correlate with the behavioral THRs are reported to be different, with generally better performance in central measures compared to peripheral ones (e.g. CAEP vs. eCAP in Abbas and Brown (2015)). Although responses from higher auditory brain areas capture the THRs better, they are less suitable for THR estimates in newborns and young infants for two reasons: higher level potentials require attention (Picton *et al.* 1971; Picton and Hillyard 1974), and the auditory pathway is not yet developed. Therefore, a compromise between more peripheral (e.g. eCAP) and more central auditory responses (e.g. CAEP) has to be found.

eCAPs overestimate the behavioral THRs with moderate correlation when the behavioral stimulation rate is low, e.g. 250 pulses-per-second (pps) (Miller *et al.* 2008) and correlation decreases when stimulation rates increase. This is due to the fact that in eCAP measurements single stimulation pulses of low stimulation rates are used, which do not reflect temporal integration effects observed when high rate pulse trains are used for clinical fittings. This limits the prediction power of the behavioral THRs (Miller *et al.* 2008; McKay *et al.* 2013; Mao *et al.* 2019). Conventional eABRs showed relatively high correlation with behavioral THRs when the behavioral stimulation rate is less than 500 pps, e.g. $r = 0.89$ at 10 pps (Hodges *et al.* 1994), $r = 0.83$ at 35-80 pps (Brown *et al.* 2000), $r = 0.98$ at 300 pps (Truy *et al.* 1998), and $r = 0.84$ and 0.74 at single pulses and pulse trains of 400 pps, respectively (Brown *et al.* 1999). However, the correlation between eABR THRs and behavioral THRs reported to decrease when the stimulation rate increased, e.g. $r = 0.69$ at 1000 pps in Brown *et al.* (1999).

In central electrophysiological recordings (e.g. eASSR and CAEP), larger correlations were found compared to those reported in eCAP and eABR measurements. In an eASSR study, Hofmann and Wouters (2012) showed high correlations between eASSR THRs and behavioral THRs either for 40 pps pulse trains ($r = 0.96$) or 900 pps amplitude modulated (AM) and phase-width modulated (PWM) pulse trains ($r = 0.96$ and $r = 0.96$, respectively). In a CI study, Visram *et al.* (2015) recorded CAEPs in response to 50 ms pulse trains presented at 900 pps, and found high correlations between behavioral THRs and cortical THRs ($r = 0.93$). Using a phase-locking feature value for CAEP growth functions, Mao *et al.* (2019) showed high correlations between CAEP THRs and behavioral THRs ($r = 0.979$ in the standard Cz-to-mastoid montage and $r = 0.96$ in recordings from channels near the CI). Although cortical potentials (eASSR and CAEP) showed promising objective THR estimates, they have still limitations that restrict their applicability for clinical purposes. For instance, subjects should remain awake and as calm as possible during the cortical measurements, which restricts the method for infant CI users. Therefore, it remains worthwhile to introduce modifications to other established measures (e.g. eABR) with the aim of improving their functionality to achieve more accurate objective THR estimates.

Neurons would respond differently to stimuli with different parameters, such as pulse shape and stimulus frequency (Mahmud and Vassanelli 2016). One modification to the conventional (single-pulse) eABR measurements could be employing multiple-pulse

(MP) stimuli with the aim to account also for loudness integration, which is prominent for typical environmental- and speech sounds. Multi-pulse integration (MPI) suggests that at a fixed stimulation rate, the detection THR improves when the number of pulses (or equivalently the stimulation duration) increases. Compared to stimulation rates below 1000 pps, the MPI slopes for rates above 1000 pps are steeper in guinea pigs (Kang *et al.* 2010; Zhou *et al.* 2015) as well as in humans (Shannon 1985; McKay and McDermott 1998; Zhou *et al.* 2012; Carlyon *et al.* 2015; Zhou *et al.* 2015). Carlyon *et al.* (2015) found that when the number of pulses increased from 1 to 16, MPI slopes decreased by about 0.68 and 1.33 dB/doubling the number of pulses, for rates of 500 and 3500 pps, respectively. Obando Leitón (2019) found that at rates of 1500 and 18000 pps, MPI slopes dropped 3.44 and 5.43 dB per tenfold increase of the number of pulses, which correspond to drops of 1.03 and 1.63 dB per doubling the number of pulses, respectively. In a previous study (Saeedi and Hemmert 2020), we measured behavioral THR and MCLs as well as eABRs in response to 1-, 2-, 4-, 8-, and 16-pulses stimuli at the rate of 10000 pps. MPs were constructed by assembling single-pulses closely together to make the stimuli more representative of high-rate clinical stimulation paradigms. We found behavioral MPI slopes of -1.30 and -0.93 dB/doubling of the number of pulses for behavioral THR and MCLs, respectively.

Our previous study (Saeedi and Hemmert 2020) aimed to assess temporal effects and efficiency of MPs in eABR. We found that eABR morphology in response to MP stimuli did not differ from those to conventional single-pulse stimuli. It was also shown that introducing more pulses led to larger wave eV amplitudes up to a certain subject-specific number of pulses. The saturation of the growth function was attributed to the destructive interference of the eABRs to later pulses in a pulse train, where time-shifted peaks and troughs of later pulses suppressed those of earlier pulses. This study aimed to 1) investigate how features extracted from the eABRs in response to MPs grow and 2) see how well the estimated THR in MP conditions correlate with the behavioral THR. We measured psychophysical THR at MP conditions as well as clinical THR. We also measured eABRs to MP stimulations from 5 to 95% of the corresponding DRs. Then, we calculated growth functions of eABR wave eV amplitudes, root mean square (RMS) values, peak phase-locking value (peak PLV), and the lowest valid data point (LVDP). We fitted and extrapolated the growth functions of these features with a linear and an exponential fitting function (FF) to estimate eABR THR. The estimated eABR THR were then compared to those from psychophysical measurements as well as to the clinical THR. We assumed that eABR THR in response to MPs could estimate clinical THR more accurately, as in our previous study (Saeedi and Hemmert 2020) psychophysical THR tended to approach the clinical THR when the number of pulses increased from 1 to 16.

4.2 Material and Methods

A total of thirteen ears from nine CI users (three males, mean age: 50.6 years) implanted with MED-EL CIs were measured. Demographic information of the participants is

eABR THR Estimation Using High-Rate Multi-Pulse Stimulation in Cochlear Implant Users

available in Table 4.1. Participants signed an informed consent and received a compensation fee for their participation. The study was approved by the Medical Ethics Committee of the Klinikum rechts der Isar, Munich.

4.2.1 Stimuli

A schematic of the stimuli used in this study is depicted in Figure 4.1. Stimuli in clinical measurements consisted of 500 ms pulse trains with a stimulation rate of 1000 pulses-per-second (pps) followed by a 1000 ms pause (Figure 4.1A). In clinical measurements, single pulses were anodic-first charge-neutral biphasic pulses with 45 μ s phase width and 2.1 μ s inter-phase gap. Stimuli for eABR measurements were same as in our previous work (Saeedi and Hemmert 2020), where electrical multi-pulse (MP) trains of 1-pulse, 2-pulses, 4-pulses, 8-pulses and 16-pulses were employed (Figure 4.1B). Multi-pulses were assembled by concatenating single pulses. Properties of single pulses in the eABR measurements were identical to those in clinical measurements. Additionally, an inter-pulse gap of 7.9 μ s was used to achieve a pulse period of 100 μ s, which corresponds to a burst rate of 10000 pps. Stimuli for eABR measurements were delivered to an electrode in the middle of the array with a repetition rate of 37 blocks-per-second.

Table 4.1 Demographic information of CI participants

Subject	Side(s)	Age range (years)	Etiology	Deafness dur. (years)	CI experience (years)	CI type	Electrode
S1	L	50-55	Inherited OM	49	4	Co	6
S2	L, R	56-60	Congenital	56	12, 10	P, So	6, 4
S3	L, R	60-65	Unknown	22	4.5, 5	So, So	4, 6
S4	L, R	56-60	Unknown	56	11, 10	P, P	6, 7
S8	L	40-45	Congenital	42	5	Co	4
S10	L, R	75-80	Unknown	30, 20	20, 12	Sy, P	4, 5
S12	R	20-25	Meningitis	22	10	So	5
S13	L	40-45	OM	40	3	Sy	7
S14	R	35-40	Inherited OM	31	6	Co	4

OM otitis Media; Co concerto; P pulsar; So sonata; Sy synchrony

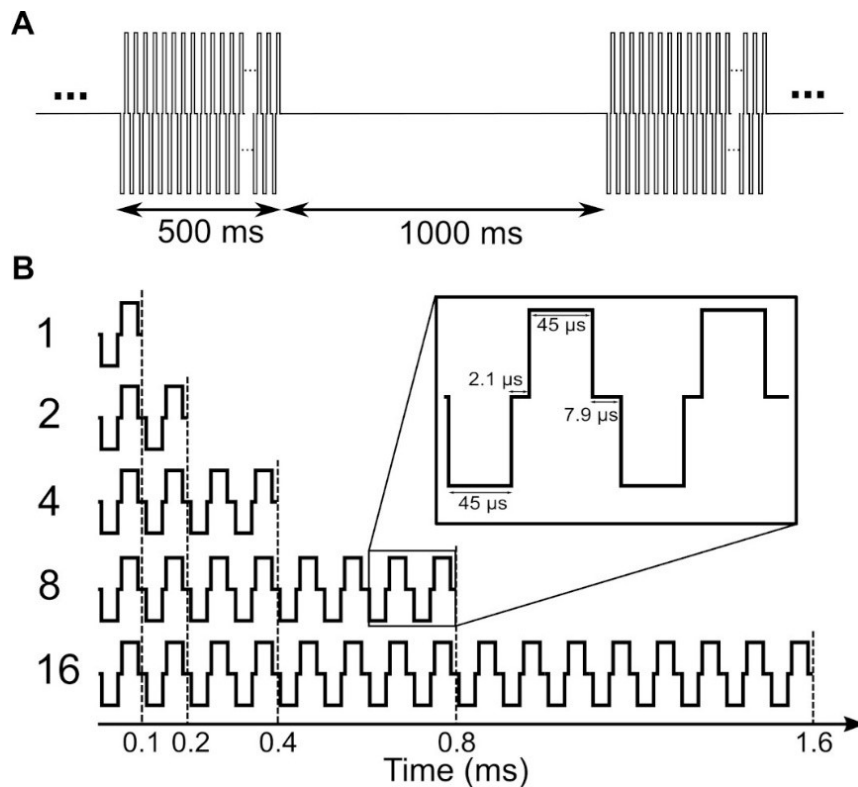


Figure 4.1 Stimuli used in clinical measurements (A) and in eABR measurements (B). Stimuli in panel b were presented at a repetition rate of 37 blocks-per-second.

4.2.2 Pretest

Psychophysical thresholds (THR) and the most comfortable levels (MCL) for eABR and clinical measurements were adjusted by the subjects in four different sessions during the same day. In psychophysical measurements, all MP conditions of THR/MCL were presented separately; e.g. all MP THR were measured in one session and all MP MCLs were measured in another session. Each THR/MCL was measured three times; one trial round and two main rounds. Only results of the main rounds were used for further analysis. The same stimuli employed in psychophysical measurements were later used in eABR measurements. The clinical THR measured in pretest sessions were compared to the estimated eABR THR. More details on psychophysical measurements can be found in (Saeedi and Hemmert 2020).

4.2.3 eABR stimulation

In order to estimate eABR THR in each MP condition, the corresponding eABR amplitude growth functions (AGFs) were measured. Stimuli with amplitudes of 5% to 95% of the dynamic range (DR) with steps of 10% were used. For two subjects, high stimulation amplitudes stimulated the facial nerve and thus resulted in artifact-corrupted eABRs. These conditions were excluded from further analysis. In most of the subjects,

no clean eABR was observed at low stimulation amplitudes, e.g. 5% of the DR. When less than 4 points remained in the AGFs, extra stimuli were used to add more points to the AGFs and thus to make the eABR estimation procedure feasible. Stimulation scripts were developed and compiled in MATLAB 9.6.0.1072779 (2019a) installed on a personal computer. The compiled scripts were then delivered through a National Instrument (NI) I/O card to a research interface box (RIB II), manufactured by the University of Innsbruck, Innsbruck, Austria. The RIB II conveyed the stimulation pulse sequences to the internal part of the implant via an induction coil.

4.2.4 eABR recording

eABRs were measured differentially from surface electrodes glued on the skin. Raw eABRs were recorded with a Biopac® MP36 system (California, USA) with a sampling rate of 100 kHz, 24-bit A/D converter and amplifier gain set to 1000. eABRs in MP conditions were measured in separate sessions. Measurements in each MP condition were randomized through the stimulation amplitudes (5% to 95% of the DR, maximum of 10 conditions). For each stimulation amplitude of MP conditions, 2184 epochs were recorded, each of which had a duration of 27 ms (totally about 59 seconds). Subjects were sitting or laying on a comfortable couch during the eABR recordings. They were asked to close their eyes, not to blink, and stay as calm as possible during stimulation to minimize myogenic/muscle artifacts. Subjects were allowed to move freely between two consecutive measurements. Regular breaks were made and subjects were also free to request a break or to terminate the experiment at any time during the measurement. In order to achieve a low recording electrode impedance, the skin beneath electrodes was cleaned with alcohol swabs, and scrubbed by subjects themselves as thorough as they possibly could. Conductive gel was used to minimize the impedance between the electrodes and the skin. Electrode impedances were monitored by the recording setup and were below 10 k Ω during the whole measurement time.

4.2.5 eABR THR estimation

Raw eABRs were processed offline using MATLAB. The procedure of eABR processing included stimulus onset detection, electrical artifact suppression by exponential fitting, band-pass filtering, and weighted averaging. We used weighted non-stationary fixed multi-points (WNSFMP) averaging method, introduced by Silva (2009), to minimize the noise mainly originated in myogenic activities as well as spontaneous activity of the brain (e.g. EEG). The WNSFMP method is a powerful method to estimate the noise even in non-stationary situations such as auditory processing. The eABR processing steps were described in detail in (Saeedi and Hemmert 2020). The WNSFMP method provides post-average residual noise (RN) estimation. In this study, eABR amplitude variances were estimated as $\hat{\sigma}_{amp}^2 = 2\hat{\sigma}_{RN}^2$, as in (Undurraga *et al.* 2013). Only eABR waves eV with amplitudes greater than $\sqrt{2}\hat{\sigma}_{RN}$ were accepted as valid responses. One can think of increasing the number of averages to improve the signal-to-noise ratio. However,

significantly larger numbers of averages beyond 2000 are not practicable due to the long measurement times. Therefore, eABRs with low amplitudes are stronger affected by noise. This is also true for longer stimulation durations of MPs, which would consider temporal integration effects better. Long stimuli smear out the eABR responses and reduce their amplitudes due to destructive interferences, as described in Saeedi and Hemmert (2020).

Four features were used for eABR THR estimation: wave eV amplitudes, root mean square (RMS) values, peaks of phase locking values (PLV) (Mao *et al.* 2018; Mao *et al.* 2019), and the lowest stimulation amplitude, where still a valid wave eABR eV could be detected (lowest valid data point: LVDP). All four features were calculated on the block average of clean epochs. eABR wave eV amplitude was defined as the difference between peak eV and the following trough amplitude. eABR RMS value was calculated for valid eABR responses in a time window from 2.5 ms to 6.5 ms after stimulus onset. eABR peak PLV was calculated by first taking the short-time Fourier transform (STFT) on a post-stimulus window from 2.5 ms to 6.5 ms after stimulus onset. A hamming window of length 150 samples and an overlap of 100 samples were used for the calculation of the STFT. The phase-locking spectrograms were calculated at 270 frequencies linearly spaced between 300 and 3000 Hz, by calculating the phase of each time-frequency point of the STFT ($\theta_i(t, f)$) and then applying the formula in Eq. 4.1 to calculate the phase-locking spectrogram (Mardia 2014). The peak PLV was the maximum value in the PLV spectrogram.

$$PLV(t, f) = \frac{1}{N} \sqrt{\left[\sum_{i=1}^N \cos(\theta_i(t, f)) \right]^2 + \left[\sum_{i=1}^N \sin(\theta_i(t, f)) \right]^2} \quad 4.1$$

Figure 4.2 illustrates the estimation of eABR THR. For each MP condition, valid points of the features' growth functions were fitted with a linear or an exponential growth function. THRs were estimated using the median from subsamples of growth functions, where one data point was excluded from the fit and the THR was extrapolated from the remaining data points. THRs were extrapolated with an exponential and a linear function, as described in Eqs. 4.2 and 4.3, respectively. In Eq. 4.2, $f(x)$ represents a feature, x represents the stimulation amplitude in %DR, a the asymptote, b the x -intercept and c the exponential growth. In Eq. 4.3, a represents the growth slope and b the x -intercept. Fitted functions were extrapolated to intersect the x -axis, where the features are zero. The intersection point was assumed as the eABR THR. Two criteria were considered in THR estimation: 1) the 25th percentile of the THRs from the leave-one-out method is positive; 2) the median (50th percentile) is bigger than the difference between 75th and 25th percentiles. The first criterion helped to remove negative THR estimates and the second criterion provided an unbiased estimation.

$$f(x) = a \left(1 - e^{-\frac{x-b}{c}} \right) \quad 4.2$$

$$f(x) = a(x - b) \quad 4.3$$

4.2.6 Statistical Analysis

Repeated-measures analysis of variance (ANOVA) was used to statistically test the effect of the number of pulses. Fisher's r to z transformation and z -test statistics were employed to compare of Pearson correlation coefficients (PCCs). MATLAB 9.6.0.1072779 (2019a) was used for all statistical analysis. For pairwise comparisons, Bonferroni corrected post hoc analysis was used. The significance level was set to $\alpha = 0.05$ for all analysis.

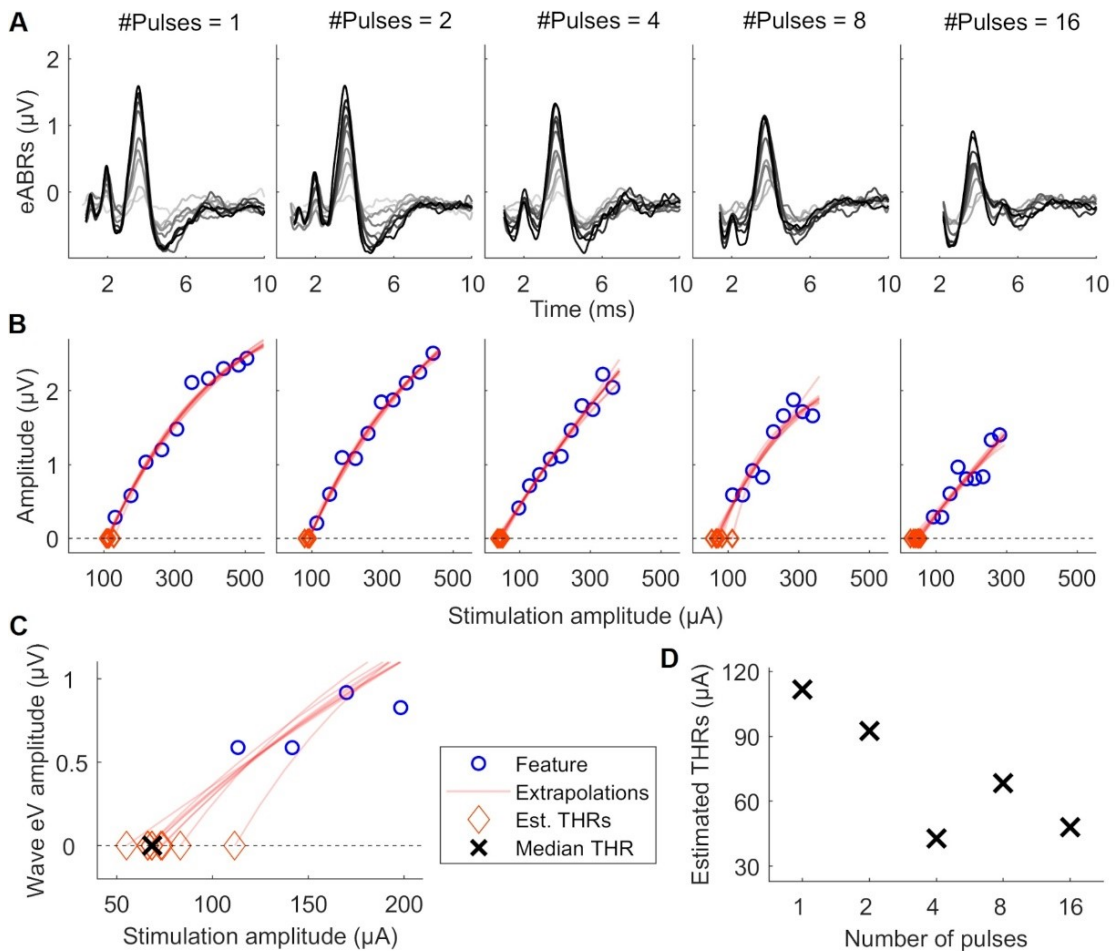


Figure 4.2 Illustration of eABR THR estimation for subject S8L. **(A)**: valid eABRs in each MP condition. In each panel, eABRs to different stimulation amplitudes are plotted. **(B)**: corresponding growth functions (blue circles) in (a), growth function fittings (red lines) and eABR THR estimations (red diamonds). **(D)**: Details of eABR estimation from b (8-pulses condition). The 'x' shows the median of estimated eABR THRs (diamonds). **(D)**: Estimated eABR THRs as a function of number of pulses.

4.3 Results

4.3.1 Psychophysical thresholds

Psychophysical thresholds are plotted in Figure 4.3, where data from individual subjects is plotted in gray while the corresponding median values are plotted in black. Figure 4.3A shows that while inter-subject variability was high, psychophysical THR_s decreased monotonically when the number of pulses increased from 1 to 16. The median THR_s dropped from 46.8 dB for a single pulse to 40.4 dB for 16 pulses. Linear regression of psychophysical THR_s revealed an average slope of -1.61 dB/doubling the number of pulses. Clinical THR_s and their corresponding median values are shown in the right side of Figure 4.3A. The difference between clinical THR_s and the psychophysical THR_s, and the corresponding absolute values of the differences are plotted in Figure 4.3B and C, respectively. This enables us to make a between-subject comparison, and on the other hand, it provides more details on the trend of psychophysical THR_s towards clinical THR_s.

The median differences between psychophysical THR_s and clinical THR_s (Figure 4.3B) decreased monotonically from 6.7 to -0.8 dB when the number of pulses increased from 1 to 16. This is equivalent to a slope of -1.8 dB/doubling the number of pulses. The between-subject range in Figure 4.3B monotonically decreased from 10.4 to 8.1 dB when the number of pulses increased from 1 to 16. The median of absolute differences between psychophysical THR_s and clinical THR_s, (Figure 4.3C) monotonically decreased from 6.70 to 2.10 dB when the number of pulses increased from 1 to 8, which is equivalent to a slope of -1.60 dB/doubling the number of pulses. It further decreased from 2.10 to 2.05 dB when the number of pulses increased from 8 to 16. The between-subject range of the absolute differences monotonically decreased from 10.4 to 5.3 dB when the number of pulses increased from 1 to 16.

4.3.2 eABR results

Figure 4.4 shows the growth of features as a function of stimulation amplitude (in %DR). Columns 1-5 show growth functions of features in 1-, 2-, 4-, 8-, and 16-pulses conditions, respectively. Rows a-c represent growth functions of wave eV amplitudes, RMS values, and peak PLVs, respectively. The thick lines show the median values of the features over all subjects and the shaded area represents the area between the 25th and 75th percentiles. Wave eV amplitudes were larger than the RMS values and peak PLVs for a given condition. The median RMS values were in most cases larger than their corresponding peak PLVs. Despite having dents, the growth functions of all features showed to be generally monotonic. In some cases, for instance in A3, A4, C3, and C5, the median features saturated at higher stimulation amplitudes. The inter-subject data variability was larger at higher stimulation amplitudes (broader shaded area).

eABR THR Estimation Using High-Rate Multi-Pulse Stimulation in Cochlear Implant Users

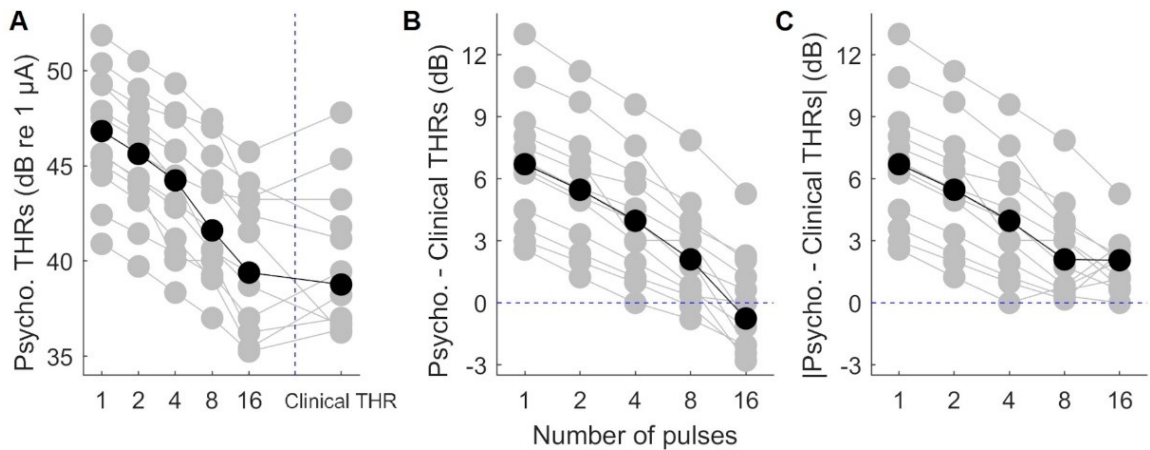


Figure 4.3 Results of psychophysical THRs. (A): Psychophysical THRs as a function of number of pulses. Clinical THRs of all subjects are plotted in the most right side of panel a. (B): The difference between psychophysical THRs and clinical THRs as a function of number of pulses. (C): The absolute values of the data in panel b. The gray circles show results of individual subjects while the black circles show the corresponding median values over all subjects.

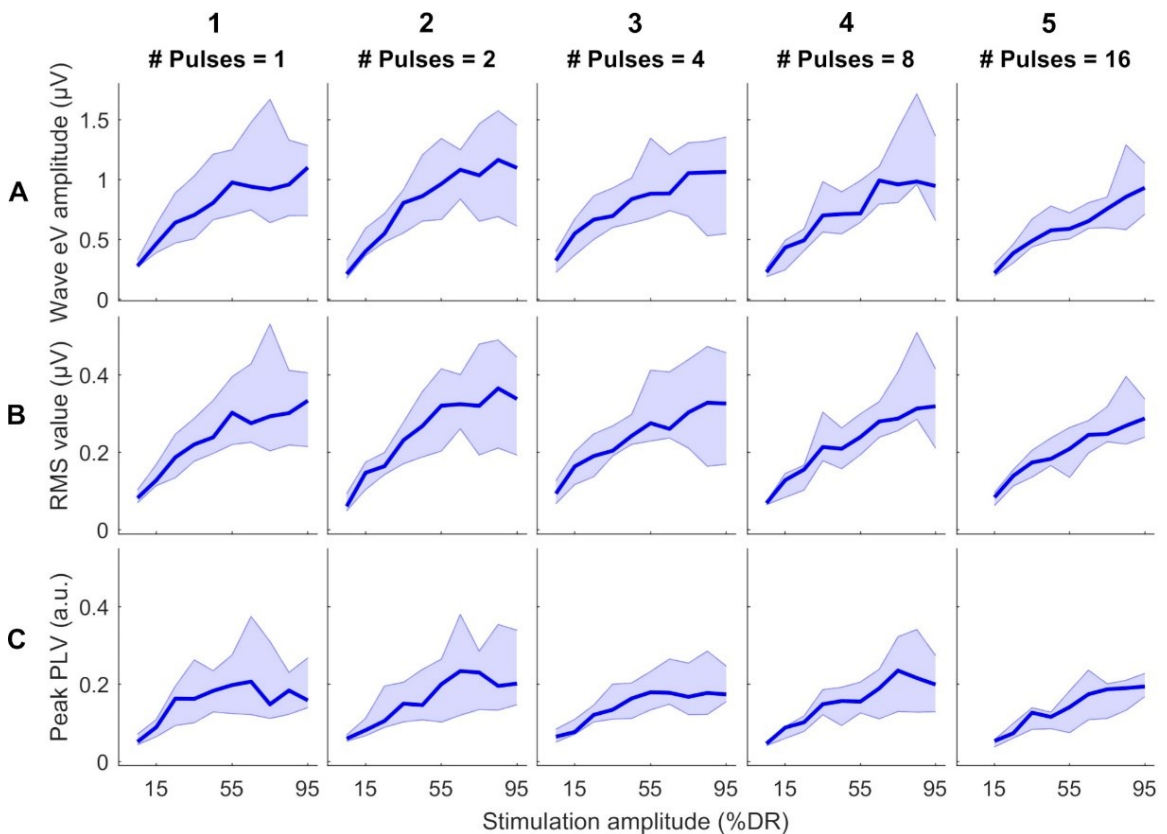


Figure 4.4 Growth functions of features used to estimate eABR THRs as a function of stimulation amplitude (%DR) in all MP conditions across all subjects. Thick lines show median values and shaded area represents the range between 25th and 75th percentiles.

Figure 4.5 shows the estimated eABR THR as a function of number of pulses. The gray circles represent results of individual subjects and the black circles show the corresponding median values across subjects. eABR THR was estimated by extrapolation of growth functions (panels A-E) or the lowest valid data point (LVDP, panel F). For each feature, an exponential and a linear function, as described in Eqs. 4.2 and 4.3, were used to fit the growth function data (left and right panels of Figure 4.5, respectively). Similar to between-subject difference in psychophysical THR and DRs, the variability of the estimated eABR THR was high across subjects. For the eV amplitude feature, eABR THR in single pulse estimated from exponential fitting functions (FFs) were significantly larger than those in 4-pulses condition, (panel A; [$F(4, 28) = 5.65, p = 0.011$]). For the RMS feature, THR in single pulse were significantly larger than that in 8-pulses condition (panel C, [$F(4, 32) = 5.08, p = 0.040$]), when estimated from exponential FFs. No significant differences were found for eABR THR estimated from the peak PLVs. However, for the LVDP feature, more conditions had significantly different estimated eABR THR. THR estimated in the single pulse condition were significantly larger than those in the rest of the MP conditions (2-, 4-, 8-, and 16-pulse conditions; panel G; [$F(4, 44) = 19.87, p = 0.002, p = 0.001, p = 0.0003, p = 0.003$, respectively]). Significantly larger THR were estimated at 2-pulses condition, when compared to 8-, and 16-pulses conditions (panel G, [$F(4, 44) = 19.87, p = 0.001, p = 0.0497$, respectively]). Note that no extrapolation was used for the LVDP feature.

The median estimated eABR THR in all panels of Figure 4.5 decreased when the number of pulses increased from 1-pulse to 4-pulses (no significant differences for individual data). As shown in Table 4.2, for exponential FFs the median THR dropped by 50.4, 65.4, and 48.5 μA , respectively for eV amplitude, eABR RMS values, and peak PLV when the number of pulses increased from single pulse to 4-pulses. For linear fittings the corresponding values dropped by 75.3, 92.2, and 50.9 μA , which suggests larger drops (not significant) for linear FFs when compared to exponential FFs. For the LVDP feature, the median THR dropped by 51.9 μA when the number of pulses increased from 1 to 4. When the number of pulses increased from 4 to 8, in most conditions the median value increased and then decreased again from 8-pulses to 16-pulses (exceptions were panels E and g). Similar to the comparison between single pulse and 4-pulses conditions, larger (insignificant) drops were observed for linear FFs compared to exponential FFs, when the number of pulses increased from 1 to 16 (details in Table 4.2).

Statistical analysis showed that for a given condition in Figure 4.5, the eABR THR estimated from exponential FFs were significantly larger than those estimated from linear FFs (worst case $p < 0.04$). Due to the inherent nature of the exponential FF compared to the linear FF, the former overestimated the clinical THR more often than the latter. For wave eV, 85.9% of eABR THR estimates were larger than clinical THR, when estimated with the exponential FF (panel A), while being 58.3% when estimated with the linear FF (panel B). For RMS feature, the ratio of overestimation for the exponential and linear FFs were 84.5% and 56.3% (panels C, D), respectively, and for peak PLV the ratios were

eABR THR Estimation Using High-Rate Multi-Pulse Stimulation in Cochlear Implant Users

80.4% and 61.7% (panels E, F), respectively.

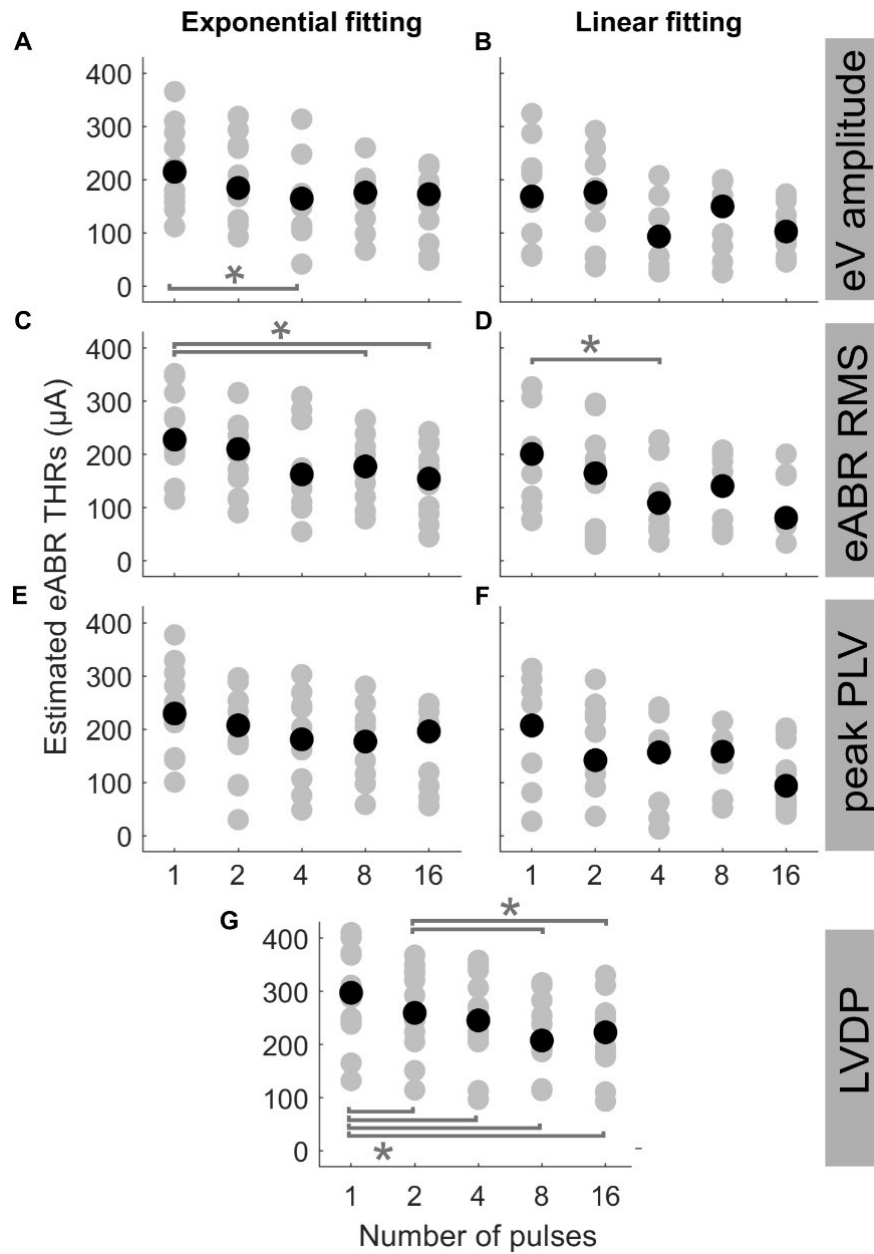


Figure 4.5 Estimated eABR THRs as a function of number of pulses, resulted from extrapolation of wave eV (panels **A** and **B**), eABR RMS value (panels **C** and **D**), peak PLV (panels **E** and **F**), and LVDP (panel **G**) growth functions. For each estimation method, an exponential function (left-side panels) and a linear function (right-side panels) were used for fitting. For the LVDP method, no estimation function was used. Data in gray shows results of individual subjects and data in black shows the corresponding median values across subjects. Asterisks show significant differences with $\alpha = 0.95$.

Table 4.2 Median estimated THR differences for different features and fitting functions.

Median estimated THR difference between	Feature	exponential	linear
1-pulse and 4-pulses (μA)	eV amplitude	-50.1*	-75.3
	RMS value	-65.4	-92.2
	Peak PLV	-48.5	-50.9
	LVDP	-51.9*	
1-pulse and 16-pulses (μA)	eV amplitude	-42.0	-66.0
	RMS value	-73.3	-119.9
	Peak PLV	-33.6	-113.7
	LVDP	-74.3*	

* shows statistically significant differences.

In order to examine the predictive power of the estimated eABR THRs presented in Figure 4.5, we plotted the ratio of estimated eABR THRs to the clinical THRs in Figure 4.6a-g, as well as the absolute difference between them in Figure 4.6H-N. The gray circles represent individual THRs and the black circles show the corresponding median values. The lower and upper error bars show the 25th and 75th percentiles, respectively. In Figure 4.6a (amplitude feature, exponential FF), the ratio of eABR THRs to the clinical THRs in single pulse and 2-pulses conditions were significantly larger than those in 4-pulses ($[F(4, 28) = 4.67, p = 0.026]$) and 8-pulses conditions ($p = 0.045$), respectively. For RMS feature in Figure 4.6C (exponential FF), the ratio between the two aforementioned THRs at single pulse was significantly larger than those at 8-pulses ($[F(4, 32) = 3.26, p = 0.009]$) and 16-pulses conditions ($p = 0.033$). For RMS features in Figure 4.6D (linear FF), the ratio at single pulse was significantly larger than those at 8-pulses ($[F(4, 20) = 6.80, p = 0.02]$) and 16-pulses conditions ($p = 0.03$). In panel G (LVDP), where median THR in single pulse condition was significantly larger than that in 2-, 4-, 8-, and 16-pulses conditions ($[F(4, 44) = 23.46, p = 0.018, p = 0.0003, p = 0.0006, \text{ and } p = 0.0002]$, respectively), and the median THR in 2-pulses condition was significantly larger than those in 8- and 16-pulses conditions ($p = 0.001, p = 0.012$], respectively).

In the absolute difference panels, significant differences were found in panels J (RMS, exponential FF) and N (LVDP). In Figure 4.6J, the absolute difference between eABR THRs and clinical THRs in single-pulse condition was significantly larger than that in 8-pulses condition ($[F(4, 32) = 3.53, p = 0.036]$). In panel N (LVDP), significant differences were found between the same pairs as in panel G (larger absolute differences for single-pulse condition compared to 2-, 4-, 8-, 16-pulses conditions: $[F(4, 44) = 19.87, p = 0.002, p = 0.001, p = 0.0003, \text{ and } p = 0.003]$, respectively]; larger absolute differences for 2-pulses condition when compared to 8-, and 16-pulses conditions: $p = 0.001, p = 0.0497$). In the ratio panels E-G, the median THRs monotonically decreased as a function of number of pulses, while for absolute difference panels, monotonic decrease of medians

eABR THR Estimation Using High-Rate Multi-Pulse Stimulation in Cochlear Implant Users

was only observed in panel N (LVDP).

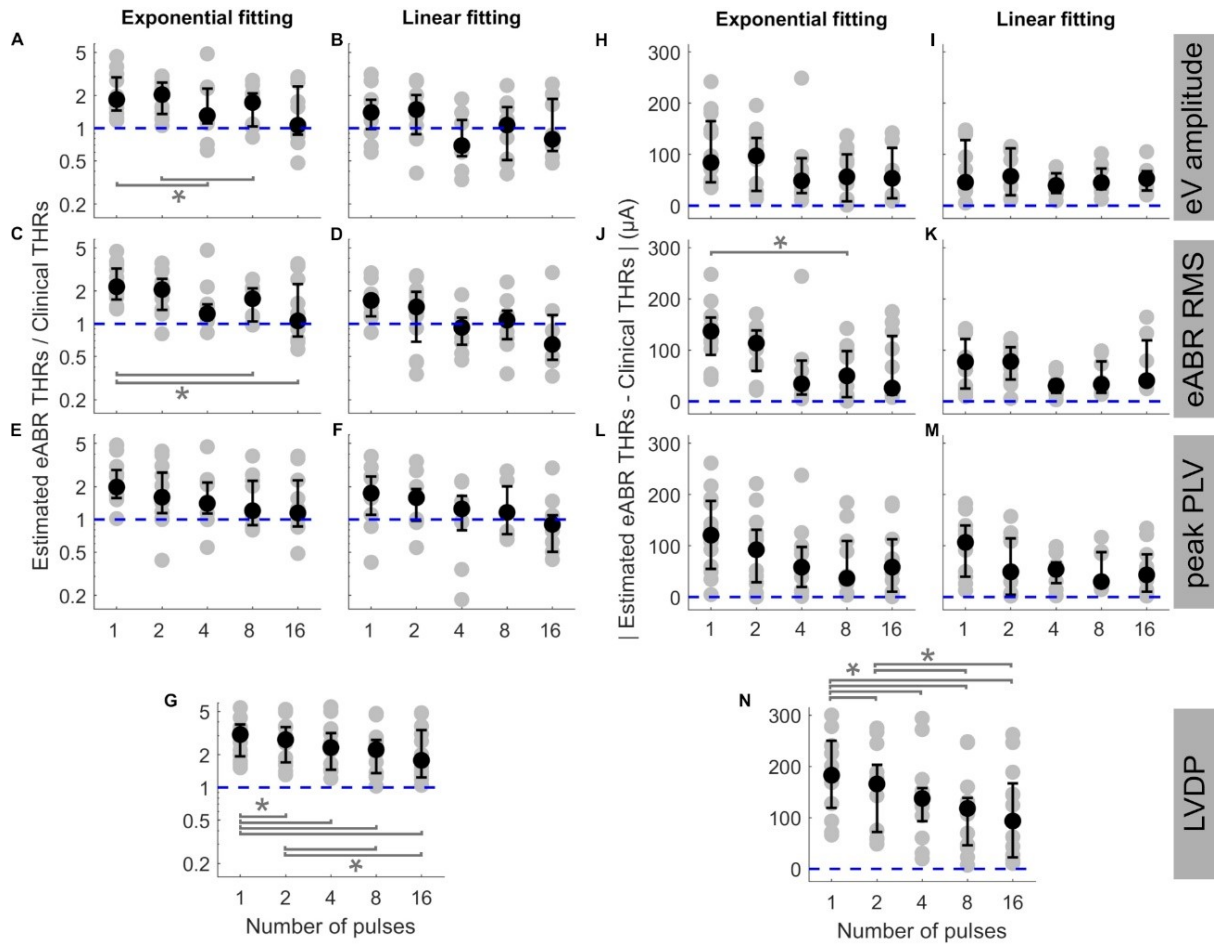


Figure 4.6 The ratio of estimated eABR THRs to clinical THRs (panels A-G) and absolute difference between them (panels H-N, respectively) as a function of number of pulses. The estimated eABR THRs were presented in Figure 4.5, which were resulted from extrapolation of growth functions of wave eV (panels A, B, H, and I), eABR RMS value (panels C, D, J, K), peak PLV (panels E, F, L, M), and LVDP (panels G and N, without any extrapolation). For each estimation method, an exponential function (left-side panels in each sub-figure) and a linear function (right-side panels in each sub-figure) were used for fitting. For the LVDP method, no estimation function was used. Data in gray shows results of individual subjects and data in black shows the corresponding median values across subjects. Lower and upper error bars show the mean 25th and 75th percentiles of median values from subsamples of growth functions, respectively. Asterisks show significant differences with 0.95 confidence intervals.

The ideal median ratio of 1 did not occur at the same MP condition. In Figure 4.6A, C, E, F, and G, the closest median ratios closest to 1 were found at 16-pulses condition (1.064, 1.065, 1.148, 0.902, and 1.778, respectively), while in Figure 4.6B and D, the ratios closest to 1 were 1.068 and 0.927. They occurred at 8-pulses and 4-pulses conditions, respectively (details in Table 4.3). Similarly, in absolute panels of Figure 4.6, the minimum of median values occurred at different MP conditions. In panels H, I, and K, the minimum median of absolute differences were found in 4-pulses condition (48.6, 39.5, 30.3 μA , respectively). In panels L and N, the minimum median values were 36.6 and 30.0 μA , respectively, which occurred at 4-pulse condition. In panels J and N, the minimum median values occurred at 16-pulses (25.9 and 93.5 μA , respectively). These results did not consider the between-subject variability and, therefore, might not reflect conditions with the best estimated eABR THRs that applies to majority of the subjects who participated in this study. Table 4.3 also shows the best conditions for the ratio of eABR THRs to clinical THRs (defined as A in Table 4.3) and the absolute difference between them (defined as B in Table 4.3), with considering the between-subject variability. For relation A , the expression $\min |A - 1|$ does not account for the between-subject variability, while the expression $\min |\log A| \times \text{mid}50$ was introduced to consider it. The variable $\text{mid}50$ represents the mid 50th percentile (75th percentile – 25th percentile). For relation B , the expression $\min B$ yields the absolute minimum of the differences between the two THRs, while the expression $\min B \times \text{mid}50$ would consider the data variability. In Table 4.3, conditions that minimized the aforementioned expressions are expressed in parenthesis. For a number of cases, conditions with the closest THR estimates remained unchanged, e.g. best conditions in expression A , when THRs were estimated with linear FFs. In other cases, however, conditions with the best THR estimates differed when considering the variable $\text{mid}50$. For instance, for RMS results and exponential FFs, the minimum of B occurred at 16-pulses, while the minimum of $B \times \text{mid}50$ occurred at 4-pulses condition. Data in Figure 4.6J is in line with this finding, as it suggests that 4-pulses condition would provide smaller median differences and at the same time smaller between-subject variability.

Figure 4.7 shows the eABR THR estimates as a function of psychophysical THRs for all MP conditions and estimation configurations. Individual data are depicted in black open circles. Each row presents eABR THRs resulted for a specific feature and a fitting function and each column shows results for a specific number of pulses. The black dotted lines show lines of equality and the blue lines show linear regressions. In each panel, the PCC (r) and the probability value (p) are shown. Except for 16-pulse conditions, PCCs were relatively high for the rest of the MP conditions and the corresponding p -values showed significance of the correlations. The eABR THRs estimated from linear FFs seem to underestimate the psychophysical THRs when compared to exponential FFs, i.e. data in panels B, D, and f tends to be below the lines of equality. Since no fitting was used for the LVDP feature, the THRs estimated with this feature overestimated the psychophysical THRs, i.e. data in panels G are above the lines of equality. High PCCs in Figure 4.7 show that it is, in principle, possible to predict behavioral THRs from eABRs. In the 16-pulses

eABR THR Estimation Using High-Rate Multi-Pulse Stimulation in Cochlear Implant Users

conditions, due to the low eABR amplitudes and the lack of enough data points of growth functions, THR estimations were unreliable and could not be performed for all subjects. This also resulted in statistically insignificant PCCs in all 16-pulses conditions. In order to compare the PCCs statistically, they were first transformed to z-scores via Fisher's r to z transformation and then z-test statistics were applied. For a given feature and MP condition, there was no significant differences between the PCCs of the two FFs (for instance, Figure 4.7C1 and D1). For neither exponential nor linear FFs, no significant differences were found between features, e.g. Figure 4.7A4 compared to C4 or E4). For a given feature and FF, comparison of PCCs of MP conditions showed significant differences only in 3 pairs (out of 60): 2- and 16-pulses, where RMS feature and exponential FF were used (Figure 4.7C2 and C5), single pulse and 16-pulses, where RMS feature and linear FF were used (Figure 4.7D1 and D5), and 2-, and 16-pulses, where amplitude feature and linear FF were used (Figure 4.7B2 and B5).

Table 4.3 Conditions with the closest eABR THRs to clinical THRs for different features and fitting FFs. For each of relations A and B , two expressions were defined, one without considering the between-subject variability ($\min|A - 1|$ and $\min B$, respectively) and the other with considering it ($\min|\log A| \times mid50$ and $\min B \times mid50$, respectively). The variable $mid50$ represents the mid 50th percentile (75th percentile – 25th percentile). Conditions (argument) in which the minima of expressions occurred are presented in parenthesis. nP: number of pulses.

	$A = \frac{eABR\ THRs}{Clinical\ THRs}$				$B = eABR\ THRs - Clinical\ THRs $			
	$\min A - 1 $ (arg min _{nPulses} A - 1)		$\min \log A \times mid50$ (arg min _{nPulses} \log A \times mid50)		$\min B$ (arg min _{nPulses} B)		$\min B \times mid50$ (arg min _{nPulses} B \times mid50)	
	exponential	linear	exponential	linear	exponential	linear	exponential	linear
Amplitude	1.064 (nP=16)	1.068 (nP= 8)	0.042 (nP=16)	0.030 (nP= 8)	48.6 (nP= 4)	39.5 (nP= 4)	3315.6 (nP=4)	1530.6 (nP= 4)
RMS	1.065 (nP=16)	0.927 (nP= 4)	0.039 (nP= 4)	0.016 (nP= 4)	25.9 (nP=16)	30.3 (nP= 4)	2295.6 (nP=4)	774.1 (nP= 4)
PLV	1.148 (nP=16)	0.902 (nP=16)	0.086 (nP=16)	0.026 (nP=16)	36.6 (nP= 8)	30.0 (nP= 8)	3013.7 (nP=8)	1968.3 (nP= 8)
LVDP	1.778 (nP=16)		0.479 (nP= 8)		93.5 (nP=16)		8921.8 (nP=4)	

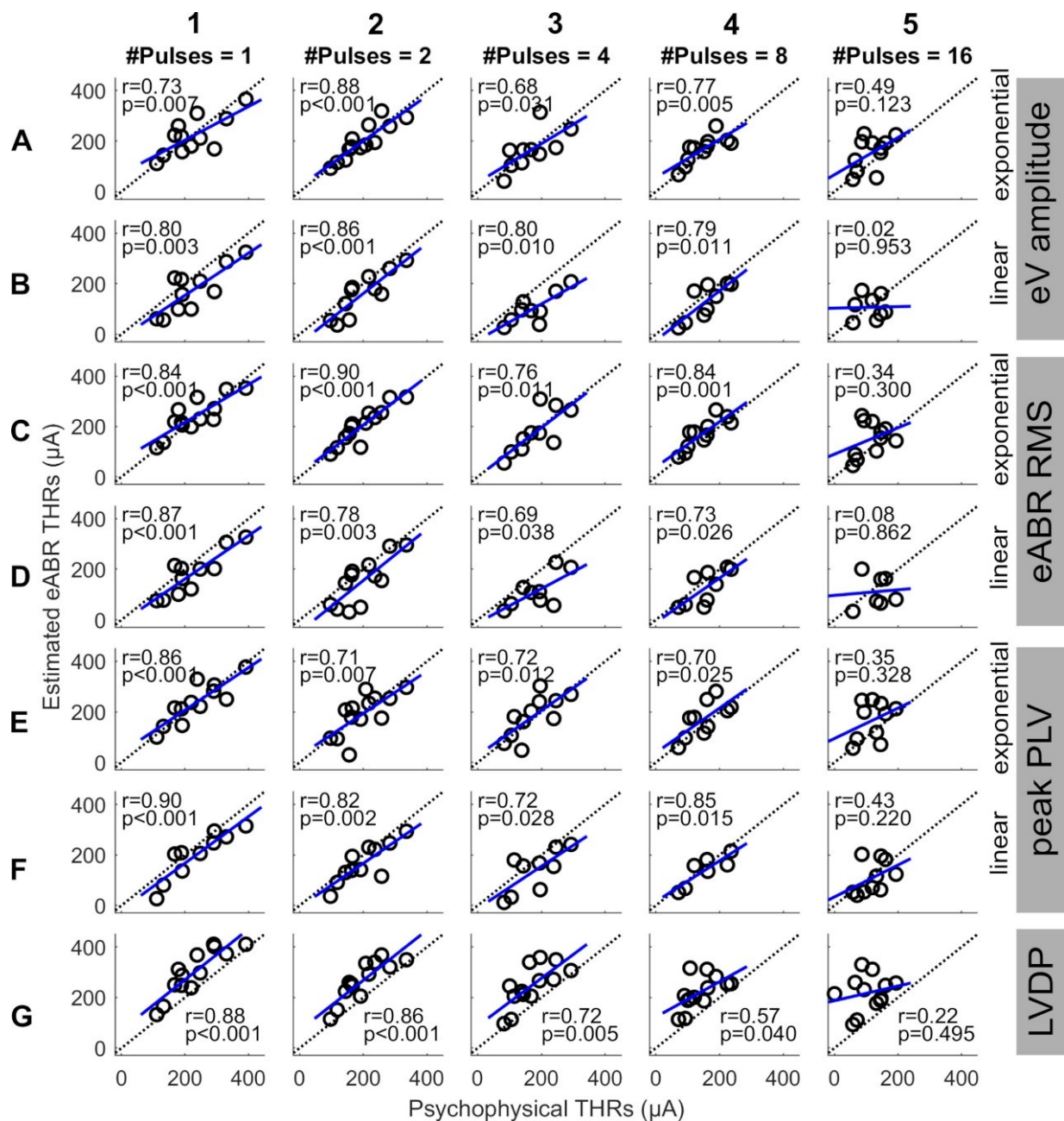


Figure 4.7 Estimated eABR THRs as a function of psychophysical THRs for multi-pulse conditions. Each column shows results of a specific number of pulses. Panels in **A** and **B** show the eABR THRs estimated from AGFs of wave eV with exponential and linear fittings, respectively. Data in panels **C** and **D** present the eABR THRs estimated from growth functions of eABR RMS values with exponential and linear fittings, respectively. Panels **E** and **F** present the eABR THRs estimated from growth functions of peak PLV with exponential and linear fittings, respectively. Panels in **G** show the eABR THRs resulted from the LVDP method. Open circles present data from individual subjects. Dotted black lines show the identity lines and the blue lines show linear regressions. In each panel, the correlation coefficient (r) and the probability value (p) are shown.

Since this study aimed to estimate clinical THRs, the estimated eABR THRs were plotted as a function of clinical THRs in Figure 4.8 and correlated. Except for 16-pulse conditions (panels in column 5) and for panel D3, the PCCs in Figure 4.8 were smaller than their corresponding values in Figure 4.7. Similar to Figure 4.7, the PCCs in the 16-pulses conditions were all statistically insignificant and thus were excluded from further analysis. For the linear FFs (panels B, D, and F), the PCCs in the 4-pulses conditions were larger than their corresponding PCCs in the other MP conditions. The largest PCC over all conditions ($r = 0.83$, $p = 0.005$) was resulted from linear fitting of growth functions of the eABR RMS values at the 4-pulses condition (panel D3). Similar to Figure 4.8, for a given feature and MP condition, comparison of PCCs of the two FFs revealed no significant differences (e.g. Figure 4.8E2 and F2). For neither exponential nor linear FFs, no significant differences were found between combinations of the two features, e.g. Figure 4.8B5 compared to D5 or F5). Finally, for a given feature and FF, comparison of PCCs of MP conditions showed significant differences only between 4- and 16-pulses conditions, where the RMS feature and linear FF were used (Figure 4.7D3 and D5).

4.4 Discussion

The aim of this study was to examine the capability of the eABR THRs in response to MP stimulations to predict clinical THRs. We employed 1-, 2-, 4-, 8-, and 16-pulse burst stimuli with a fast burst rate of 10000 pps. We found that the behavioral THRs in response to MP stimuli approached clinical THRs when the number of pulses increased from 1 to 16 (Figure 4.3). Moreover, the between-subject range of the difference between psychophysical THRs and clinical THRs dropped by about 2.3 dB (Figure 4.3B), and the range of absolute difference by about 4.9 dB (Figure 4.3C), when the number of pulses increased from 1 to 16. These findings were the motivation to see whether similar findings can be observed in eABR measurements, too. We have tested various methods to extrapolate eABR THRs and evaluated, how well they coincided with clinical THRs and found that MP stimulation protocols indeed provide a better estimate than single pulses, although, inter-subject variability was high. Recording of each stimulation amplitude of MP conditions took about 59 seconds. If the time spent for subject preparation is excluded from the total measurement time, and if only one MP condition is used to extrapolate THRs, the recording time would be below 10 minutes (10 stimulation amplitude steps for the AGF \times 59 seconds). This is comparable to the smallest recording time reported by Mao *et al.* (2018) (12.7 ± 3.1 minutes), and to the 10-minute measurement conditions reported by Mao *et al.* (2019), but still larger than the 5-minute measurement conditions in the same study.

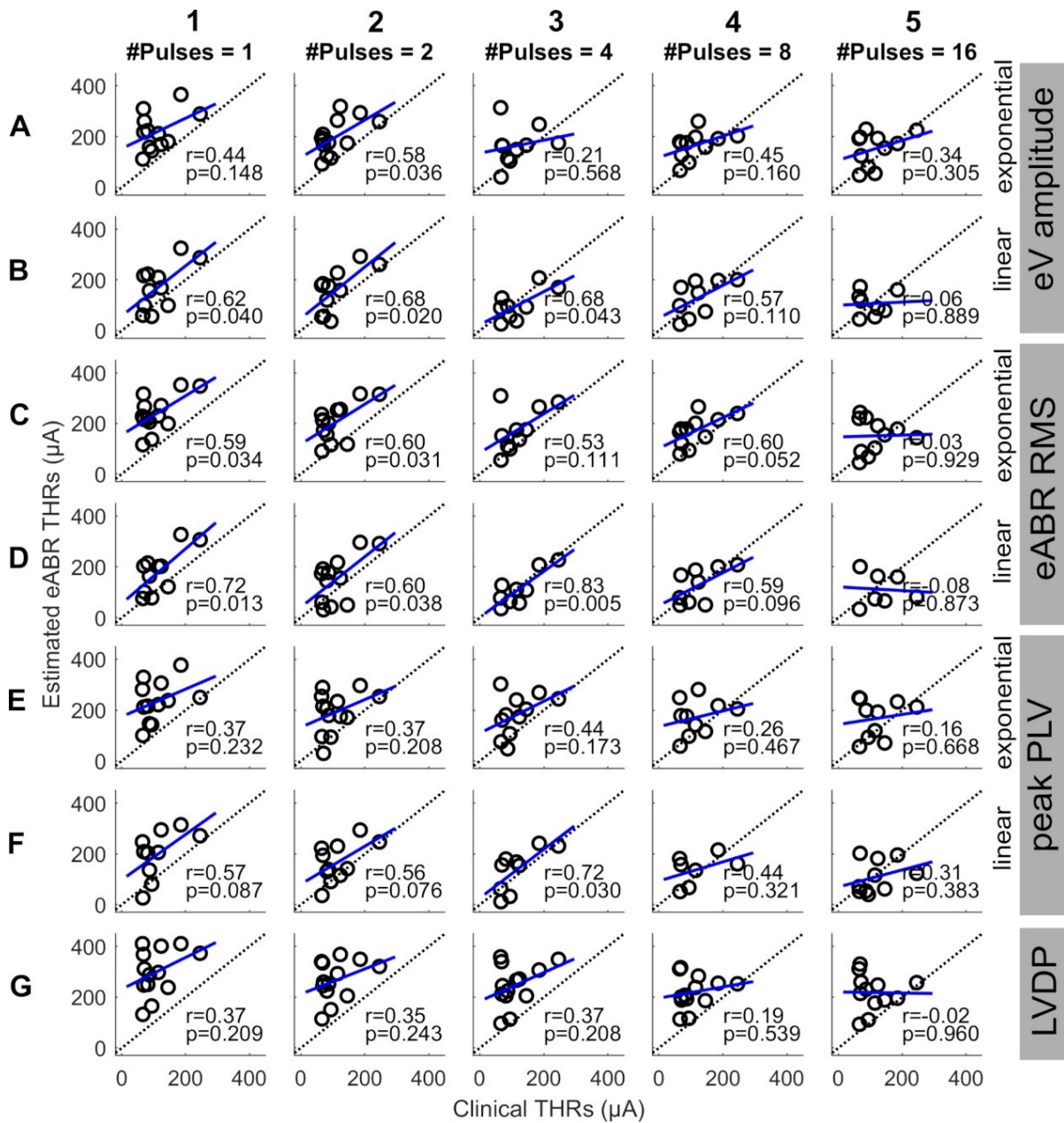


Figure 4.8 Estimated eABR THRs as a function of clinical THRs for multi-pulse conditions. Each column shows results of a specific number of pulses. Panels in **A** and **B** show the eABR THRs estimated from AGFs of wave eV with exponential and linear fittings, respectively. Data in panels **C** and **D** present the eABR THRs estimated from growth functions of eABR RMS values with exponential and linear fittings, respectively. Panels **E** and **F** present the eABR THRs estimated from growth functions of peak PLV with exponential and linear fittings, respectively. Panels **G** show the eABR THRs resulted from the LVDP method. Open circles present data from individual subjects. Dotted black lines show the identity lines and the blue lines show linear regressions. In each panel, the correlation coefficient (r) and the probability value (p) are shown.

4.4.1 eABR THR estimation

Due to the variable trend of the AGFs of electric and acoustic hearing, linear (Mao *et al.* 2018) and non-linear regressions (Ross *et al.* 1999; Abbas and Brown 2015; Visram *et al.* 2015; Mao *et al.* 2019) were used for extrapolation of the AGFs. Mao *et al.* (2018) showed that linear regression can perform equally well when compared to exponential regression. In the study of Mao *et al.* (2018), the baseline value was defined as the point where the extrapolated FF was zero (x-intercept) while Visram *et al.* (2015) and Mao *et al.* (2019) defined the baseline as the point where the extrapolated FF equals to the response to -20 dB sensation level (noise floor). The THRs estimated from the latter were usually larger than those estimated from the former, due to the monotonic increase of the exponential function. In this study, we used growth functions of two time features (wave eV amplitude and RMS value) and one time-frequency feature (peak PLV) to estimate eABR THRs and the zero baseline criterion for THR estimation (Figure 4.6).

As Table 4.3 suggests, for the two criteria (ratio and absolute difference) the closest eABR THRs to clinical THRs occurred at different MP conditions depending on the two FFs as well as on different expressions used to find the minima. Results in Table 4.3 showed that without considering the between-subject variability, the MP condition with the closest eABR THRs to clinical THRs could be misleading. As expressions *A* and *B* (in Table 4.3) treat the relation between the estimated eABR THRs and clinical THRs differently, it is not possible to directly compare the corresponding conditions in each expression. The dimensionless expression *A* cares about the relative difference of the eABR THRs, while expression *B* considers the absolute linear difference between the two THRs. Presuming two subjects with hugely different hearing DRs, estimation errors of $\pm 50 \mu\text{A}$ would be treated identically by the expression *B*, while expression *A* would treat them differently and more realistically. On the other hand, expression *A* differentiates underestimations from overestimations, and, thus, it treats them differently. For instance, for a given clinical THR of $50 \mu\text{A}$ with estimation errors of $\pm 25 \mu\text{A}$, expression *A* would result in ratios of 1.5 ($75\mu\text{A}/50 \mu\text{A}$) and 0.5 ($25\mu\text{A}/50\mu\text{A}$), while expression *B* would treat both errors identically, and assuming an enough large DR, more realistically. Therefore, depending on the THR value, the DR, and required accuracy and sensitivity of estimation, one expression could be used over the other.

In this study, no attempt was made to measure the noise floor in response to stimulus far below the THRs. Therefore, it was not possible to compare the zero baseline method with the noise floor method used for THR estimation. Similar to Visram *et al.* (2015) and Ross *et al.* (1999), we defined the THR at a location where the extrapolated FFs were zero. This procedure is responsible for the small underestimation of eABR THRs relative to psychophysical THRs, which can be detected in most conditions of Figure 4.7. Therefore, when data with more subjects is available, a compensation of this bias could further improve the accuracy of eABR THR extrapolation. (Mao *et al.* 2018).

4.4.2 eABR THR vs. psychophysical THR and clinical THR

In Figure 4.3B, C, the difference and the absolute difference between psychophysical THR and clinical THR monotonically decreased when the number of pulses increased from 1 to 8. From 8-pulses to 16-pulses, the difference further decreased while the absolute difference remained almost the same. Yet, the between-subject range was smaller in the 16-pulse condition when compared to that in the 8-pulse condition. This suggests that psychophysical THR with 16-pulses could be used as estimations of the clinical THR with the smallest offset of about 2.0 dB and the smallest between-subject variability of 5.3 dB, when compared to other MP conditions. However, in Figure 4.6 the absolute difference between estimated eABR THR and clinical THR in 16-pulses condition were not always the smallest. This can be explained by the insignificant correlations between psychophysical THR and estimated eABR THR (Figure 4.7, column 5). The fact that eABR THR estimates at 16-pulses failed to show significant correlation with psychophysical THR could be attributed to two factors: first, the subject-dependent desynchronization of the auditory nerves is largest at 16-pulses condition (especially for the PLV feature), and second, the small number of data points in 16-pulses conditions due to the smaller eABR amplitudes. These reasons severely compromised the precision of THR estimates (right column in Figure 4.7) and led to large differences to clinical THR (Figure 4.6).

Although the PCCs in single pulse conditions of this study (between 0.73 and 0.90) were smaller than those reported in the literature (e.g. $R = 0.98$ in Truy *et al.* (1998)), we observed that the PCCs were significant and still relatively large for all but 16-pulses conditions (Figure 4.7). This suggests that up to 8-pulses, the eABR THR seem to be able to well represent their corresponding psychophysical THR, and thus, could be able to estimated clinical THR. As Figure 4.6 and **Table 4.3** suggest, with considering between-subject variability, eABR THR in 4- and 8-pulses conditions estimated the clinical THR better than the other MP conditions. However, as the medium values of the PCCs in shows, eABR THR in none of the MP conditions were able to represent all aspects of the temporal integration elicited by clinical stimuli. The PCCs of the PLV feature in the single pulse condition (0.73 and 0.80, respectively for exponential and linear FFs) were smaller than the PCCs of 0.979 and 0.966 reported in Mao *et al.* (2019) for Cz-M and Cz-closest montages, respectively. Such a better performance in their study might be due to the fact that they measured responses from more central locations of the auditory pathway, thus resulted in higher correlations between behavioral THR and CAEP THR. Since Mao *et al.* (2019) did not measure clinical THR (they measured response to 50-ms electric stimuli), and therefore, it is not possible to compare the PCCs between clinical THR and eABR THR measured from the PLV feature. However, they mentioned two methods to estimate clinical thresholds with longer (500 ms) clinical stimulation: using a correction factor to compensate for the longer stimulation duration, or using longer stimuli, however, these would cause interference with the recorded CAEPs. In this study, we have hypothesized that packing as many pulses as possible within a short stimulation

period (longest duration was 1.6 ms) would at least partially consider integration effects and allow us to estimate clinical THRs with higher precision. We plan to extend the multi-pulse stimulation paradigm for CAEP modalities in the future. With the stimulation configuration used in this study, one can pack up to 500 pulses (each of length 100 μ s) to construct a 50-ms burst. We assume that measurements with more pulses at more central locations of the auditory pathway could potentially yield even better objective THR estimates.

Fully objective estimation of thresholds of normal and electrical hearing is still challenging from some aspects such as accuracy of the method, measurement equipment, and measurement time. Intra-cochlear measurements, e.g. eCAP, which are provided by the telemetry systems of current implants have their limitations as they can only assess peripheral effects and responses to single pulses. Therefore eCAPs are unable to cover temporal loudness integration, which occurs at higher levels of the auditory pathway. Measurements from mid- to central locations of the auditory pathway usually need additional equipment and longer measurement time to capture more epochs to increase the signal-to-noise ratio. In some measurements such as event-related potential measurements, active listening of participants is required. This makes these methods not applicable to estimate THRs in young babies. However, methods with high precision estimation of THRs are proposed (Visram *et al.* 2015; Mao *et al.* 2018; Mao *et al.* 2019), where they used CAEPs to estimate behavioral THRs. Another issue regarding estimation of behavioral THRs is overestimation, where estimated THRs are larger than behavioral THRs, which reduces the available dynamic range of the CI users.

The eABR seems to be able to estimate behavioral THRs (particularly clinical THRs) at least to some extent. Results of this study show that eABR THRs in response to high-rate multi pulse stimuli could in principle improve objective estimation of clinical THRs. As the stimulation to elicit eABR has to be shorter than some milliseconds to separate stimulation artifacts from eABR responses, loudness integration, which has still longer time constants, cannot be completely covered. Yet, the longer stimulation duration in MP eABRs compared to single pulse measurements (eCAP, single pulse eABRs) at least cover some of the temporal processing aspects and therefore provide a more precise estimation of clinical THRs. Still higher and later potentials might enable even longer lasting stimuli and be able to cover slower effects as loudness integration at more central levels of the auditory system (Abbas and Brown 2015) with higher precision. On the other hand, higher potentials (CAEPs, eASSR) in young children depend highly on the development of the auditory pathway, which makes their measurement and interpretation harder. However, studies have shown that CAEPs are developed in months-old children (Sharma *et al.* 2002, 2002), with quite stable latencies from birth to age 6, and decreasing P1 and N2 amplitudes and increasing N1 and P2 amplitudes (Wunderlich *et al.* 2006). It is straight-forward to extend the methods to higher auditory potentials. Our paper provides methods for THR extrapolation of eABRs with extended stimulus durations which should cover higher processing steps as facilitation and, at least partly, temporal

loudness integration. These features hold the potential to improve the process of clinical THR estimation with objective measurements.

Accurate clinical THR estimation is important for improvement of CIs' functionality. Among CI manufacturers, MED-EL and Advanced Bionics set the THRs to 0 clinical units (CU) or 10% of the maximum acceptable levels (Wolfe and Schafer 2014). The 0 CU would underestimate real THRs while 10% of the MAL could either under- or overestimate the real THRs. In both cases, speech would not be optimally coded within the small dynamic range available for CI users and accurate estimation of the THRs with MP stimulation could improve the performance of the CIs in either case.

In summary, the main contributions of this study are:

- eABRs to bursts of high rate could estimate clinical THRs with smaller errors.
- For the longest pulse trains (1.6 ms, 16 pulses) eABR amplitudes were reduced due to interference, which limited the measurement precision.
- Correlation between eABR THRs and their corresponding psychophysical THRs was generally large (except for 16-pulses) when compared to those between eABR THRs and clinical THRs.
- MP condition at which the smallest difference between eABR THRs and clinical THRs occurred, varied between 4-, 8-, and 16-pulses conditions.

Chapter 5

Summary, Conclusion, and Outlook

This thesis investigated characteristics of eABRs to multi-pulse stimuli at very high burst rates (10 kpps) and examined the feasibility of estimation of clinical THR_s using eABR THR_s in response to such high-rate stimuli. Main findings of the thesis were published in two research papers and their contents were presented in Chapter 3 and 4.

Chapter 3 investigated the psychophysical THR_s and MCL_s as well as characteristics of eABRs to single-pulse, 2-, 4-, 8-, and 16-pulses stimuli, including eABRs' general morphology, amplitude and latency growth functions, and the effect of number of pulses on the eABRs. As an effect of temporal and loudness integration, THR_s and MCL_s decreased monotonically with slopes of -1.30 and -0.93 dB/doubling the number of pulses, respectively. These slopes are equivalent to decrements of 6.30 and 4.65 dB for THR_s and MCL_s, respectively, when the number of pulses increased from 1 to 16. When the total charge of the burst (total burst charge: TBC) that is needed to reach THR_s and MCL_s was considered, it significantly increased as a function of number of pulses. This is, at least partially, an underlying reason which explains the reduction in the THR_s and MCL_s, and consequently the temporal integration. However, comparing the slopes of THR_s (or MCL_s) drop and the slope of increase of TBC in a given MP condition suggests that MP stimuli are inefficient (see Figure 3.6). If the efficacy was 100%, one would expect that in comparison to the single-pulse condition, m -pulses stimulus would need a reduced amplitude by a factor of $\frac{1}{m}$ to elicit the same THR as in single-pulse condition. However, such a proportionality was by far not observed in our measurements, which indicates that the neuronal integration process must be quite leaky.

The general morphology of eABRs to MPs did not differ from that of ordinary (single-pulse) eABR. Therefore, the traditional wave eV amplitudes were used for analysis. Despite occasional dents, amplitude growth functions were almost monotonic in all MP conditions. However, there was a decreasing tendency in wave eV amplitude and an increasing tendency in wave eV latency, when the number of pulses increased from 1 to 16 (Figure 3.11). However, as Figure 3.7 suggests, the degree of eABR multi-pulse integration was not consistent within subjects. For a few subjects (e.g. S2L, S3L, and S4R), wave eV amplitudes grew as more pulses were presented, with the stimulation amplitude kept constant. For other subjects, wave eV amplitudes increased up to a certain subject-specific number of pulses and then saturated or decreased. In S3L, for instance, the amplitude decrease started at 2-pulses condition, while for S4L, in MSA16, the decrease started at 4-pulses condition. Even for a given subject, the condition where the

decrease occurred was not always identical. For S6L, the start of negative slope in MSA4, MSA8, and MSA16 happened at 2-pulses, 4-pulses, and 8-pulses conditions, respectively.

Comparing the eABR wave eV amplitudes at maximum stimulation amplitude (MSA) of each MP condition also supports the finding of large charge loss in multi-pulse stimulation. We assumed that all MSAs (MSA1-MSA16) would probably induce similar, if not the same, hearing sensation, which were close to the corresponding MCLs. Thus, one would expect the eABR characteristics and amplitudes to these stimuli, e.g. wave eV amplitudes, to be similar. However, Figure 3.13A shows that wave eV amplitudes at MSAs (95% of the corresponding DRs of MP conditions) decreased monotonically and, in most of the cases, significantly. At the same time, as depicted in Figure 3.13B, charge at MCLs and consequently at MSAs significantly increased as a function of number of pulses. Therefore, it seems that using more charge led to a decrease in eABR wave eV amplitudes, which one might usually not expect. In Figure 3.12, we suggested one possible reason for such a contradiction, where we estimated the individual and group components of eABRs by subtracting responses with the same stimulation amplitude, but with different stimulation amplitude. As shown in Figure 3.12, the amplitude of the first pulse dominated the overall response, whereas the amplitudes of the following components were smaller and also delayed systematically. For instance, the response peak of the component $eABR_{9..16}$ (extracted eABR to the 9th-16th pulses in the train) occurred at around 5.2 ms after stimulus onset, while the latency of the response peak of the second pulse ($eABR_2$) was at around 4.0 ms. The differences in latencies led to destructive interference, which generally suppressed the overall response. Therefore, a reduced wave eV amplitude might not necessarily be a result of less activity of brainstem neurons, but might be caused by the interactions between different and time-shifted components of the original responses.

The extent of temporal- and loudness integration is thought to be closely related to the neural survival and health state (Zhou and Dong 2017) of the SGNs. Therefore, eABR wave eV MP integration characteristics could be a predictor for neural population health. If there would be a high correlation, this objective measure could be used in conjunction with or even instead of imaging techniques (MRI or CT-scans) used now to estimate the health state of neurons and thus candidacy of a CI. This speculation, however, requires further examinations.

In Chapter 4, we have investigated the feasibility of using eABRs for estimation of clinical THR. The choice of eABR as an objective measure was a compromise between peripheral and central measures of auditory neuronal responses. Peripheral measures such as eCAPs usually overestimate clinical THR, as they characterize responses to single pulse stimuli with low-rate. Therefore, they fail to account for the temporal integration effects observed in the clinical setting, where pulse trains of relatively high-rates are applied. There are limitations when centrally evoked potentials are recorded in infants and newborns, as the auditory pathway may not be developed at their age. Moreover, as

Summary, Conclusion, and Outlook

such cortical potentials are sensitive to attention, it can be difficult to measure them in this population. We hypothesized that using eABRs to high-rate multi-pulses could, at least partially, compensate the temporal integration missed in eCAPs.

The same MP stimuli as described in Chapter 3 was employed and growth functions of four features were used to obtain eABR THRs in each of MP conditions. The features were the amplitude, RMS value, and peak of phase-locking value (peak-PLV, as used by Mao *et al.* (2018); Mao *et al.* (2019)), and lowest valid data point (above the noise floor) in the amplitude growth function. The growth functions of the features were fitted and extrapolated with linear- and an exponential functions. The value at which the fitting function crossed zero was selected as the eABR THR. Although extraction of objective THRs share some general steps such as the usage of growth functions of some features and extrapolation of such features, they still differ in some aspects. For instance, different studies have used different temporal and/or spectral features for THR estimation. The details of the procedures of THR estimation also varies. For example, Visram *et al.* (2015) and the study in Chapter 4 of this thesis have defined the estimated THR at a location, where the fitting function of a given feature equals to zero (parameter b in fitting functions of Eqs. 4.2 and 4.3), to a baseline value (Mao *et al.* 2018; Mao *et al.* 2019) or to a fixed value of $0.1 \mu\text{V}$ (Macherey *et al.* 2021). Although no study has attempted to investigate the effect of such variabilities, one can intrinsically observe how different methods could lead to different results. For instance, using a baseline value for THR estimation leads to larger estimations, when compared to the zero crossing. Therefore, besides the natural differences in responses which are, at least partly, due to different stimulation configurations, such technical variations could also play a role in the precision of the proposed methods.

Psychophysical THRs evoked from MP stimuli in **Figure 4.3** showed that they can closely approach clinical THRs. In 16-pulses condition, the median difference between psychophysical and clinical THRs was about -0.80 dB (absolute difference of 2.1 dB in **Figure 4.3C**), which suggests that it is worthwhile to employ these MP stimuli for eABR measurements. Both time (wave eV amplitude and the RMS value) and time-frequency features used for eABR THR estimation, generally showed monotonic growth functions (see **Figure 4.4**). In **Figure 4.6**, we used the ratio as well as the absolute difference of estimated eABR THRs and clinical THRs (expressions A and B in **Table 4.3**) to examine the goodness of THR estimates. The best values of expressions A and B (ratio of 1 and absolute difference of 0, respectively) for different features and fitting functions were observed at different MP conditions. For instance, the best value of expression A for PLV features and exponential fit occurred in 16-pulses condition ($A = 1.148$), while the best value of expression B for the same condition was observed in 8-pulses condition ($B = 36.6$). As the inter-subject variability was high in **Figure 4.6**, we also considered the mid-50th (*mid50*) percentile as a measure of dispersion. Therefore, we also calculated the best values of expressions A and B with considering the *mid50* values (see **Table 4.3**).

Figure 4.7 suggests that up to 8-pulses, the correlation between psychophysical THR_s and eABR THR_s was relatively high for all features and fitting functions. Therefore, it seems that eABR_s in response to MP conditions up to 8-pulses can well represent their corresponding psychophysical THR_s. As **Figure 4.8** shows, in only a few conditions, the correlation between eABR THR_s and clinical THR_s was fairly high (e.g. 0.83 for the RMS feature and the linear fit). This suggests that although MP stimuli might be able to partially account for temporal loudness integration occurring in the auditory pathway, they are still unable to fully represent such temporal integrations. This is, at least partly, because of the fact that the integration mechanisms remain active up to the most central stations of the auditory pathway. Therefore, eABR_s seem to be unable to cover such integration activities which occurred after the lateral lemniscus. In order to cover the integrations missed by eABR_s, employing central potentials such as CAEP_s could be beneficial. With a 100 μ s-long pulse train, one can pack up to 500 pulses into a 50-ms window, which is short enough to allow capturing cortical potentials (e.g. N1-P2 complex, which occurs about 100 ms after the stimulus) without being interfered by the stimulation artifact. This would remain as a future topic for investigation.

Objective estimation of THR_s in normal and electric hearing is an ongoing research topic and it still faces challenging aspects such as the precision and the amount of time needed for measurements. Hearing THR_s are perceptual concepts, which means they result from the interactions between different stations of the auditory pathway, from the outer ear in normal hearing listeners or auditory nerve fibers in CI users to the central auditory cortex. Therefore, one might imply that objective estimation of such THR_s is only possible by using measures from the central auditory system, such as CAEP_s. However, we showed that eABR_s are capable of objectively estimating psychophysical and, at least to some extents, clinical THR_s. This is especially important for situations, where measuring of central potentials are not possible. This is the case in young children, whose auditory pathway is not not-fully developed. Nevertheless, investigating CAEP THR_s remains worthwhile for investigation of objective estimation of clinical THR_s.

A

Supplementary material for Chapter 3

In this chapter, appendices are shown. Note that, you can add up to two levels to the appendices, e.g. A1.1.

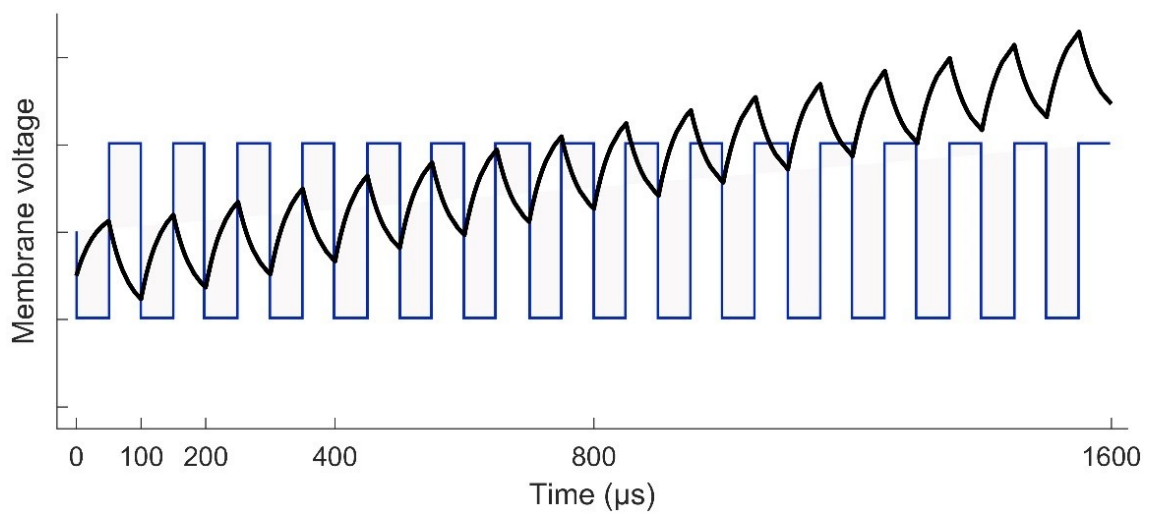


Figure A.1 Schematic illustration of charge integration of a neuron with nonlinear conductance in 16-pulses condition.

List of Figures

Figure 1.1 Monopolar (A) and Bipolar (C) stimulation configuration and their corresponding electric fields (B and D). The drawings in B and D were adapted with modification from (Schnupp <i>et al.</i> 2011).	4
Figure 1.2 Schematic illustration of virtual electrode (current steering). The focus of stimulation will in the midpoint of the two electrodes when the stimulation currents on the two adjacent electrodes are equal (A). When the stimulation current dominates at one electrode, the stimulation focus will be toward that electrode (B).....	4
Figure 1.3 Schematic illustration of continues interleaved sampling (CIS).....	7
Figure 1.4 Schematic presentation of n-of-m strategies (e.g. ACE). Filter outputs with the highest amplitude are with electric pulses and delivered to the electrodes (here electrodes 2, 3, and 6). The remaining channels are not used during this cycle, as they had lower amplitudes.	9
Figure 1.5 Schematic illustration of three common methods to reduce artifact stimulation in calculation of eCAPs.....	12
Figure 1.6 Sample ABR (A) and eABR (B) signals in response to low, medium, and high stimulation amplitudes.	15
Figure 2.1 Temporal response properties of stimulus-response phenomena in auditory nerve fiber. (A): Refractoriness, (B): facilitation (temporal summation), (C) accommodation (subthreshold adaptation), and (D): spike-rate adaptation. The gray curves represent stimuli and the black ones show nerve responses. Figure adapted and modified from Boulet <i>et al.</i> (2016).	18
Figure 3.1 Shape of multi-pulse stimuli used in the study.	33
Figure 3.2 eABR multi-pulse measurement conditions (n.m. means not measured). ...	35
Figure 3.3 Setup for electrical stimulation via CI and eABR recording.	35
Figure 3.4 Surface electrode recordings (blue curves) and exponential fittings of stimulation artifacts (only after stimulation, red curves). Left column shows two-exponential fittings and right panels show one-exponential fittings. In each panel, the number of pulses and the stimulation amplitude is indicated. Note that the stimulation artifact exceeds the range displayed in the figure.	37
Figure 3.5 Exemplary final eABRs for three subjects (columns) in multi-pulse conditions (rows). The stimulation amplitudes and the number of pulses are indicated in each panel. Significant peaks and troughs eIII are marked with filled black and red diamonds, respectively. Peaks and troughs of eV are shown with filled black and red circles, respectively. Horizontal red lines indicate $\pm 2\sigma RN2$. The minimum number of epochs used for averaging (min N) is indicated for each subject.....	38
Figure 3.6 (A) Psychophysical THR and MCL currents (in dB re 1 μ A) and (B) Total burst charge (TBC) (dB re 1 nC) for 14 subjects (19 ears). Values differed significantly between all conditions ($p < 0.05$).	39
Figure 3.7 eABR wave eV amplitudes corresponding to the 15 measurement conditions mentioned in Figure 3.2. Curves with specific colors represent responses to stimuli with	

fixed stimulation amplitude and varying number of pulses. Error bars indicate $\pm 2\sigma RN2$.	41
Figure 3.8 eABR wave eV latencies corresponding to the 15 measurement conditions mentioned in Figure 3.2. Curves with specific colors represent responses to stimuli with fixed stimulation amplitude and varying number of pulses.	42
Figure 3.9 eABR eV amplitudes of multi-pulse conditions over all subjects. In each panel, the stimulation amplitude is constant (MSA2, MSA4, MSA8, MSA16 in panels (A-D), respectively). Data from individual subjects are plotted in gray circles and their corresponding median values in colors, which match the colors in Figure 3.7. In each panel, data were normalized to (divided by) the corresponding responses at the largest number of pulses (2-, 4-, 8-, and 16-pulses in panels A-D, respectively). Data of MSA1 condition (blue points in Figure 3.7) are not plotted, as all were 1 due to normalization. The asterisk shows pairs with significant difference.	43
Figure 3.10 eABR eV latencies of multi-pulse conditions over all subjects. In each panel, the stimulation amplitude is constant (MSA2, MSA4, MSA8, MSA16 in panels (A-D), respectively). Data from individual subjects are plotted in gray circles and their corresponding median values in colors, which match the colors in Figure 3.7. Data of MSA1 condition (blue points in Figure 3.7) are not plotted, as all were 0 due to normalization. The asterisk shows pairs with significant difference.	45
Figure 3.11 Wave eV amplitude growth functions (A) and latency functions (B) as a function of stimulation amplitude in all MP conditions for 8 ears (last column of Table 3.1). The amplitude data was normalized to the largest valid wave eV amplitudes in 1-pulse condition for each ear. Results from individual subjects are plotted in open gray circles, while the corresponding median values are plotted in filled black circles.	46
Figure 3.12 eABRs to individual pulses and groups of pulses in 16-pulses condition for subject S8L. Note the peaks and troughs of responses to successive pulses and groups of pulses, which suppress the response to the first pulse (eABR _{1p}). This destructive interference effect may explain the decrease of the eV amplitude in multi-pulse conditions.	49
Figure 3.13 Comparison of psychophysical and eABR results. eABR wave eV amplitude at MSAs (95% of psychophysical MCLs) (A), and corresponding stimulation TBCs led to psychophysical MCLs (B). All data are normalized to their corresponding values at 16-pulses condition. The ‘n.s.’ in red in panel (A) show <i>not significant</i> differences between 1-pulse and 2-pulses and between 4-pulses and 8-pulses. The difference between the rest of the pairs were significant. In panel (B), all pairs were significantly different.	50
Figure 4.1 Stimuli used in clinical measurements (A) and in eABR measurements (B). Stimuli in panel b were presented at a repetition rate of 37 bocks-per-second.	57
Figure 4.2 Illustration of eABR THR estimation for subject S8L. (A): valid eABRs in each MP condition. In each panel, eABRs to different stimulation amplitudes are plotted. (B): corresponding growth functions (blue circles) in (a), growth function fittings (red lines) and eABR THR estimations (red diamonds). (C): Details of eABR estimation from b (8-pulses condition). The ‘×’ shows the median of estimated eABR THRs (diamonds). (D): Estimated eABR THRs as a function of number of pulses.	60

Figure 4.3 Results of psychophysical THRs. **(A)**: Psychophysical THRs as a function of number of pulses. Clinical THRs of all subjects are plotted in the most right side of panel a. **(B)**: The difference between psychophysical THRs and clinical THRs as a function of number of pulses. **(C)**: The absolute values of the data in panel b. The gray circles show results of individual subjects while the black circles show the corresponding median values over all subjects.....62

Figure 4.4 Growth functions of features used to estimate eABR THRs as a function of stimulation amplitude (%DR) in all MP conditions across all subjects. Thick lines show median values and shaded area represents the range between 25th and 75th percentiles.62

Figure 4.5 Estimated eABR THRs as a function of number of pulses, resulted from extrapolation of wave eV (panels **A** and **B**), eABR RMS value (panels **C** and **D**), peak PLV (panels **E** and **F**), and LVDP (panel **G**) growth functions. For each estimation method, an exponential function (left-side panels) and a linear function (right-side panels) were used for fitting. For the LVDP method, no estimation function was used. Data in gray shows results of individual subjects and data in black shows the corresponding median values across subjects. Asterisks show significant differences with $\alpha = 0.95$64

Figure 4.6 The ratio of estimated eABR THRs to clinical THRs (panels **A-G**) and absolute difference between them (panels **H-N**, respectively) as a function of number of pulses. The estimated eABR THRs were presented in Figure 4.5, which were resulted from extrapolation of growth functions of wave eV (panels **A**, **B**, **H**, and **I**), eABR RMS value (panels **C**, **D**, **J**, **K**), peak PLV (panels **E**, **F**, **L**, **M**), and LVDP (panels **G** and **N**, without any extrapolation). For each estimation method, an exponential function (left-side panels in each sub-figure) and a linear function (right-side panels in each sub-figure) were used for fitting. For the LVDP method, no estimation function was used. Data in gray shows results of individual subjects and data in black shows the corresponding median values across subjects. Lower and upper error bars show the mean 25th and 75th percentiles of median values from subsamples of growth functions, respectively. Asterisks show significant differences with 0.95 confidence intervals.66

Figure 4.7 Estimated eABR THRs as a function of psychophysical THRs for multi-pulse conditions. Each column shows results of a specific number of pulses. Panels in **A** and **B** show the eABR THRs estimated from AGFs of wave eV with exponential and linear fittings, respectively. Data in panels **C** and **D** present the eABR THRs estimated from growth functions of eABR RMS values with exponential and linear fittings, respectively. Panels **E** and **F** present the eABR THRs estimated from growth functions of peak PLV with exponential and linear fittings, respectively. Panels in **G** show the eABR THRs resulted from the LVDP method. Open circles present data from individual subjects. Dotted black lines show the identity lines and the blue lines show linear regressions. In each panel, the correlation coefficient (r) and the probability value (p) are shown.69

Figure 4.8 Estimated eABR THRs as a function of clinical THRs for multi-pulse conditions. Each column shows results of a specific number of pulses. Panels in **A** and **B** show the eABR THRs estimated from AGFs of wave eV with exponential and linear fittings, respectively. Data in panels **C** and **D** present the eABR THRs estimated from growth functions of eABR RMS values with exponential and linear fittings, respectively.

Panels **E** and **F** present the eABR THR_s estimated from growth functions of peak PLV with exponential and linear fittings, respectively. Panels **G** show the eABR THR_s resulted from the LVDP method. Open circles present data from individual subjects. Dotted black lines show the identity lines and the blue lines show linear regressions. In each panel, the correlation coefficient (r) and the probability value (p) are shown. 71

List of Tables

Table 2.1 Details of studies that investigated the eABR THRs and behavioral THRs. .24	24
Table 3.1 Demographic information of CI subjects participated in the study.....32	32
Table 4.1 Demographic information of CI participants56	56
Table 4.2 Median estimated THR differences for different features and fitting functions.65	65
Table 4.3 Conditions with the closest eABR THRs to clinical THRs for different features and fitting FFs. For each of relations A and B , two expressions were defined, one without considering the between-subject variability ($\min A - 1$ and $\min B$, respectively) and the other with considering it ($\min \log A \times \text{mid}50$ and $\min B \times \text{mid}50$, respectively). The variable $\text{mid}50$ represents the mid 50th percentile (75th percentile – 25th percentile). Conditions (argument) in which the minima of expressions occurred are presented in parenthesis. nP: number of pulses.68	68

References

- Abbas PJ and Brown CJ (1991). Electrically evoked auditory brainstem response: growth of response with current level. *Hearing research*, 51(1), 123-137. [https://doi.org/10.1016/0378-5955\(91\)90011-w](https://doi.org/10.1016/0378-5955(91)90011-w).
- Abbas PJ and Brown CJ (1991). Electrically evoked auditory brainstem response: refractory properties and strength-duration functions. *Hearing research*, 51(1), 139-147.
- Abbas PJ and Brown CJ (2015). Assessment of responses to cochlear implant stimulation at different levels of the auditory pathway. *Hearing research*, 322, 67-76. <https://doi.org/10.1016/j.heares.2014.10.011>.
- Abbas PJ, *et al.* (1999). Summary of results using the nucleus CI24M implant to record the electrically evoked compound action potential. *Ear and hearing*, 20(1), 45-59.
- Allen JB, Hall JL and Jeng PS (1990). Loudness growth in 1/2-octave bands (LGOB)—A procedure for the assessment of loudness. *The Journal of the Acoustical Society of America*, 88(2), 745-753. <https://doi.org/10.1121/1.399778>.
- Anwar A, *et al.* (2017). The value of intraoperative EABRs in auditory brainstem implantation. *International Journal of Pediatric Otorhinolaryngology*, 101, 158-163. <https://doi.org/10.1016/j.ijporl.2017.08.007>.
- Bahmer A and Baumann U (2012). Application of triphasic pulses with adjustable phase amplitude ratio (PAR) for cochlear ECAP recording: II. Recovery functions. *Journal of Neuroscience Methods*, 205(1), 212-220. <https://doi.org/10.1016/j.jneumeth.2011.12.006>.
- Bahmer A, Peter O and Baumann U (2008). Recording of electrically evoked auditory brainstem responses (E-ABR) with an integrated stimulus generator in Matlab. *Journal of neuroscience methods*, 173(2), 306-314.
- Bahmer A, Polak M and Baumann U (2010). Recording of electrically evoked auditory brainstem responses after electrical stimulation with biphasic, triphasic and precision triphasic pulses. *Hearing research*, 259(1), 75-85.
- Bai S, *et al.* (2019). Electrical Stimulation in the Human Cochlea: A Computational Study Based on High-Resolution Micro-CT Scans. *Frontiers in Neuroscience*, 13, 1312.
- Balkany T, *et al.* (2007). Nucleus freedom North American clinical trial. *Otolaryngology—Head and Neck Surgery*, 136(5), 757-762. <https://doi.org/10.1016/j.otohns.2007.01.006>.
- Baudhuin JL, Hughes ML and Goehring JL (2016). A comparison of alternating polarity and forward masking artifact-reduction methods to resolve the electrically evoked compound action potential. *Ear and hearing*, 37(4), e247. <https://10.1097/AUD.0000000000000288>.
- Baudhuin JL, Hughes ML and Goehring JL (2016). A Comparison of Alternating Polarity and Forward Masking Artifact-Reduction Methods to Resolve the Electrically Evoked

Compound Action Potential. Ear and hearing, 37(4), e247-e255.
<https://doi.org/10.1097/AUD.0000000000000288>.

Bierer JA and Middlebrooks JC (2002). Auditory cortical images of cochlear-implant stimuli: dependence on electrode configuration. Journal of neurophysiology, 87(1), 478-492. <https://doi.org/10.1152/jn.00212.2001>.

Black RC, Clark GM, O'Leary SJ and Walters C (1983). Intracochlear electrical stimulation of normal and deaf cats investigated using brainstem response audiometry. Acta Oto-Laryngologica, 95(sup399), 5-17.
<https://doi.org/10.3109/00016488309105588>.

Boons T, *et al.* (2012). Predictors of spoken language development following pediatric cochlear implantation. Ear and hearing, 33(5), 617-639.
<https://doi.org/10.1097/AUD.0b013e3182503e47>.

Botros A and Psarros C (2010). Neural response telemetry reconsidered: II. The influence of neural population on the ECAP recovery function and refractoriness. Ear and hearing, 31(3), 380-391. <https://doi.org/10.1097/AUD.0b013e3181cb41aa>.

Boulet J, White M and Bruce IC (2016). Temporal considerations for stimulating spiral ganglion neurons with cochlear implants. Journal of the Association for Research in Otolaryngology, 17(1), 1-17.

Brackett D and Zara CV (1998). Communication outcomes related to early implantation. The American journal of otology, 19(4), 453-460.

Brand T and Hohmann V (2002). An adaptive procedure for categorical loudness scaling. The Journal of the Acoustical Society of America, 112(4), 1597-1604.
<https://doi.org/10.1121/1.1502902>.

Brochier T, McKay CM and Carlyon RP (2021). Interpreting the Effect of Stimulus Parameters on the Electrically Evoked Compound Action Potential and on Neural Health Estimates. Journal of the Association for Research in Otolaryngology, 22(1), 81-94.
<https://doi.org/10.1007/s10162-020-00774-z>.

Brown CJ (2003). Clinical uses of electrically evoked auditory nerve and brainstem responses. Current opinion in otolaryngology & head and neck surgery, 11(5), 383-387.

Brown CJ, Abbas PJ and Gantz B (1990). Electrically evoked whole-nerve action potentials: Data from human cochlear implant users. The Journal of the Acoustical Society of America, 88(3), 1385-1391. <https://doi.org/10.1121/1.399716>.

Brown CJ, Hughes ML, Luk B, Abbas PJ, Wolaver A and Gervais J (2000). The relationship between EAP and EABR thresholds and levels used to program the nucleus 24 speech processor: data from adults. Ear and hearing, 21(2), 151-163.
<https://doi.org/10.1097/00003446-200004000-00009>.

Brown CJ, Lopez SM, Hughes ML and Abbas PJ (1999). Relationship between Eabr Thresholds and Levels Used to Program the Clarion® Speech Processor. Annals of Otolaryngology, Rhinology & Laryngology, 108(4_suppl), 50-57.

<https://doi.org/10.1177/00034894991080S411>.

Büchner A, Frohne-Büchner C, D. Battmer R and Lenarz T (2004). Two years of experience using stimulation rates between 800 and 5000 pps with the clarion CII implant. International Congress Series, 1273, 48-51. <https://doi.org/10.1016/j.ics.2004.09.012>.

Büchner A, Frohne-Büchner C, Gaertner L, Stoever T, Battmer RD and Lenarz T (2010). The Advanced Bionics High Resolution Mode: Stimulation rates up to 5000 pps. Acta Oto-Laryngologica, 130(1), 114-123. <https://doi.org/10.3109/00016480902971239>.

Busby PA and Arora K (2016). Effects of threshold adjustment on speech perception in Nucleus cochlear implant recipients. Ear and hearing, 37(3), 303-311. <https://doi.org/10.1097/AUD.0000000000000248>.

Carhart R and Jerger JF (1959). Preferred method for clinical determination of pure-tone thresholds. Journal of speech and hearing disorders, 24(4), 330-345.

Carlyon RP, Deeks JM and McKay CM (2015). Effect of Pulse Rate and Polarity on the Sensitivity of Auditory Brainstem and Cochlear Implant Users to Electrical Stimulation. J Assoc Res Otolaryngol, 16(5), 653-668. <https://doi.org/10.1007/s10162-015-0530-z>.

Cartee LA, Miller CA and van den Honert C (2006). Spiral ganglion cell site of excitation I: Comparison of scala tympani and intrameatal electrode responses. Hearing Research, 215(1), 10-21. <https://doi.org/10.1016/j.heares.2006.02.012>.

Cartee LA, van den Honert C, Finley CC and Miller RL (2000). Evaluation of a model of the cochlear neural membrane. I. Physiological measurement of membrane characteristics in response to intrameatal electrical stimulation. Hearing Research, 146(1), 143-152. [https://doi.org/10.1016/S0378-5955\(00\)00109-X](https://doi.org/10.1016/S0378-5955(00)00109-X).

Chouard CH, Meyer B and Donadieu F (1979). Auditory brainstem potentials in man evoked by electrical stimulation of the round window. Acta oto-laryngologica, 87(3-6), 287-293. <https://doi.org/10.3109/00016487909126422>.

Colletti L, Mandalà M, Zoccante L, Shannon RV and Colletti V (2011). Infants versus older children fitted with cochlear implants: performance over 10 years. International Journal of Pediatric Otorhinolaryngology, 75(4), 504-509. <https://doi.org/10.1016/j.ijporl.2011.01.005>.

Colrain IM and Campbell KB (2007). The use of evoked potentials in sleep research. Sleep medicine reviews, 11(4), 277-293. <https://doi.org/10.1016/j.smrv.2007.05.001>.

Danieli F, *et al.* (2021). Clinical implications of intraoperative eABRs to the Evo®-CI electrode array recipients. Brazilian Journal of Otorhinolaryngology. <https://doi.org/10.1016/j.bjorl.2021.04.012>.

Davis H (1965). Slow cortical responses evoked by acoustic stimuli. Acta Oto-laryngologica, 59(2-6), 179-185. <https://doi.org/10.3109/00016486509124551>.

Dees DC, *et al.* (2005). Normative findings of electrically evoked compound action potential measurements using the neural response telemetry of the Nucleus CI24M cochlear implant system. Audiology and Neurotology, 10(2), 105-116.

<https://doi.org/10.1159/000083366>.

Dettman SJ, *et al.* (2016). Long-term communication outcomes for children receiving cochlear implants younger than 12 months: A multicenter study. *Otology & Neurotology*, 37(2), e82-e95. <https://doi.org/10.1097/MAO.0000000000000915>.

Djourno A and Eyries C (1957). Prothèse auditive par excitation électrique à distance du nerf sensoriel à l'aide d'un bobinage inclus à demeure. *Presse médicale*, 65(63), 1417-1417.

Donaldson GS, Viemeister NF and Nelson DA (1997). Psychometric functions and temporal integration in electric hearing. *The Journal of the Acoustical Society of America*, 101(6), 3706-3721.

Dynes SBC (1996). Discharge characteristics of auditory nerve fibers for pulsatile electrical stimuli.

Elberling C and Nielsen C (1993). The dynamics of speech and the auditory dynamic range in sensorineural hearing impairment. *Recent developments in hearing instrument technology*, 99-133.

Firszt JB, Chambers RD and Kraus N (2002). Neurophysiology of cochlear implant users II: comparison among speech perception, dynamic range, and physiological measures. *Ear and hearing*, 23(6), 516-531.

Firszt JB, Chambers RD, Rotz LA and Novak MA (1999). Electrically evoked potentials recorded in adult and pediatric CLARION® implant users. *Annals of Otology, Rhinology & Laryngology*, 108(4_suppl), 58-63. <https://doi.org/10.1177/00034894991080S412>.

Florentine M, Fastl H and Buus Sr (1988). Temporal integration in normal hearing, cochlear impairment, and impairment simulated by masking. *The Journal of the Acoustical Society of America*, 84(1), 195-203. <https://doi.org/10.1121/1.2024393>.

Friesen LM, Shannon RV and Cruz RJ (2005). Effects of stimulation rate on speech recognition with cochlear implants. *Audiology and Neurotology*, 10(3), 169-184. <https://doi.org/10.1159/000084027>.

Frijns JHM, Briaire JJ, de Laat JAPM and Grote JJ (2002). Initial evaluation of the Clarion CII cochlear implant: speech perception and neural response imaging. *Ear and Hearing*, 23(3), 184-197.

Frijns JHM, Briaire JJ, de Laat JAPM and Grote JJ (2002). Initial Evaluation of the Clarion CII Cochlear Implant: Speech Perception and Neural Response Imaging. *Ear and Hearing*, 23(3).

Fryauf-Bertschy H, Tyler RS, Kelsay DM, Gantz BJ and Woodworth GG (1997). Cochlear implant use by prelingually deafened children: the influences of age at implant and length of device use. *Journal of speech, language, and hearing research*, 40(1), 183-199. <https://doi.org/10.1044/jslhr.4001.183>.

Gallégo S, Frachet B, Micheyl C, Truy E and Collet L (1998). Cochlear implant performance and electrically-evoked auditory brain-stem response characteristics.

Electroencephalography and Clinical Neurophysiology/Evoked Potentials Section, 108(6), 521-525. [https://doi.org/10.1016/S0168-5597\(98\)00030-6](https://doi.org/10.1016/S0168-5597(98)00030-6).

Gallégo S, Truy E, Morgon A and Collet L (1997). EABRs and Surface Potentials with a Transcutaneous Multielectrode Cochlear Implant. *Acta Oto-Laryngologica*, 117(2), 164-168. 10.3109/00016489709117761.

Geers A, Brenner C and Davidson L (2003). Factors associated with development of speech perception skills in children implanted by age five. *Ear and hearing*, 24(1), 24S-35S. <https://doi.org/10.1097/01.AUD.0000051687.99218.0F>.

Gerken GM, Bhat VK and Hutchison-Clutter M (1990). Auditory temporal integration and the power function model. *J Acoust Soc Am*, 88(2), 767-778.

Gordon KA, Papsin BC and Harrison RV (2003). Activity-Dependent Developmental Plasticity of the Auditory Brain Stem in Children Who Use Cochlear Implants. *Ear and Hearing*, 24(6). <https://doi.org/10.1097/01.AUD.0000100203.65990.D4>.

Gordon KA, Valero J, van Hoesel R and Papsin BC (2008). Abnormal timing delays in auditory brainstem responses evoked by bilateral cochlear implant use in children. *Otology & Neurotology*, 29(2), 193-198. DOI 10.1097/mao.0b013e318162514c.

Grant GD, Cheng AK and Niparko JK (1999). Meta-analysis of pediatric cochlear implant literature. *Annals of Otology, Rhinology & Laryngology*, 108(4_suppl), 124-128. <https://doi.org/10.1177/00034894991080S425>.

Harris MS, Capretta NR, Henning SC, Feeney L, Pitt MA and Moberly AC (2016). Postoperative Rehabilitation Strategies Used by Adults With Cochlear Implants: A Pilot Study. *Laryngoscope Investigative Otolaryngology*, 1(3), 42-48. <https://doi.org/10.1002/lio2.20>.

Heffer LF, Sly DJ, Fallon JB, White MW, Shepherd RK and O'Leary SJ (2010). Examining the auditory nerve fiber response to high rate cochlear implant stimulation: chronic sensorineural hearing loss and facilitation. *J Neurophysiol*, 104(6), 3124-3135. <https://doi.org/10.1152/jn.00500.2010>.

Hellbruück J and Moser LM (1985). Hörgeräte-Audiometrie: ein computerunterstütztes psychologisches Verfahren zur Hörgeräteanpassung;. *Psychologische Beiträge* (Lengerich), 27(4), 494-508.

Helms J, *et al.* (2004). Analysis of ceiling effects occurring with speech recognition tests in adult cochlear-implanted patients. *ORL*, 66(3), 130-135. <https://doi.org/10.1159/000079332>.

Hochmair I, *et al.* (2006). MED-EL Cochlear implants: state of the art and a glimpse into the future. *Trends in amplification*, 10(4), 201-219. <https://doi.org/10.1177/1084713806296720>.

Hodges AV, Ruth RA, Lambert PR and Balkany TJ (1994). Electric auditory brain-stem responses in Nucleus multichannel cochlear implant users. *Archives of Otolaryngology–Head & Neck Surgery*, 120(10), 1093-1099.

<https://doi.org/10.1001/archotol.1994.01880340037007>.

Hodgkin AL (1938). The subthreshold potentials in a crustacean nerve fibre. Proceedings of the Royal Society of London Series B-Biological Sciences, 126(842), 87-121.

Hodgkin AL and Huxley AF (1952). A quantitative description of membrane current and its application to conduction and excitation in nerve. The Journal of physiology, 117(4), 500-544.

Hofmann M and Wouters J (2012). Improved electrically evoked auditory steady-state response thresholds in humans. Journal of the Association for Research in Otolaryngology, 13(4), 573-589. <https://doi.org/10.1007/s10162-012-0321-8>.

Holden LK, Reeder RM, Firszt JB and Finley CC (2011). Optimizing the perception of soft speech and speech in noise with the Advanced Bionics cochlear implant system. International journal of audiology, 50(4), 255-269. <https://doi.org/10.3109/14992027.2010.533200>.

Hosoya M, Minami SB, Enomoto C, Matsunaga T and Kaga K (2018). Elongated EABR wave latencies observed in patients with auditory neuropathy caused by OTOF mutation. Laryngoscope Investigative Otolaryngology, 3(5), 388-393. <https://doi.org/10.1002/liv2.210>.

Hu H, Kollmeier B and Dietz M (2015). Reduction of stimulation coherent artifacts in electrically evoked auditory brainstem responses. Biomedical Signal Processing and Control, 21, 74-81.

Hughes ML, Brown CJ, Abbas PJ, Wolaver AA and Gervais JP (2000). Comparison of EAP thresholds with MAP levels in the nucleus 24 cochlear implant: data from children. Ear and hearing, 21(2), 164-174. <https://doi.org/10.1097/00003446-200004000-00010>.

Hughes ML, Castioni EE, Goehring JL and Baudhuin JL (2012). Temporal response properties of the auditory nerve: data from human cochlear-implant recipients. Hear Res, 285(1-2), 46-57. 10.1016/j.heares.2012.01.010.

Hughes ML, *et al.* (2001). A Longitudinal Study of Electrode Impedance, the Electrically Evoked Compound Action Potential, and Behavioral Measures in Nucleus 24 Cochlear Implant Users. Ear and Hearing, 22(6).

Jeon JH, Bae MR, Song MH, Noh SH, Choi KH and Choi JY (2013). Relationship Between Electrically Evoked Auditory Brainstem Response and Auditory Performance After Cochlear Implant in Patients With Auditory Neuropathy Spectrum Disorder. Otolaryngology & Neurotology, 34(7). <https://doi.org/10.1097/MAO.0b013e318291c632>.

Kang SY, Colesa DJ, Swiderski DL, Su GL, Raphael Y and Pfungst BE (2010). Effects of hearing preservation on psychophysical responses to cochlear implant stimulation. Journal of the Association for Research in Otolaryngology, 11(2), 245-265. <https://doi.org/10.1007/s10162-009-0194-7>.

Karg SA, Lackner C and Hemmert W (2013). Temporal interaction in electrical hearing elucidates auditory nerve dynamics in humans. Hearing Research, 299, 10-18.

<https://doi.org/10.1016/j.heares.2013.01.015>.

Kileny PR, Zwolan TA, Boerst A and Telian SA (1997). Electrically evoked auditory potentials: current clinical applications in children with cochlear implants. *The American journal of otology*, 18(6 Suppl), S90-92.

Kim AH, Kileny PR, Arts HA, El-Kashlan HK, Telian SA and Zwolan TA (2008). Role of electrically evoked auditory brainstem response in cochlear implantation of children with inner ear malformations. *Otology & Neurotology*, 29(5), 626-634. <https://doi.org/10.1097/MAO.0b013e31817781f5>.

Kim J-R, Abbas PJ, Brown CJ, Etler CP, O'Brien S and Kim L-S (2010). The relationship between electrically evoked compound action potential and speech perception: a study in cochlear implant users with short electrode array. *Otology & neurotology*, 31(7), 1041-1048. <https://doi.org/10.1097/MAO.0b013e3181ec1d92>.

Kirk KI, Ying E, Miyamoto RT, O'Neill T, Lento CL and Fears B (2002). Effects of Age at Implantation in Young Children. *Annals of Otology, Rhinology & Laryngology*, 111(5_suppl), 69-73. <https://doi.org/10.1177/00034894021110S515>.

Koch DB, Downing M, Osberger MJ and Litvak L (2007). Using Current Steering to Increase Spectral Resolution in CII and HiRes 90K Users. *Ear and Hearing*, 28(2), 38S-41S. <https://doi.org/10.1097/AUD.0b013e31803150de>.

Koch DB, Osberger MJ, Segel P and Kessler D (2004). HiResolution™ and conventional sound processing in the HiResolution™ bionic ear: using appropriate outcome measures to assess speech recognition ability. *Audiology and Neurotology*, 9(4), 214-223. <https://doi.org/10.1159/000078391>.

Launer S (1995). Loudness perception in listeners with sensorineural hearing impairment.

Litvak LM, Smith ZM, Delgutte B and Eddington DK (2003). Desynchronization of electrically evoked auditory-nerve activity by high-frequency pulse trains of long duration. *The Journal of the Acoustical Society of America*, 114(4), 2066-2078.

Liu Q, Lee E and Davis RL (2014). Heterogeneous intrinsic excitability of murine spiral ganglion neurons is determined by Kv1 and HCN channels. *Neuroscience*, 257, 96-110. <https://doi.org/10.1016/j.neuroscience.2013.10.065>.

Lundin K, Stillesjö F and Rask-Andersen H (2015). Prognostic value of electrically evoked auditory brainstem responses in cochlear implantation. *Cochlear implants international*, 16(5), 254-261. <https://doi.org/10.1179/1754762815Y.0000000005>.

Macherey O, Stahl P, Intartaglia B, Meunier S, Roman S and Schön D (2021). Temporal integration of short-duration pulse trains in cochlear implant listeners: Psychophysical and electrophysiological measurements. *Hearing Research*, 403, 108176. <https://doi.org/10.1016/j.heares.2021.108176>.

Macherey O, van Wieringen A, Carlyon RP, Deeks JM and Wouters J (2006). Asymmetric pulses in cochlear implants: effects of pulse shape, polarity, and rate. *J Assoc Res Otolaryngol*, 7(3), 253-266. 10.1007/s10162-006-0040-0.

- Mahmud M and Vassanelli S (2016). Differential Modulation of Excitatory and Inhibitory Neurons during Periodic Stimulation. *Frontiers in Neuroscience*, 10, 62. <https://doi.org/10.3389/fnins.2016.00062>.
- Makhdoum MJ, Groenen PAP, Snik AFM and Broek Pvd (1998). Intra-and interindividual correlations between auditory evoked potentials and speech perception in cochlear implant users. *Scandinavian audiology*, 27(1), 13-20. <https://doi.org/10.1080/010503998419650>.
- Mao D, Innes-Brown H, Petoe M, McKay CM and Wong YT (2021). Spectral features of cortical auditory evoked potentials inform hearing threshold and intensity percepts in acoustic and electric hearing. *Journal of Neural Engineering*. <https://doi.org/10.1088/1741-2552/ac02db>.
- Mao D, Innes-Brown H, Petoe MA, Wong YT and McKay CM (2018). Cortical auditory evoked potential time-frequency growth functions for fully objective hearing threshold estimation. *Hearing research*, 370, 74-83. <https://doi.org/10.1016/j.heares.2018.09.006>.
- Mao D, Innes-Brown H, Petoe MA, Wong YT and McKay CM (2019). Fully objective hearing threshold estimation in cochlear implant users using phase-locking value growth functions. *Hear Res*, 377, 24-33. <https://doi.org/10.1016/j.heares.2019.02.013>.
- Mardia KV (2014). *Statistics of directional data*, Academic press.
- Matsuoka AJ, Rubinstein JT, Abbas PJ and Miller CA (2001). The effects of interpulse interval on stochastic properties of electrical stimulation: models and measurements. *IEEE Transactions on Biomedical Engineering*, 48(4), 416-424. <https://doi.org/10.1109/10.915706>.
- McKay CM, Chandan K, Akhoun I, Siciliano C and Kluk K (2013). Can ECAP Measures Be Used for Totally Objective Programming of Cochlear Implants? *Journal of the Association for Research in Otolaryngology*, 14(6), 879-890. <https://doi.org/10.1007/s10162-013-0417-9>.
- McKay CM, Fewster L and Dawson P (2005). A different approach to using neural response telemetry for automated cochlear implant processor programming. *Ear and hearing*, 26(4), 38S-44S.
- McKay CM and McDermott HJ (1998). Loudness perception with pulsatile electrical stimulation: the effect of interpulse intervals. *The Journal of the Acoustical Society of America*, 104(2), 1061-1074. <https://doi.org/10.1121/1.423316>.
- McKay CM and McDermott HJ (1999). The perceptual effects of current pulse duration in electrical stimulation of the auditory nerve. *The Journal of the Acoustical Society of America*, 106(2), 998-1009.
- McKay CM and Smale N (2017). The relation between ECAP measurements and the effect of rate on behavioral thresholds in cochlear implant users. *Hearing research*, 346, 62-70. <https://doi.org/10.1016/j.heares.2017.02.009>.
- Middlebrooks JC (2004). Effects of cochlear-implant pulse rate and inter-channel timing

on channel interactions and thresholds. *The Journal of the Acoustical Society of America*, 116(1), 452-468.

Miller CA, Abbas PJ and Brown CJ (1993). Electrically evoked auditory brainstem response to stimulation of different sites in the cochlea. *Hearing Research*, 66(2), 130-142. [https://doi.org/10.1016/0378-5955\(93\)90134-M](https://doi.org/10.1016/0378-5955(93)90134-M).

Miller CA, Abbas PJ and Brown CJ (2000). An improved method of reducing stimulus artifact in the electrically evoked whole-nerve potential. *Ear and hearing*, 21(4), 280-290. 10.1097/00003446-200008000-00003.

Miller CA, Abbas PJ and Robinson BK (2001). Response properties of the refractory auditory nerve fiber. *JARO-Journal of the Association for Research in Otolaryngology*, 2(3), 216-232.

Miller CA, Abbas PJ, Rubinstein JT, Robinson BK, Matsuoka AJ and Woodworth G (1998). Electrically evoked compound action potentials of guinea pig and cat: responses to monopolar, monophasic stimulation. *Hearing Research*, 119(1), 142-154. [https://doi.org/10.1016/S0378-5955\(98\)00046-X](https://doi.org/10.1016/S0378-5955(98)00046-X).

Miller CA, Brown CJ, Abbas PJ and Chi S-L (2008). The clinical application of potentials evoked from the peripheral auditory system. *Hearing Research*, 242(1), 184-197. <https://doi.org/10.1016/j.heares.2008.04.005>.

Miller CA, Hu N, Zhang F, Robinson BK and Abbas PJ (2008). Changes Across Time in the Temporal Responses of Auditory Nerve Fibers Stimulated by Electric Pulse Trains. *Journal of the Association for Research in Otolaryngology*, 9(1), 122-137. 10.1007/s10162-007-0108-5.

Miller CA, Woo J, Abbas PJ, Hu N and Robinson BK (2011). Neural masking by sub-threshold electric stimuli: animal and computer model results. *Journal of the Association for Research in Otolaryngology*, 12(2), 219-232.

Miyamoto RT (1986). Electrically evoked potentials in cochlear implant subjects. *The Laryngoscope*, 96(2), 178-185. <https://doi.org/10.1288/00005537-198602000-00009>.

Miyamoto RT, Kirk KI, Svirsky MA and Sehgal ST (1999). Communication skills in pediatric cochlear implant recipients. *Acta oto-laryngologica*, 119(2), 219-224. <https://doi.org/10.1080/00016489950181701>.

Moon AK, Zwolan TA and Pfungst BE (1993). Effects of phase duration on detection of electrical stimulation of the human cochlea. *Hearing research*, 67(1-2), 166-178.

Negm MH and Bruce IC (2014). The Effects of HCN and KLT Ion Channels on Adaptation and Refractoriness in a Stochastic Auditory Nerve Model. *IEEE Transactions on Biomedical Engineering*, 61(11), 2749-2759. <https://doi.org/10.1109/TBME.2014.2327055>.

Nie K, Barco A and Zeng F-G (2006). Spectral and temporal cues in cochlear implant speech perception. *Ear and hearing*, 27(2), 208-217. <https://doi.org/10.1097/01.aud.0000202312.31837.25>.

- Obando Leitón ME (2019). Temporal integration in cochlear implants and the effect of high pulse rates. PhD thesis, Ludwig Maximilian University of Munich. <https://doi.org/10.5282/edoc.25312>.
- Papsin B, Gysin C, Picton N, Nedzelski J and Harrison R (2001). Speech Perception Outcome Measures in Prelingually Deaf Children up to Four Years after Cochlear Implantation. *The Annals of otology, rhinology & laryngology Supplement*, 185, 38-42. 10.1177/0003489400109S1216.
- Perl ER, Galambos R and Glorig A (1953). The estimation of hearing threshold by electroencephalography. *Electroencephalography and Clinical Neurophysiology*, 5(4), 501-512. [https://doi.org/10.1016/0013-4694\(53\)90026-1](https://doi.org/10.1016/0013-4694(53)90026-1).
- Pfingst BE, *et al.* (2011). Detection of pulse trains in the electrically stimulated cochlea: Effects of cochlear health. *The Journal of the Acoustical Society of America*, 130(6), 3954-3968.
- Pfingst BE, *et al.* (2015). Importance of cochlear health for implant function. *Hearing research*, 322, 77-88. <https://doi.org/10.1016/j.heares.2014.09.009>.
- Picton TW (2011). Late auditory evoked potentials: Changing the things which are. *Human auditory evoked potentials*, 335-398.
- Picton TW and Hillyard SA (1974). Human auditory evoked potentials. II: Effects of attention. *Electroencephalography and Clinical Neurophysiology*, 36, 191-200. [https://doi.org/10.1016/0013-4694\(74\)90156-4](https://doi.org/10.1016/0013-4694(74)90156-4).
- Picton TW, Hillyard SA, Galambos R and Schiff M (1971). Human Auditory Attention: A Central or Peripheral Process? *Science*, 173(3994), 351. <https://doi.org/10.1126/science.173.3994.351>.
- Polak M, Hodges AV, King JE and Balkany TJ (2004). Further prospective findings with compound action potentials from Nucleus 24 cochlear implants. *Hearing Research*, 188(1), 104-116. [https://doi.org/10.1016/S0378-5955\(03\)00309-5](https://doi.org/10.1016/S0378-5955(03)00309-5).
- Prado-Guitierrez P, Fewster LM, Heasman JM, McKay CM and Shepherd RK (2006). Effect of interphase gap and pulse duration on electrically evoked potentials is correlated with auditory nerve survival. *Hear Res*, 215(1-2), 47-55. <https://doi.org/10.1016/j.heares.2006.03.006>.
- Prado-Guitierrez P, Fewster LM, Heasman JM, McKay CM and Shepherd RK (2006). Effect of interphase gap and pulse duration on electrically evoked potentials is correlated with auditory nerve survival. *Hearing research*, 215(1-2), 47-55. <https://doi.org/10.1016/j.heares.2006.03.006>.
- Prasher D, Mula M and Luxon L (1993). Cortical evoked potential criteria in the objective assessment of auditory threshold: a comparison of noise induced hearing loss with Ménière's disease. *The Journal of Laryngology & Otology*, 107(9), 780-786. <https://doi.org/10.1017/S0022215100124429>.
- Rader T, Doms P, Adel Y, Weissgerber T, Strieth S and Baumann U (2018). A method

for determining precise electrical hearing thresholds in cochlear implant users. *International Journal of Audiology*, 57(7), 502-509. <https://doi.org/10.1080/14992027.2017.1412519>.

Ramekers D, Versnel H, Strahl SB, Smeets EM, Klis SFL and Grolman W (2014). Auditory-nerve responses to varied inter-phase gap and phase duration of the electric pulse stimulus as predictors for neuronal degeneration. *Journal of the Association for Research in Otolaryngology*, 15(2), 187-202. <https://doi.org/10.1007/s10162-013-0440-x>.

Ross B, Lütkenhöner B, Pantev C and Hoke M (1999). Frequency-Specific Threshold Determination with the CERAGram Method: Basic Principle and Retrospective Evaluation of Data. *Audiology and Neurotology*, 4(1), 12-27. <https://doi.org/10.1159/000013816>.

Rubinstein JT, Wilson BS, Finley CC and Abbas PJ (1999). Pseudospontaneous activity: stochastic independence of auditory nerve fibers with electrical stimulation. *Hearing research*, 127(1-2), 108-118.

Saeedi A and Hemmert W (2020). Investigation of Electrically-Evoked Auditory Brainstem Responses to Multi-Pulse Stimulation of High Frequency in Cochlear Implant Users. *Frontiers in Neuroscience*, 14(615). <https://doi.org/10.3389/fnins.2020.00615>.

Schnupp J, Nelken I and King A (2011). *Auditory neuroscience: Making sense of sound*, MIT press.

Schwartz-Leyzac KC and Pfingst BE (2016). Across-site patterns of electrically evoked compound action potential amplitude-growth functions in multichannel cochlear implant recipients and the effects of the interphase gap. *Hearing research*, 341, 50-65. <https://doi.org/10.1016/j.heares.2016.08.002>.

Shader MJ, *et al.* (2020). Effect of Stimulation Rate on Speech Understanding in Older Cochlear-Implant Users. *Ear and Hearing*, 41(3). <https://doi.org/10.1097/AUD.0000000000000793>.

Shallop JK, Beiter AL, Goin DW and Mischke RE (1990). Electrically evoked auditory brain stem responses (EABR) and middle latency responses (EMLR) obtained from patients with the nucleus multichannel cochlear implant. *Ear and hearing*, 11(1), 5-15.

Shallop JK, Goin DW, VanDyke L and Mischke RE (1991). Prediction of Behavioral Threshold and Comfort Values for Nucleus 22-Channel Implant Patients from Electrical Auditory Brain Stem Response Test Results. *Annals of Otology, Rhinology & Laryngology*, 100(11), 896-898. <https://doi.org/10.1177/000348949110001107>.

Shannon RV (1983). Multichannel electrical stimulation of the auditory nerve in man. I. Basic psychophysics. *Hearing Research*, 11(2), 157-189. [https://doi.org/10.1016/0378-5955\(83\)90077-1](https://doi.org/10.1016/0378-5955(83)90077-1).

Shannon RV (1985). Threshold and loudness functions for pulsatile stimulation of cochlear implants. *Hearing Research*, 18(2), 135-143. [https://doi.org/10.1016/0378-5955\(85\)90005-X](https://doi.org/10.1016/0378-5955(85)90005-X).

- Shapiro WH and Bradham TS (2012). Cochlear implant programming. *Otolaryngologic Clinics of North America*, 45(1), 111-127. <https://doi.org/10.1016/j.otc.2011.08.020>.
- Sharma A, Dorman MF and Spahr AJ (2002). Rapid development of cortical auditory evoked potentials after early cochlear implantation. *Neuroreport*, 13(10), 1365-1368.
- Sharma A, Dorman MF and Spahr AJ (2002). A sensitive period for the development of the central auditory system in children with cochlear implants: implications for age of implantation. *Ear and hearing*, 23(6), 532-539. <https://doi.org/10.1097/01.AUD.0000042223.62381.01>.
- Shepherd RK, Hardie NA and Baxi JH (2001). Electrical Stimulation of the Auditory Nerve: Single Neuron Strength-Duration Functions in Deafened Animals. *Annals of Biomedical Engineering*, 29(3), 195-201. <https://doi.org/10.1114/1.1355276>.
- Shepherd RK and Javel E (1999). Electrical stimulation of the auditory nerve: II. Effect of stimulus waveshape on single fibre response properties. *Hearing research*, 130(1), 171-188.
- Silva I (2009). Estimation of postaverage SNR from evoked responses under nonstationary noise. *IEEE Transactions on Biomedical Engineering*, 56(8), 2123-2130. <https://doi.org/10.1109/TBME.2009.2021400>.
- Simmons FB, Meyers T, Lusted HS and Shelton C (1984). Electrically induced auditory brainstem response as a clinical tool in estimating nerve survival. *Annals of Otolaryngology & Laryngology*, 93(4_suppl), 97-100. <https://doi.org/10.1177/00034894840930S417>.
- Skinner MW, Holden LK, Holden TA and Demorest ME (1995). Comparison of procedures for obtaining thresholds and maximum acceptable loudness levels with the Nucleus cochlear implant system. *Journal of Speech, Language, and Hearing Research*, 38(3), 677-689.
- Skinner MW, Holden LK, Holden TA and Demorest ME (2000). Effect of stimulation rate on cochlear implant recipients' thresholds and maximum acceptable loudness levels. *Journal of the American Academy of Audiology*, 11(4), 203-213.
- Smith L and Simmons FB (1983). Estimating eighth nerve survival by electrical stimulation. *Annals of Otolaryngology & Laryngology*, 92(1), 19-23. <https://doi.org/10.1111/j.1749-6632.1983.tb31656.x>.
- Snyder RL, Middlebrooks JC and Bonham BH (2008). Cochlear implant electrode configuration effects on activation threshold and tonotopic selectivity. *Hearing Research*, 235(1), 23-38. <https://doi.org/10.1016/j.heares.2007.09.013>.
- Spahr AJ and Dorman MF (2005). Effects of Minimum Stimulation Settings for the Med El Tempo+ Speech Processor on Speech Understanding. *Ear and Hearing*, 26(4).
- Spitzer P, Zierhofer C and Hochmair E (2006). Algorithm for multi-curve-fitting with shared parameters and a possible application in evoked compound action potential measurements. *Biomedical engineering online*, 5(1), 13.

- Starr A and Brackmann DE (1979). Brain stem potentials evoked by electrical stimulation of the cochlea in human subjects. *Annals of Otology, Rhinology & Laryngology*, 88(4), 550-556. <https://doi.org/10.1177/000348947908800419>.
- Tabibi S, Kegel A, Lai WK, Bruce IC and Dillier N (2019). Measuring temporal response properties of auditory nerve fibers in cochlear implant recipients. *Hearing Research*, 380, 187-196. <https://doi.org/10.1016/j.heares.2019.07.004>.
- Tabibi S, Kegel A, Lai WK and Dillier N (2020). A bio-inspired coding (BIC) strategy for cochlear implants. *Hearing Research*, 388, 107885. <https://doi.org/10.1016/j.heares.2020.107885>.
- Tejani VD, Abbas PJ and Brown CJ (2017). Relationship between peripheral and psychophysical measures of amplitude modulation detection in cochlear implant users. *Ear and hearing*, 38(5), e268. <https://doi.org/10.1097/AUD.0000000000000417>.
- Truy E, Gallego S, Chanal JM, Collet L and Morgon A (1998). Correlation between electrical auditory brainstem response and perceptual thresholds in Digisonic cochlear implant users. *The Laryngoscope*, 108(4), 554-559. <https://doi.org/10.1097/00005537-199804000-00017>.
- Turner C, Mehr M, Hughes M, Brown C and Abbas P (2002). Within-subject predictors of speech recognition in cochlear implants: A null result. *Acoustics Research Letters Online*, 3(3), 95-100. <https://doi.org/10.1121/1.1477875>.
- Tykocinski M, Shepherd RK and Clark GM (1995). Reduction in excitability of the auditory nerve following electrical stimulation at high stimulus rates. *Hearing research*, 88(1), 124-142.
- Tyler RS, Parkinson AJ, Woodworth GG, Lowder MW and Gantz BJ (1997). Performance over time of adult patients using the Ineraid or Nucleus cochlear implant. *The Journal of the Acoustical Society of America*, 102(1), 508-522. <https://doi.org/10.1121/1.419724>.
- Undurraga JA, Carlyon RP, Wouters J and van Wieringen A (2013). The Polarity Sensitivity of the Electrically Stimulated Human Auditory Nerve Measured at the Level of the Brainstem. *Journal of the Association for Research in Otolaryngology*, 14(3), 359-377. <https://doi.org/10.1007/s10162-013-0377-0>.
- Vaerenberg B, *et al.* (2014). Cochlear implant programming: a global survey on the state of the art. *The Scientific World Journal*, 2014. <https://doi.org/10.1155/2014/501738>.
- Valencia DM, Rimell FL, Friedman BJ, Oblander MR and Helmbrecht J (2008). Cochlear implantation in infants less than 12 months of age. *International Journal of Pediatric Otorhinolaryngology*, 72(6), 767-773. <https://doi.org/10.1016/j.ijporl.2008.02.009>.
- van den Honert C and Stypulkowski PH (1986). Characterization of the electrically evoked auditory brainstem response (ABR) in cats and humans. *Hearing Research*, 21(2), 109-126. [https://doi.org/10.1016/0378-5955\(86\)90033-X](https://doi.org/10.1016/0378-5955(86)90033-X).
- Van Dun B, Dillon H and Seeto M (2015). Estimating hearing thresholds in hearing-

impaired adults through objective detection of cortical auditory evoked potentials. *Journal of the American Academy of Audiology*, 26(04), 370-383. <https://doi.org/10.3766/jaaa.26.4.5>.

Van Wieringen A and Wouters J (2001). Comparison of procedures to determine electrical stimulation thresholds in cochlear implant users. *Ear and hearing*, 22(6), 528-538.

Vandali AE, Whitford LA, Plant KL, Clark and Graeme M (2000). Speech Perception as a Function of Electrical Stimulation Rate: Using the Nucleus 24 Cochlear Implant System. *Ear and Hearing*, 21(6). <https://doi.org/10.1097/00003446-200012000-00008>.

Vandali AE, Whitford LA, Plant KL and Clark GM (2000). Speech perception as a function of electrical stimulation rate: using the Nucleus 24 cochlear implant system. *Ear and hearing*, 21(6), 608-624.

Verschuur CA (2005). Effect of stimulation rate on speech perception in adult users of the Med-El CIS speech processing strategy Efectos de la tasa de estimulación en la percepción del lenguaje en usuarios adultos de la estrategia de procesamiento Med-El CIS. *International journal of audiology*, 44(1), 58-63. <https://doi.org/10.1080/14992020400022488>.

Visram AS, Innes-Brown H, El-Dereedy W and McKay CM (2015). Cortical auditory evoked potentials as an objective measure of behavioral thresholds in cochlear implant users. *Hearing Research*, 327, 35-42. <https://doi.org/10.1016/j.heares.2015.04.012>.

Walsh SM and Leake-Jones PA (1982). Chronic electrical stimulation of auditory nerve in cat: Physiological and histological results. *Hearing research*, 7(3), 281-304. [https://doi.org/10.1016/0378-5955\(82\)90041-7](https://doi.org/10.1016/0378-5955(82)90041-7).

Walton J, Gibson WPR, Sanli H and Prelog K (2008). Predicting cochlear implant outcomes in children with auditory neuropathy. *Otology & Neurotology*, 29(3), 302-309.

Wang Y, Pan T, Deshpande Shruti B and Ma F (2015). The Relationship Between EABR and Auditory Performance and Speech Intelligibility Outcomes in Pediatric Cochlear Implant Recipients. *American Journal of Audiology*, 24(2), 226-234. https://doi.org/10.1044/2015_AJA-14-0023.

Weber BP, *et al.* (2007). Performance and preference for ACE stimulation rates obtained with nucleus RP 8 and freedom system. *Ear and hearing*, 28(2), 46S-48S. <https://doi.org/10.1097/AUD.0b013e3180315442>.

WHO (2021). World Report on Hearing. Online, Visited on 05.05.2021.

Wilson BS (2004). Engineering design of cochlear implants. *Cochlear implants: auditory prostheses and electric hearing*, Springer: 14-52.

Wolfe J and Kasulis H (2008). Relationships among objective measures and speech perception in adult users of the HiResolution Bionic Ear. *Cochlear implants international*, 9(2), 70-81. <https://doi.org/10.1002/cii.354>.

Wolfe J and Schafer E (2014). Programming cochlear implants, Plural publishing.

- Wouters J, McDermott HJ and Francart T (2015). Sound coding in cochlear implants: From electric pulses to hearing. *IEEE Signal Processing Magazine*, 32(2), 67-80. <https://doi.org/10.1109/MSP.2014.2371671>.
- Wunderlich JL, Cone-Wesson BK and Shepherd R (2006). Maturation of the cortical auditory evoked potential in infants and young children. *Hearing research*, 212(1-2), 185-202. <https://doi.org/10.1016/j.heares.2005.11.010>.
- Yamazaki H, *et al.* (2014). Electrically Evoked Auditory Brainstem Response–Based Evaluation of the Spatial Distribution of Auditory Neuronal Tissue in Common Cavity Deformities. *Otology & neurotology*, 35(8), 1394-1402.
- Yeung KNK and Wong LLN (2007). Prediction of hearing thresholds: Comparison of cortical evoked response audiometry and auditory steady state response audiometry techniques. *International Journal of Audiology*, 46(1), 17-25. <https://doi.org/10.1080/14992020601102238>.
- Zeng F-G (2017). Challenges in improving cochlear implant performance and accessibility. *IEEE Transactions on Biomedical Engineering*, 64(8), 1662-1664. <https://doi.org/10.1109/TBME.2017.2718939>.
- Zeng FG, Rebscher S, Harrison W, Sun X and Feng H (2008). Cochlear Implants: System Design, Integration, and Evaluation. *IEEE Reviews in Biomedical Engineering*, 1, 115-142. <https://doi.org/10.1109/RBME.2008.2008250>.
- Zhang F, Miller CA, Robinson BK, Abbas PJ and Hu N (2007). Changes Across Time in Spike Rate and Spike Amplitude of Auditory Nerve Fibers Stimulated by Electric Pulse Trains. *Journal of the Association for Research in Otolaryngology*, 8(3), 356-372. <https://doi.org/10.1007/s10162-007-0086-7>.
- Zhou N and Dong L (2017). Evaluating Multipulse Integration as a Neural-Health Correlate in Human Cochlear-Implant Users: Relationship to Psychometric Functions for Detection. *Trends in Hearing*, 21, 2331216517690108. 10.1177/2331216517690108.
- Zhou N, Dong L and Hang M (2018). Evaluating multipulse integration as a neural-health correlate in human cochlear implant users: effects of stimulation mode. *Journal of the Association for Research in Otolaryngology*, 19(1), 99-111.
- Zhou N, Kraft CT, Colesa DJ and Pfingst BE (2015). Integration of Pulse Trains in Humans and Guinea Pigs with Cochlear Implants. *J Assoc Res Otolaryngol*, 16(4), 523-534. <https://doi.org/10.1007/s10162-015-0521-0>.
- Zhou N and Pfingst BE (2016). Evaluating multipulse integration as a neural-health correlate in human cochlear-implant users: Relationship to spatial selectivity. *The Journal of the Acoustical Society of America*, 140(3), 1537-1547.
- Zhou N, Xu L and Pfingst BE (2012). Characteristics of detection thresholds and maximum comfortable loudness levels as a function of pulse rate in human cochlear implant users. *Hear Res*, 284(1-2), 25-32. <https://doi.org/10.1016/j.heares.2011.12.008>.